GEOLOGIC CHARACTERIZATION OF A SALINE RESERVOIR FOR CARBON SEQUESTRATION: THE PALUXY FORMATION, CITRONELLE DOME, GULF OF MEXICO BASIN, ALABAMA

By

AYOBAMI TIMOTHY FOLARANMI

Bachelor of Science in Geosciences

Midwestern State University

Wichita Falls, Texas

2012

Submitted to the Faculty of the
Graduate College of the
Oklahoma State University
in partial fulfillment of
the requirements for
the Degree of
MASTER OF SCIENCE
May, 2015

GEOLOGIC CHARACTERIZATION OF A SALINE RESERVOIR FOR CARBON SEQUESTRATION: THE PALUXY FORMATION, CITRONELLE DOME, GULF OF MEXICO BASIN, ALABAMA

Thesis Approved:

Dr. Jack Pashin

Thesis Adviser

Dr. Mary Hileman

Dr. Joseph F. Donoghue

ACKNOWLEDGEMENTS

First and foremost, I would like to thank God Almighty for being my strength and support throughout this journey.

I would also like to thank the U.S Department of Energy, Southern Company, and Advanced Resources International for their support of this work, which was conducted under contract DE-FE0009785.

Words do no justice to the immense help my advisor, Dr. Jack Pashin has been over the past two years. He has provided a lot of support to make this a success.

I appreciate Dr. Jim Puckette for helping me with my XRD Analysis. Jingyao Meng (Jenny) and Ibrahim Al Atwah who have helped me tremendously with the art of making better graphical illustrations for my thesis. Finally, I would like to thank my parents. To my parents David and Felicia, I cannot thank you enough for your prayers, unconditional love, and support through all these years. You guys are the real MVPs.

Name: AYOBAMI TIMOTHY FOLARANMI

Date of Degree: MAY, 2015

Title of Study: GEOLOGIC CHARACTERIZATION OF A SALINE RESERVOIR FOR CARBON SEQUESTRATION: THE PALUXY FORMATION, CITRONELLE DOME, GULF OF MEXICO BASIN, ALABAMA

Major Field: GEOLOGY

ABSTRACT

The purpose of this study is to characterize a saline formation that is actively being used to store CO_2 as part of the SECARB III Anthropogenic test in Citronelle Field in southwest Alabama. The study is designed to understand the potential of the Paluxy Formation in Citronelle Field to store commercial quantities of anthropogenic CO_2. This entails detailed analysis of core data and geophysical logs from three recently drilled wells in the Southeast Citronelle Oil Unit. The field is developed in the crestal region of Citronelle Dome, which is a simple salt-cored anticline that lacks faults and contains abundant reservoir sandstone bodies and mudstone, evaporite, and carbonate seals.

The Paluxy has an average thickness of about 1,100 ft in Citronelle Dome. Sedimentologic analysis indicates that the Paluxy Formation was deposited in a fluvial environment that included bedload-dominated fluvial systems and interfluvial paleosols. The Paluxy Formation is a coarsening-upward, succession composed of numerous stacked, aggradational sandstone-mudstone packages. Individual sandstone bodies have sharp bases, typically fine upward, and range in thickness from less than 10 ft to more than 40 ft. Although some sandstone units have great lateral continuity, each well may have substantially different geophysical log signatures, reflecting internal reservoir heterogeneity among wells.

Analysis of cores and geophysical logs was performed to determine framework sandstone composition, sandstone diagenesis, and reservoir architecture. Results show that the sandstone units are predominantly arkosic. Porosity and permeability are well-developed in the sandstone especially in the Upper Paluxy, where average porosity and permeability values are 19 percent and 200 mD respectively. Intergranular pores predominate, and intragranular pores are common within feldspar grains. Quartz is the most abundant authigenic cement and is expressed primarily as overgrowths; pore-filling calcite and ferroan dolomite also are common. Authigenic clay includes grain-coating illite and pore-filling kaolinite. An understanding of reservoir composition and the formative depositional and diagenetic factors will provide a predictive framework to help facilitate field-scale commercialization of anthropogenic CO_2 storage.

TABLE OF CONTENTS

LIST OF FIGURES

Figure Page

LIST OF PLATES

CHAPTER I

INTRODUCTION

Purpose

This study is a critical analysis of the geologic data acquired from the Southeastern Regional Carbon Sequestration Partnership (SECARB) Phase III Anthropogenic Test and help define a pathway towards commercial field-scale storage of anthropogenic CO_2. The primary purpose of this study is to characterize siliciclastic strata of the Paluxy Formation, which is a saline formation constituting the injection target for the Phase III Anthropogenic Test in Alabama (Figure 1). This test was led by the Southeastern Regional Carbon Sequestration Partnership (SECARB) under the sponsorship of the U.S. Department of Energy. This test applied an integrated approach to geologic CO_2 storage in which (1) a CO_2 capture plant was built at a major coal-fired power plant, and (2) CO_2 was separated from flue gas and piped about 12 miles to the Citronelle Oil Field, where (3) a cumulative mass of about 150,000 tons of CO_2 was injected into the subsurface and stored in Cretaceous-age sandstone of the Paluxy Formation. A broad range of techniques were used to characterize Paluxy CO_2 sinks, including core description, facies analysis, sandstone petrology, petrophysical well log and core analysis. The results were synthesized into a larger analysis of reservoir

heterogeneity and seal continuity that helps define the way forward for field-scale deployment of CO_2 storage technology in the Paluxy Formation in Citronelle Field.

Core description and facies analysis were used to interpret depositional processes, paleoenvironments, and reservoir architecture. Petrologic and well log analysis were performed to analyze framework sandstone composition, sandstone diagenesis, and reservoir properties. Sandstone body geometry and seal continuity were analyzed through stratigraphic analysis and subsurface mapping in order to understand reservoir heterogeneity and develop a viable geologic storage strategy for Citronelle Dome.

Project Summary

Carbon capture and storage (CCS) has been identified as a critical technology for mitigating the large quantities of CO_2 emitted to the atmosphere from coal-fired power plants (Esposito et al., 2011). The United States Department of Energy (DOE) has sought to validate the feasibility of injecting, storing, and monitoring CO_2 in the subsurface by establishing seven Regional Carbon Sequestration Partnerships (RCSPs) (NETL, 2012).

The SECARB Anthropogenic Test is a landmark study because it is the only storage test performed by the RCSPs that integrates the separation, capture, transportation, and subsurface storage of CO_2 from a coal-fired power facility (Koperna, 2012). More than 150,000 metric tonnes of CO_2 has been sequestered to date, and operations are now nearing completion. The Anthropogenic test has yielded a wealth of information on geologic storage operations, and the next step is to define the pathway toward larger scale, commercial operations in the Citronelle area. Geological

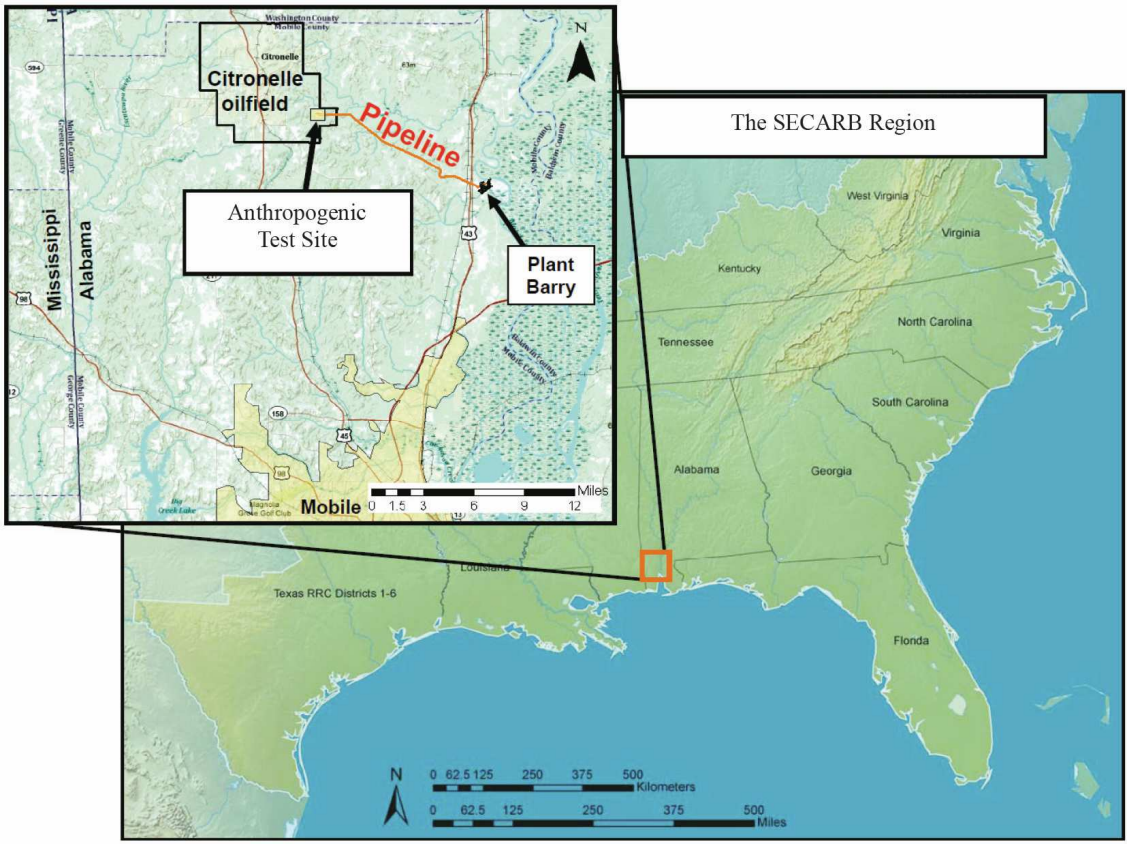

Figure 1. General location map of Plant Barry and the SECARB injection site in Citronelle Field (after Koperna et al., 2012).

characterization is a basic need for defining this pathway because it helps identify injection targets and seals, supports reservoir modeling, guides operations, and helps ensure that long-term geological storage is safe and effective. This thesis research is funded by Advanced Resources International (ARI) through grants from the U.S. Department of Energy (DOE) and Southern Company and is part of a larger initiative designed to evaluate the potential for commercial deployment of carbon sequestration technology in the Citronelle area.

The James M. Barry Electric Generating Plant, which is operated by Alabama Power Company, is a major coal-fired power plant that is located along the eastern margin of the Mississippi Interior Salt Basin in southwest Alabama. The power plant is in

an area of active oil and gas production, and the plant hosts a pilot facility for the capture, separation, and pipeline transport of CO_2. The nameplate capacity of the coal-fired unit at Plant Barry is 750 megawatts (Mw). The pilot plant processes a slipstream of flue gas equivalent to 25 Mw, which is equivalent to 3.3 percent of the CO_2 generated by the coal-fired unit. The capture plant has the capacity to generate about 500 tonnes of CO_2 per day, and achieving a goal of zero CO_2 emissions would require a large capture plant with capacity of about 15,000 tonnes per day. The CO_2 is being transported to the Citronelle Oil Field, which has the potential to store more than a century's worth of greenhouse gas emissions (Esposito et al., 2007, 2010). In the SECARB Anthropogenic Test, CO_2 from Plant Barry is being injected into saline reservoirs of the Paluxy Formation in Citronelle Field, which contains stacked sandstone bodies with complex geometry and internal heterogeneity.

Citronelle Field

The Citronelle oil field was discovered in 1955 by the Zack Brooks Drilling Company in Mobile County, Alabama. It is located approximately 30 miles north of Mobile County, Alabama. The discovery well, the Brooks Donovan No. 1 (SW¼, NW¼, Sec. 25, T. 2 N., R. 3 W.), was drilled to a total depth of 11,517 ft and produced oil from the Lower Cretaceous Donovan sandstone at a total depth of 10,879 ft (Eaves, 1976).

Citronelle is the largest oil field in Alabama (Esposito et al., 2010). The field is in the crestal region of an anticlinal structure called Citronelle Dome and has produced more than 173 million barrels of 42-46° API gravity oil from Donovan sandstone (Esposito et al., 2008; Pashin et al., 2014).

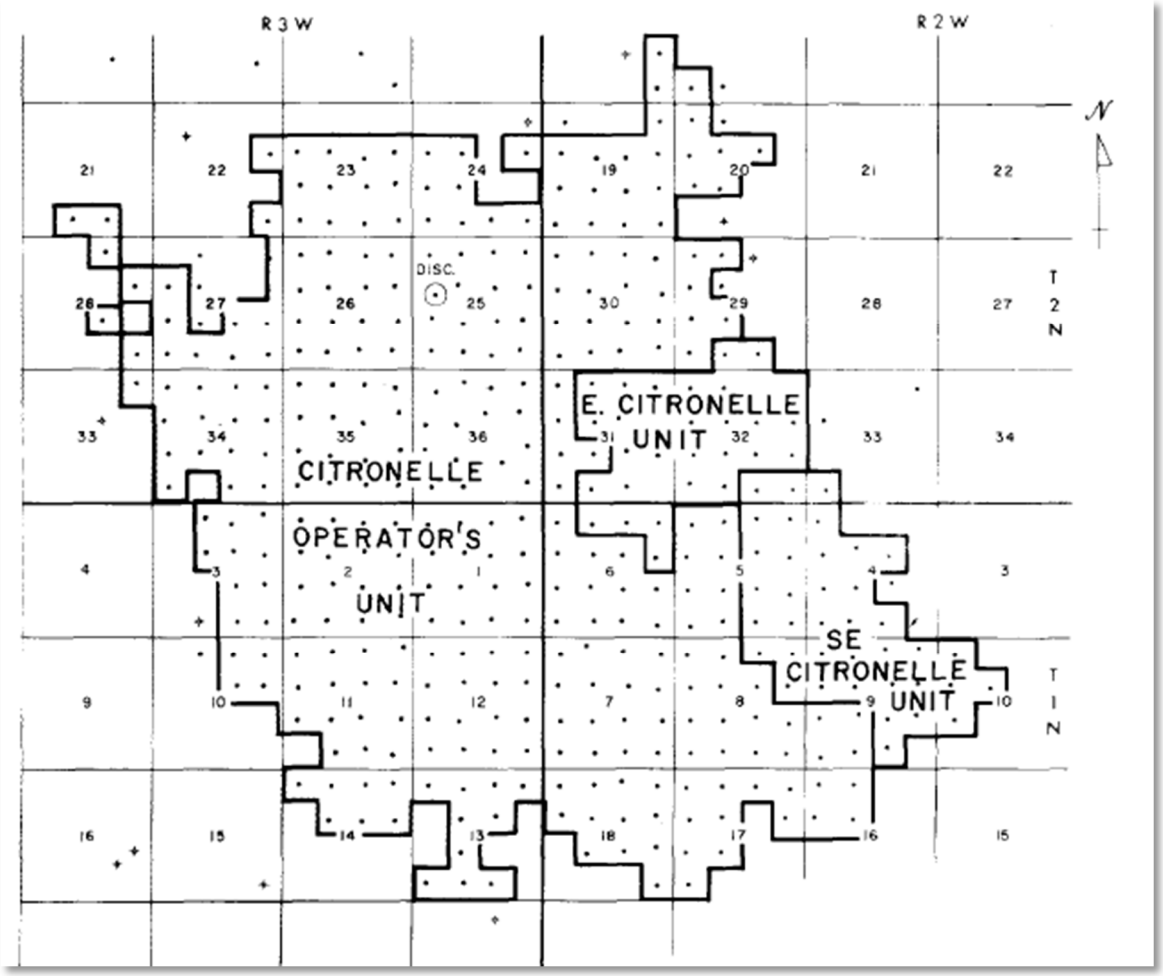

Figure 2. Map showing extent of the Citronelle Field and its unitized areas (after Eaves, 1977).

As of June 2014, 524 wells had been drilled in the field, with 506 wells listed as active or temporarily abandoned by the State Oil and Gas Board of Alabama. Unitization of the field for waterflood started in 1961 and proved successful. By May 1966, all wells in the field were unitized (Figure 2; Eaves, 1976).

This field is a favorable site for carbon sequestration for several reasons:

1. The field is within 10 miles of a coal-fired power plant that emits about 10 million tons of CO_2 per year (Esposito et al., 2010).
2. It contains stacked porous and permeable sandstone bodies that lack faults (Esposito et al., 2008, 2010; Pashin et al., 2014).
3. Multiple regional seals are present, including anhydrite, mudstone, and chalk (Esposito et al., 2008; Pashin et al., 2014).
4. Citronelle is a mature field with a well-documented history of commercial waterflooding, pilot CO_2-enhanced recovery operations (Gilchrist, 1981, 1982), and well-developed infrastructure for tertiary recovery of hydrocarbons and carbon storage (Esposito et al., 2010; Pashin et al. 2014).

Sandstone bodies containing saline water in this field are highly heterogeneous and require extensive geologic characterization in order to predict the outcome of carbon sequestration operations (Esposito et al., 2010). The total static storage capacity of the Citronelle Field is estimated by Esposito et al. (2010) to be between 500 million and 2 billion tonnes of CO_2 and this estimate did not include the Paluxy Formation or the Washita-Fredericksburg Group, which have additional capacity exceeding 1 Gt (Pashin et al., 2008). Based on these estimates, the Citronelle Dome has capacity to store more than century of emissions from all major power plants in the region.

CHAPTER II

GEOLOGIC SETTING

Overview of the Geologic Setting of the Mississippi Interior Salt Basin

Citronelle Field is in the Mississippi Interior Salt Basin (Figure 3), which is an onshore sub-basin of the Gulf of Mexico sedimentary basin. In the Citronelle area, the Mississippi Interior Salt Basin contains a succession of Mesozoic and Cenozoic strata that is commonly between 12,000 and 20,000 ft thick (Pashin et al., 2014). These strata accumulated as part of the passive margin succession along the northern rim of the Gulf of Mexico. The sedimentary fill of the salt basin unconformably overlies basement strata of the Paleozoic-age Appalachian-Ouachita orogenic belt and Triassic grabens that formed during Pangaean rifting (Pashin et al., 2014).

The mid Jurassic Louann Salt unconformably overlies basement. This unconformity apparently marks the transition from active rifting during Triassic time to passive margin development associated with the opening of the Atlantic Ocean and the Gulf of Mexico, which began during the Jurassic (Withjack et al., 1998). Above the Louann Salt is a thick Jurassic section that consists primarily of sandstone, carbonate, and evaporite. Early Cretaceous strata in the Citronelle area are thicker than 6,000 ft; they are dominated by siliciclastic redbeds containing thin carbonate and evaporite intervals. Late

Cretaceous and Tertiary strata in the Citronelle area include sandstone, mudstone, chalk, and limestone, and are about 7,200 ft thick (Pashin et al., 2014).

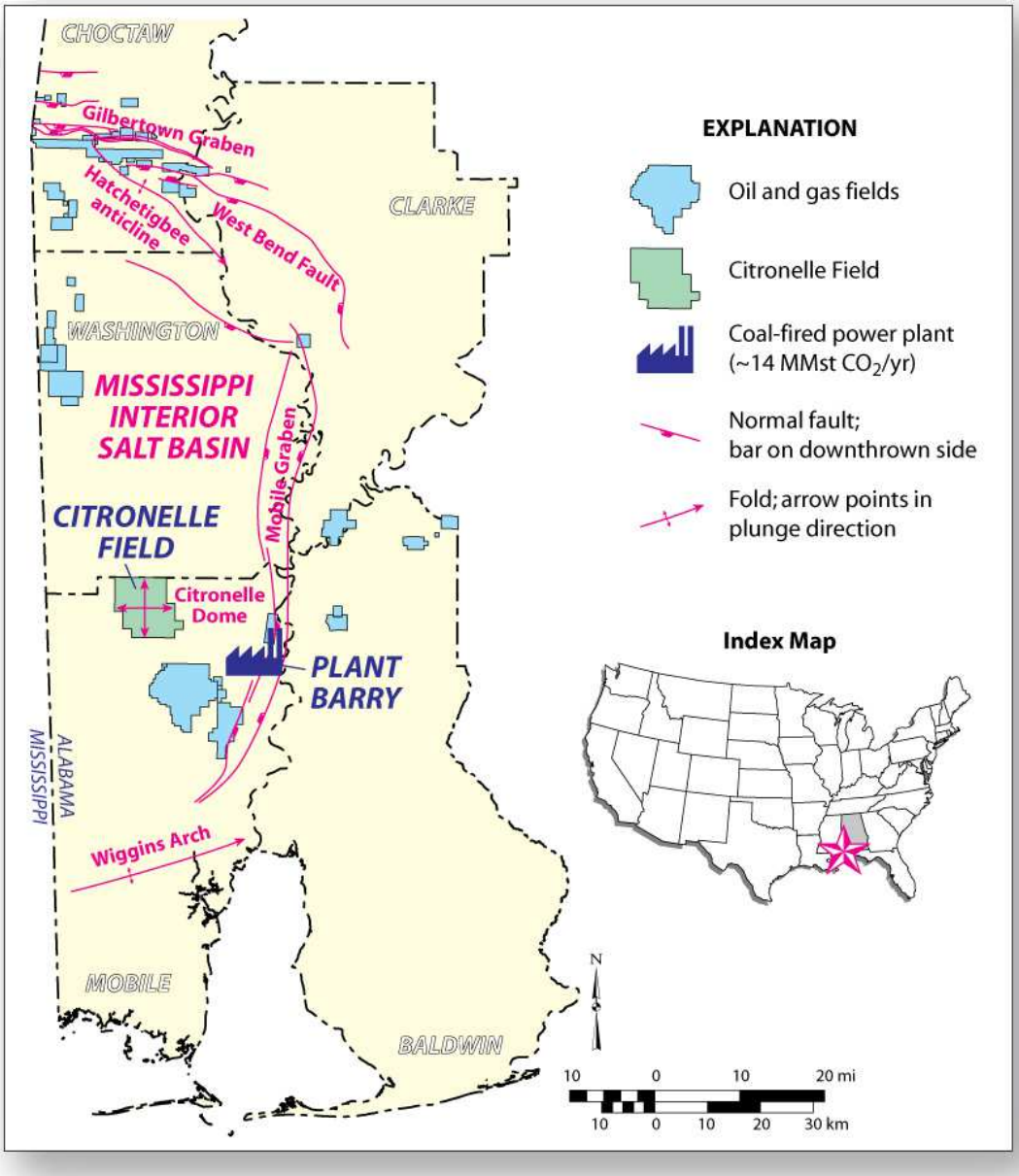

Figure 3. Map showing location of Plant Barry and the Citronelle Oil Field in the Mississippi Interior salt basin in southwest Alabama (after Pashin et al., 2014).

Stratigraphic Framework

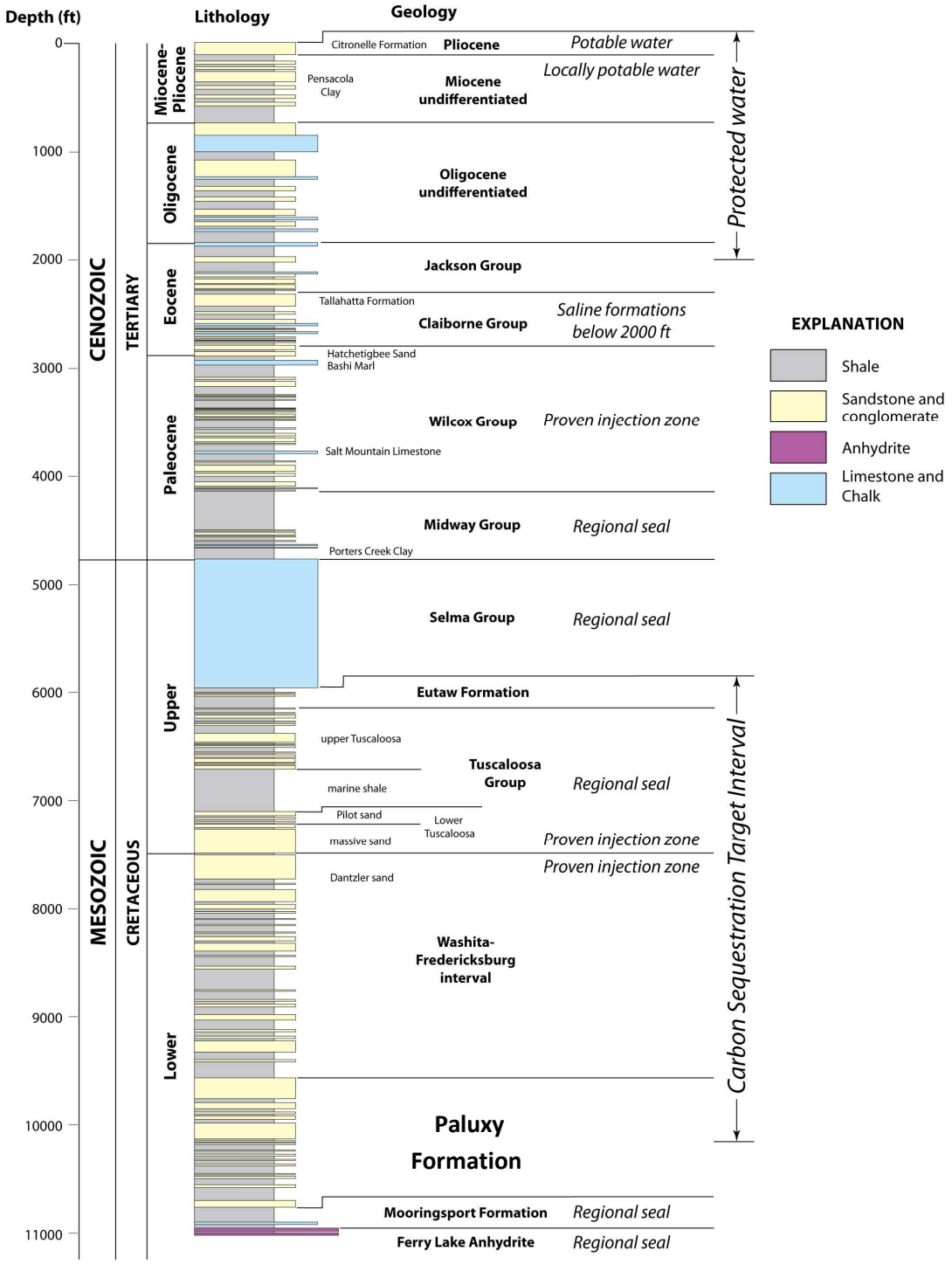

Figure 4. Stratigraphic column showing saline reservoirs, seals, and underground sources of drinking water (modified from Pashin et al., 2008).

Figure 4 shows the basic stratigraphic section from the Lower Cretaceous Ferry Lake Anhydrite to the surface, including the distribution of saline formations, sealing strata, and underground sources of drinking water in Mobile County, Alabama. The Ferry Lake Anhydrite is about 50 ft thick in Citronelle Field and consists of two anhydrite beds separated by shale that can be correlated throughout the field. It is one of the most distinctive lithostratigraphic units in the Gulf Coastal Plain and is widely used for regional correlation (Mancini and Puckett, 2002). It serves as the primary seal for the Donovan oil reservoirs in the Citronelle Dome (Esposito et al., 2008).

The Mooringsport Formation is about 240 ft thick in the Citronelle Field (Pashin et al., 2014). It is composed primarily of variegated shale, limestone, and fine-grained sandstone (Mancini and Puckett, 2002). The Paluxy Formation, which constitutes the injection target for the SECARB Anthropogenic Test, occurs at a depth of about 9,400 ft in the Southeast Citronelle Oil Unit. It is an overall coarsening-upward succession of variegated shale and sandstone.

Above the Paluxy Formation is the Washita-Fredericksburg interval, a net coarsening-upward succession composed of variegated shale and sandstone (e.g., Mancini and Puckett, 2005). The basal shale of the Washita-Fredericksburg appears to be continuous, and has an average thickness of 150 ft in the Southeast Oil Unit. It is considered the confining zone for the SECARB Phase III CO_2 injection test (Koperna et al., 2012).

The Upper Cretaceous Tuscaloosa Group disconformably overlies the Lower Cretaceous Washita-Fredericksburg Interval. It is about 1,500 ft thick in the Citronelle Field. It is subdivided into Lower, Marine (middle) and Upper Tuscaloosa Group. The

Lower Tuscaloosa Group is subdivided informally into the Massive sand and Pilot sand. The Pilot sand contains significant oil in southwest Alabama. It is overlain by the so-called marine Tuscaloosa, which is a regionally extensive shale unit that serves as a topseal for the Lower Tuscaloosa oil reservoirs. The marine Tuscaloosa shale also serves as a secondary regional seal for the CO_2 injection test. The shale coarsens upward into the interbedded shale and sandstone of the upper Tuscaloosa Group. The Massive sand and upper Tuscaloosa have been identified as attractive saline formations for the storage of CO_2 (Esposito et al., 2008).

The Eutaw Formation overlies the Tuscaloosa Group and is about 150 ft thick in the injection area. It is primarily composed of shale and glauconitic sandstone. It has also been identified as a target for CO_2 storage. The Eutaw Formation is overlain by about 1,200 ft of chalk which is assigned to the Selma Group. The Selma Group acts as the topseal for Eutaw reservoirs and saline formations for CO_2 storage (Pashin et al., 2000). It also separates the oil reservoirs from underground sources of drinking water in the Tertiary section (Esposito et al., 2008).

The Midway Group is of Paleocene age and overlies the Selma Group. It is composed of the Clayton Formation, Porter's Creek Clay, and Naheola formations (in ascending order). It is about 800 ft thick in the Citronelle dome area and is composed of marl, limestone, sandstone, and shale. Porter's Creek Clay is a dark brown to black clay containing thin beds of fossilliferous limestone (Raymond et al., 1988). Along with the Selma Group, Porters Creek Clay forms a regionally extensive confining unit that seals fractured chalk reservoirs along faults at the margin of the Mississippi Interior Salt Basin (Pashin et al., 2000).

The Eocene Wilcox Group comprises, in ascending order, the Nanafalia Formation, Salt Mountain Limestone, Tuscahoma Sand, and Hatchetighee Formation. It is composed of sand, shale, marl, and limestone. It is about 2,000 ft thick in the area. The Eocene Claiborne Group is composed of the Tallahatta Formation, Lisbon Formation, and Gosport Sand. It is about 100 ft thick in the area. It is primarily composed of shale, limestone, and sandstone. The Upper Eocene Jackson Group is about 1,100 ft thick and is composed of marl and clay (Raymond et al., 1988). According to a report by CH2M Hill (1986), the deepest protected USDW in the Citronelle area is in the Jackson Group at a depth of about 1,200 ft.

Above the Eocene strata is a succession of Oligocene-age strata composed of limestone, clay, and sand. They are approximately 200 ft thick in the Citronelle area. Undifferentiated Miocene strata succeeds this strata and is about 100 ft thick in Citronelle Field. The Citronelle Formation forms the surface stratum in this area and is a major aquifer that forms the water supply for the city of Citronelle and for waterflood operations in Citronelle Field. The Citronelle Formation consists of deeply weathered red sand, fine quartz, chert pebble gravel, variegated clays (Raymond et al., 1988).

Structure and Tectonics

The Citronelle Dome is a giant, salt-cored anticline in the eastern Mississippi Interior Salt Basin of southern. The dome is a subtle fold with limbs dipping less than 3° (Figure 5). The fold is underlain by a broad pillow of Louann Salt, and the origin of the dome has long been understood to be a product of regional salt movement (Eaves, 1976, Cottingham, 1988). The Hatter's Pond fault is mapped southeast of Citronelle Field and underlies Plant Barry. The Hatter's Pond fault forms the western margin of the Mobile graben (Figures 5, 6, and 7). Leakage risks associated with the fault is the primary reason there is no storage opportunity at Plant Barry (Pashin et al., 2008).

The dome forms an elliptical, four-way structural closure (Pashin and Jin, 2004; Esposito et al., 2007; Pashin et al., 2008). A structural contour map of the base of the Ferry Lake Anhydrite demonstrates the structural simplicity of Citronelle Dome (Figure 6). The axial trace of the dome trends northwest, and the southwest flank is steeper than the northeast flank (Figure 6; Pashin et al., 2014). Figure 6 also shows that the anticline has more than 500 ft of four-way structural closure. The dense well spacing in the crestal region of the dome follows the general footprint of the oil accumulation (Pashin et al., 2014).

The saddle between the dome and a footwall uplift along the western boundary of the Mobile graben defines the spillpoint of the anticline (Pashin et al., 2014). The reservoir is under filled with oil such that the oil-water contact is about 200 ft above the structural spillpoint (Esposito et al., 2008). There are no regionally correlatable stratigraphic surfaces between the Ferry Lake Anhydrite and the top of the lower Tuscaloosa Group. Figure 7 shows a structural contour map of the top of the Lower

Tuscaloosa, which also is the base of the marine Tuscaloosa shale, which is an important regional seal. This seal sits about 2,400 ft above the Paluxy Formation. The area of the structural closure of the dome increases upward from 36 square miles in at the base of the Ferry Lake Anhydrite (Figure 6) to more than 72 square miles in the Tuscaloosa Group (Figure 7) (Esposito et al., 2008). Importantly, no faults are known in the Citronelle Dome, and so all of the regional seals in the section contribute positively to storage security.

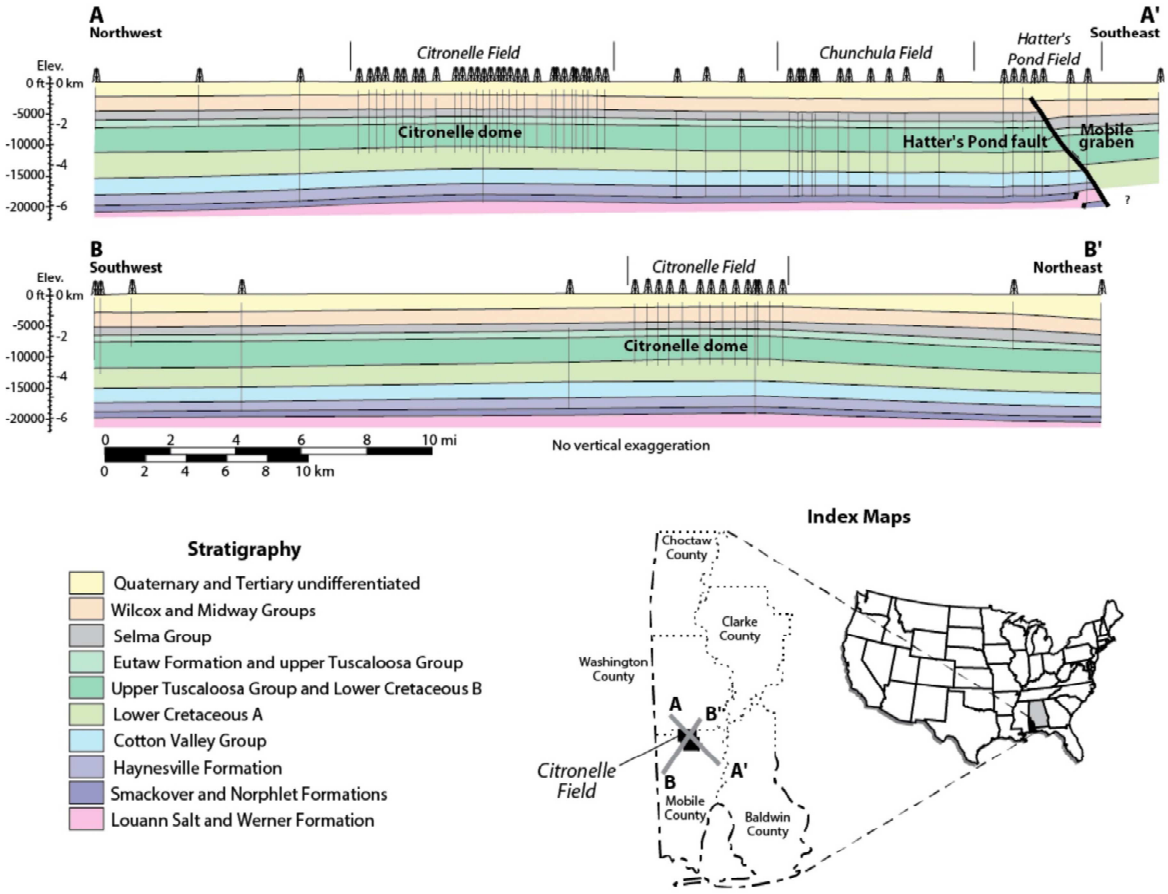

Figure 5. Structural cross sections of Citronelle dome showing location of Citronelle Field in the Lower Cretaceous section (Pashin and Jin, 2004).

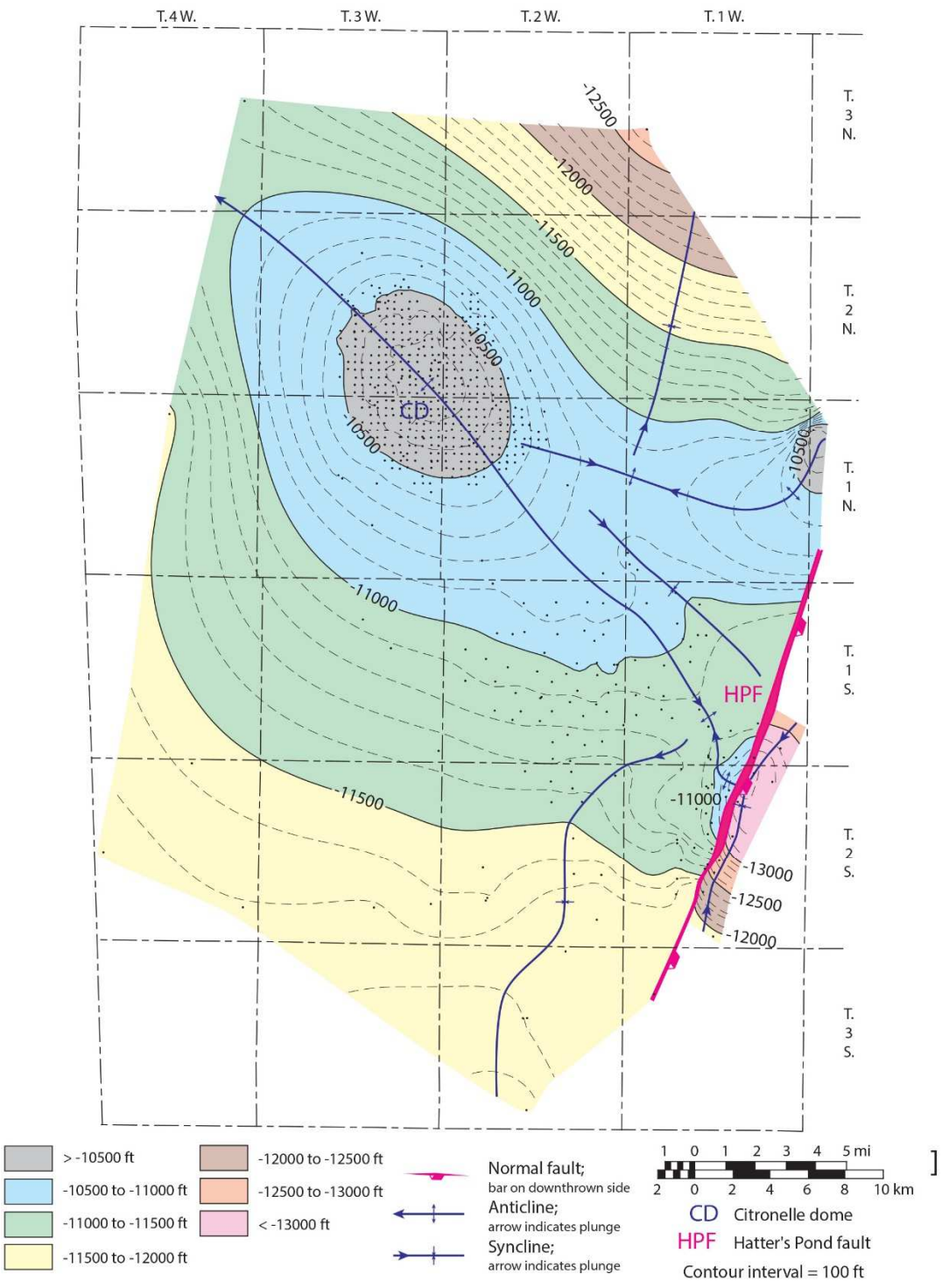

Figure 6. Structural contour map of the base of the Lower Cretaceous Ferry Lake Anhydrite showing areal geometry of the Citronelle dome in the Citronelle-Hatters Pond area, Mobile County, Alabama (modified from Pashin and Jin, 2004).

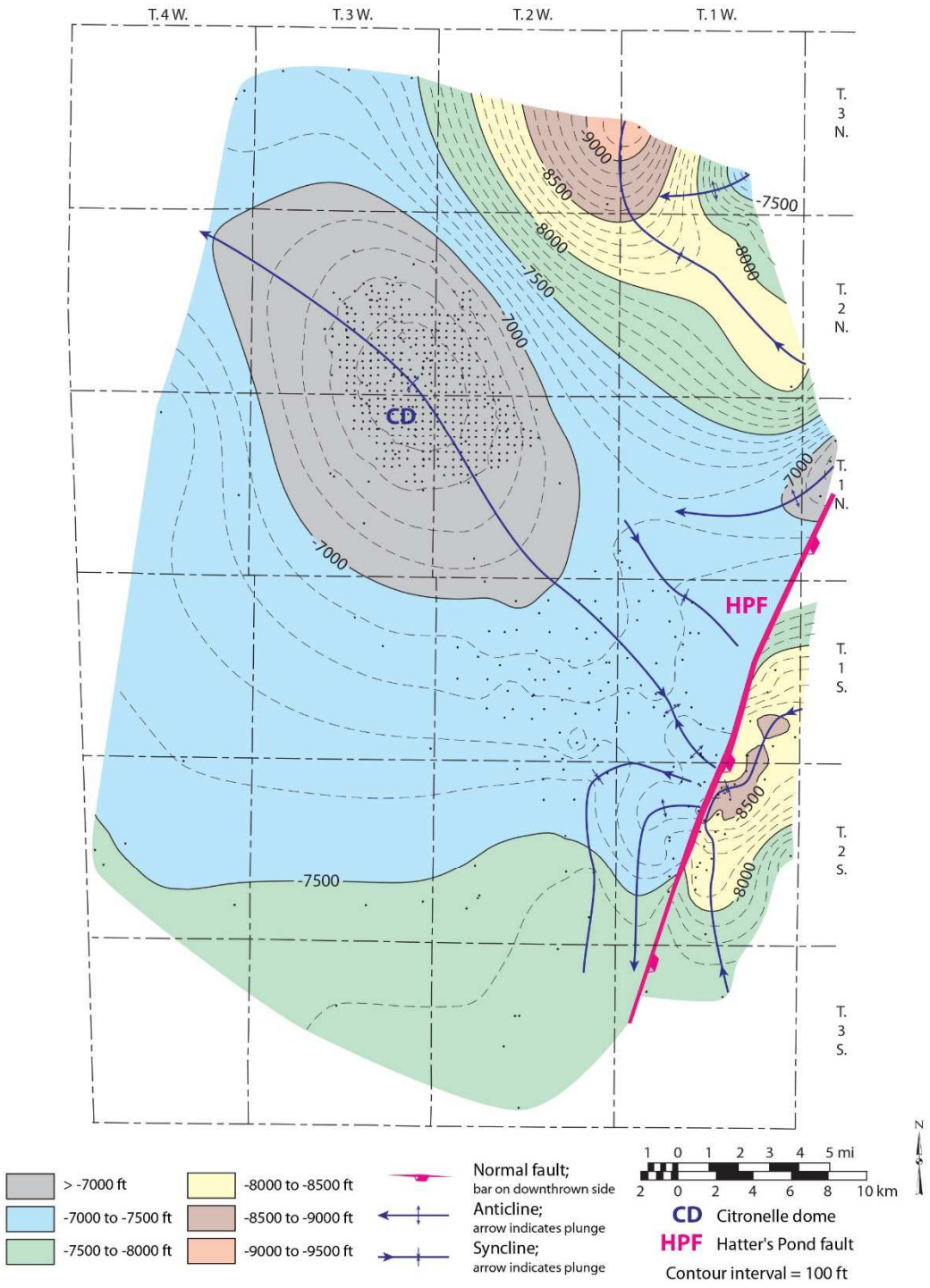

Figure 7. Structural contour map of the top of the Upper Cretaceous Lower Tuscaloosa Group in the Citronelle-Hatters Pond area, Mobile County, Alabama (modified from Pashin and Jin, 2004).

Paluxy Formation

The Paluxy Formation in Alabama has not been studied in detail. Mancini and Puckett (2002) provided a modern synthesis in their brief description of the Paluxy in the Mississippi Interior Salt Basin. In this area, they defined the Paluxy as the stratigraphic interval between the shale of the Mooringsport Formation and either the carbonate rocks of the Andrew Formation (basinward of Citronelle Field) or the interbedded sandstone and mudstone of the Fredericksburg Group (in updip areas, including Citronelle Field). The Andrew Formation and Fredericksburg Group are not defined in Alabama and have been mapped informally as the Washita-Fredericksburg interval (Pashin et al., 2008).

Figure 8 is a regional correlation chart. This chart shows that in Arkansas, the Paluxy Formation is a siliciclastic unit that overlies the Mooringsport Formation, while in Texas, it includes carbonate, overlies the Glen Rose Limestone, and is overlain by the Walnut Formation, which is the basal unit of the Fredericksburg Group (Hayward & Brown, 1967; Young, 1967). In Louisiana, the Paluxy Formation overlies the shale and limestone units of the Glen Rose Formation and is overlain by the siliciclastic and carbonate strata of the Fredericksburg Group (Yurewicz et al., 1993).

In the Mississippi Interior Salt Basin, the Paluxy Formation was originally described by Nunnally and Fowler (1954) as containing fine- to coarse-grained micaceous sandstone, including redbeds, interbedded with variegated shale. They further interpreted the Paluxy as fluvial, coastal, and shallow marine deposits. The Mooringsport-Paluxy contact was also thought to be gradational. Biostratigraphic data indicate that the Paluxy in the Mississisisipi Interior Salt Basin ranges in age from early to

middle Albian, spanning an interval of about 3 million years (Figure 8) (Mancini and Puckett, 2002).

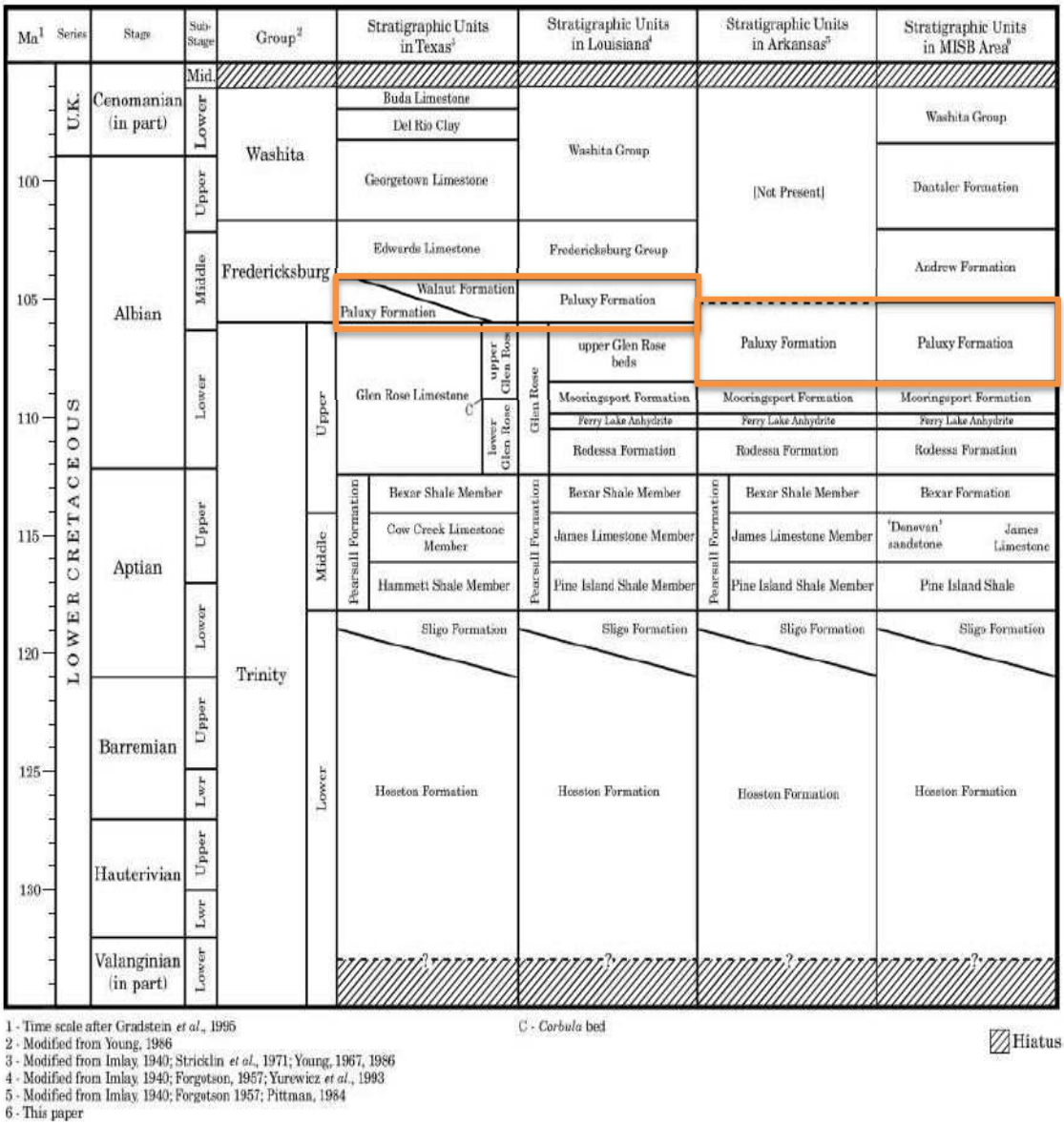

Figure 8. Absolute ages, chronostratigraphic units, and lithostratigraphic units of Lower Cretaceous strata in Texas, Louisiana, Arkansas and the Mississippi Interior Salt Basin area (Modified from Mancini et al., 2002).

CHAPTER III

METHODOLOGY

Core and Thin Section Dataset

Four cores were acquired from three recently drilled wells in the Southeast Citronelle Oil Unit. These wells are named D-9-7 #2, D-9-8 #2, and D-9-9 #2. The D-9-7 #2 was drilled as an injection well, whereas the other two were drilled as monitoring wells that could be converted to injectors should the need arise. Core was recovered from various intervals in the three wells. In well D-9-8 #2 core was recovered from the basal Paluxy sandstone units at depths of 10,430-10,465 ft and the upper part of the Paluxy at 9,400-9461 ft. One sandstone interval was cored in each of the other two wells and a depth of 9,568-9,636 ft in D-9-7 #2 and 9,404-9,448 ft in D-9-9 #2.

Cores were described using standard stratigraphic and sedimentologic techniques to define lithofacies and characterize the depositional framework. This was done by describing and graphically logging the cores to characterize rock types, bedding types, physical sedimentary structures, and biogenic sedimentary structures. Grain size was determined with a graphical comparator and hand lens, and color was determined using the Munsell soil color chart. Cores were photographed using a digital camera to document lithologic and paleontologic features. After logging and photographing the

cores, lithofacies were defined, and interpretations of depositional process and depositional environment were made on the basis of the modern and ancient analogs that have been documented in the geological literature. Standard petrographic thin sections were made from 37 core samples. All thin sections were impregnated with blue epoxy to help identify porosity. Ten thin sections were stained with Alizarin red S to identify calcite and with cobalt nitrite to identify potassium feldspar. Due to carcinogenic concerns associated with the use of sodium cobalt nitrite, only ten (10) thin sections were stained. The thin sections were examined for framework grain composition, size, fabric, and diagenesis, pore geometry, and pore fillings.

Sandstone composition was determined by using a grain count method; a modified Chayes method was used due to abundant porosity in most sandstone. An average of 400 point counts was made to get 300 grain counts in thin section samples. Proportions of various rock constituents and open pore space were calculated for each thin section. Standard ternary diagrams of detrital composition were used to classify the sandstone and evaluate provenance.

Core plug analysis was carried out by Core Lab using the CMS-300 conventional plug analysis protocol to determine porosity and permeability. Samples were prepared by drilling 1.5 inch diameter plugs with liquid nitrogen and trimming samples into right cylinders with a diamond-blade trim saw. Select samples were encapsulated in Teflon tape, nickel foil, and stainless steel screens. Core extraction was conducted by placing plugs in Soxhlet extraction cycling between a chloroform/methanol (87:13) azeotrope and methanol. Samples were oven dried at 240 °F to weight equilibrium (+/- 0.001 g). Porosity was determined using Boyle's Law technique by measuring grain volume at

ambient conditions and pore volume at indicated confining stresses (NCS). Grain density values were calculated by direct measurement of grain volume and weight on dried plug samples. Grain volume was measured by Boyle's Law technique. Permeability to air was measured on each sample using unsteady-state method at indicated NCS.

Geophysical Well Log Cross Sections

Electric logs in the Citronelle field were digitized using Petra software and Adobe Illustrator for correlation, and analysis. Formation tops were picked using SP and resistivity log curves by Advanced Resources International. Most wells were drilled between 1955 and 1965, and so vintage well logs constitute the vast majority of the available subsurface data. Because of this, the style of display among well logs was inconsistent, and it was difficult to identify and follow deep and shallow resistivity curves. Accordingly, efforts focused on digitizing and characterizing SP curves.

Spontaneous potential (SP) curves of 44 well logs were digitized for the construction of two stratigraphic cross sections that trend northwest to southeast (Plate 1) and west to east (Plate 2). These two stratigraphic cross sections were constructed to traverse the Citronelle Oil Field and intersect the wells drilled as part of the SECARB Phase III program.

The cross sections were constructed using the top of the Ferry Lake Anhydrite as a datum, which is the only stratigraphic marker that can be correlated regionally with confidence near the level of the Paluxy Formation. The top of the Ferry Lake Anhydrite was identified by a sharp increase in resistivity values (130-150 ohm-metres). Sandstone units were defined where the SP curve marks a negative deflection from the shale

baseline. By contrast, mudstone units were defined where the SP curve shows a positive deflection from the shale baseline.

X-Ray Diffraction

X-ray diffraction analysis was performed using a Phillips PW3020 computer automated X-ray diffractometer for qualitative mineralogical analysis of select powdered core samples. The goal was to help identify the dominant clay and framework minerals. The dominant framework grains were determined qualitatively by powdering samples to less than 0.01 mm using a ball mill. The powder was then placed onto slides, which were placed into the diffractometer for analysis

For identifying dominant clay minerals, pebble-sized (~50 mm) chips of select core samples were also crushed to powdered form (< 0.01 mm) and placed in individual plastic test tubes. Clay minerals were concentrated by dissolving carbonate in Na_2CO_3. After the sample stopped effervescing, the sample was washed repeatedly with distilled water to remove chemical impurities. The test tubes containing the samples were filled with water until they were two-thirds full. The tubes were then placed in a centrifuge, and thin films of clay were allowed to accumulate at the top of the water column. The clay was removed from each test tube by pipette and smeared onto slides for XRD analysis. Minerals were identified by their distinct peaks after plotting raw data acquired from XRD machine on a crossplot of 2Θ versus counts.

Scanning Electron Microscopy

A FEI Quanta 600 field-emission gun Environmental Scanning Electron Microscope (SEM) was used to examine select samples from the cores. Core chips were mounted on stubs and were then coated with carbon to achieve the best images of samples under the SEM machine. Samples were scanned to examine the surface morphology of broken rock surfaces, particularly the surfaces of pores that reveal grain and crystal morphology. Photographs were then taken using the SEM digital camera system illustrate morphology of mineral grains and cement.

CHAPTER IV

LITHOFACIES AND DEPOSITIONAL ENVIRONMENTS

Three major lithofacies were identified within the Paluxy formation based upon rock type. These are (1) the conglomerate facies, (2) the sandstone facies, and (3) the mudstone facies. In this section, each lithofacies is describe in terms of rock type, color, composition, grain size and shape, physical sedimentary structures, and biogenic structures.

Conglomerate Facies

Characteristics

The conglomerate facies is characterized by red and gray colored, sub-angular to sub-rounded granules to cobble sized clasts of mudstone and carbonate origin within a sandstone matrix (Figure 9). Rock types include intraclastic conglomerate (Figures 10B and 11) and conglomeratic sandstone (Figure 10A). Clasts range in size from granules to cobbles; pebbles are the predominant clast size. Clasts are typically sub-angular to sub-rounded, and the conglomerate is typically clast-supported within a fine- to coarse-grained sandstone matrix. Clasts that have a gray to brownish-gray color are most common within a calcite cemented sandstone matrix; the calcite cement gives the sandstone matrix a pale color (Figures 10C and 11). Reddish-brown to very dusky red

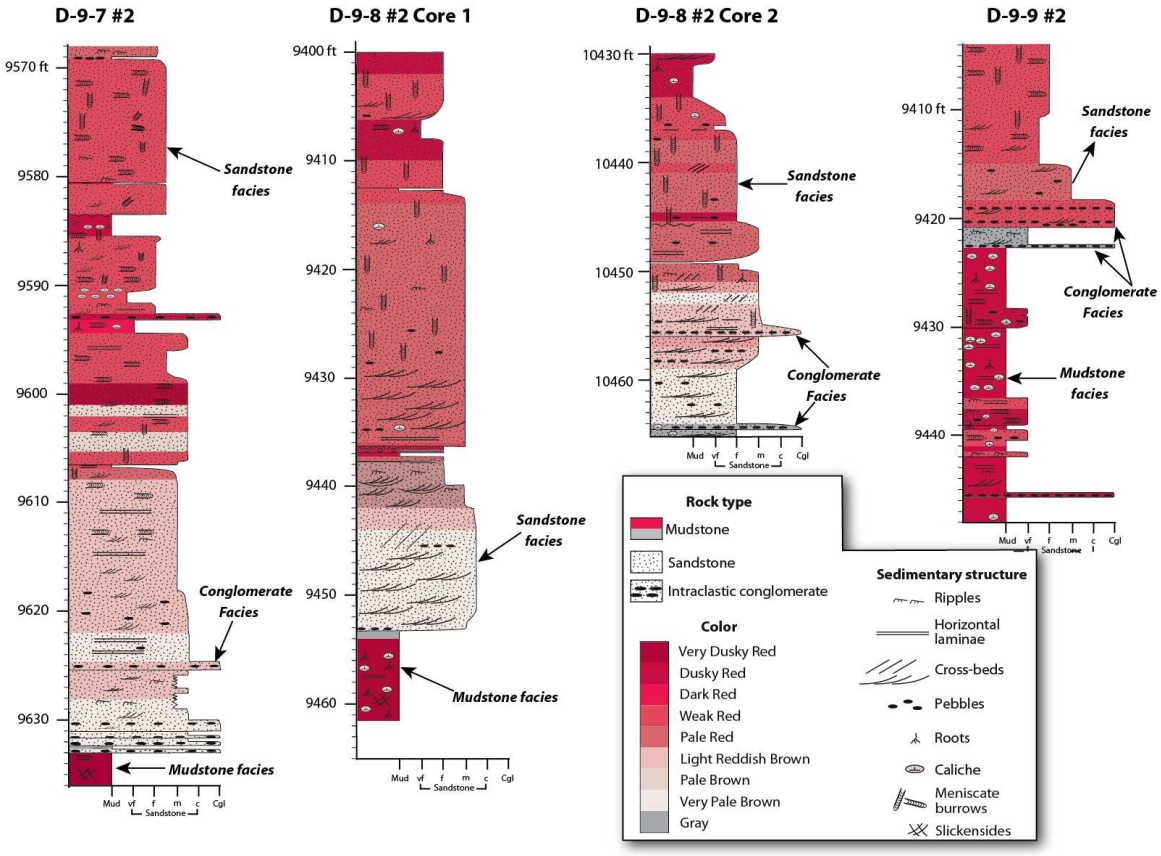

Figure 9. Graphical core logs showing major lithofacies, rock types, color variations, sedimentary and biogenic structures, and common vertical successions in the Paluxy Formation.

clasts tend to be in sandstone matrix where calcite cementation is less pervasive (Figures 10A and B).

Types of clasts include argillaceous mudstone (Figures 10 and 11) and dolomitic mudstone (Figure 11). Most of the clasts are either clay-coated or are composed of mud. In many cases, clay coats have faded or bleached rims. Thickness of conglomeratic beds varies from less than 1 foot to more than 3 ft. The beds have sharp bases and are commonly present at or near the base of sandstone units (Figures 10C and 12). The upper part of the conglomeratic units, by contrast, have sharp to gradational contacts (Figures 10 and 12).

Argillaceous mudstone clasts are typically platy and poorly sorted (Figures 10 and 11). The mudstone is silty and sandy, and clasts tend to be randomly distributed. Color is typically red; gray clasts are also common (Figure 10C and Figure 11). Sandstone matrix is commonly calcareous and can contain reworked caliche clasts probably derived from soil (Figure 10B).

Dolomitic mudstone clasts are sub-spherical and moderately well sorted (Figure 11). The clasts typically have grayish hues (Figures 10 C and 11). This facies is predominantly clast-supported and the matrix consists of calcite-cemented sandstone. The matrix is typically fine to medium grained sandstone and for the most part is light gray in color. The clasts are commonly coated with clay, and many have faded or bleached rims. Calcite-filled septaria are commonly found within some of these clasts (Figure 11).

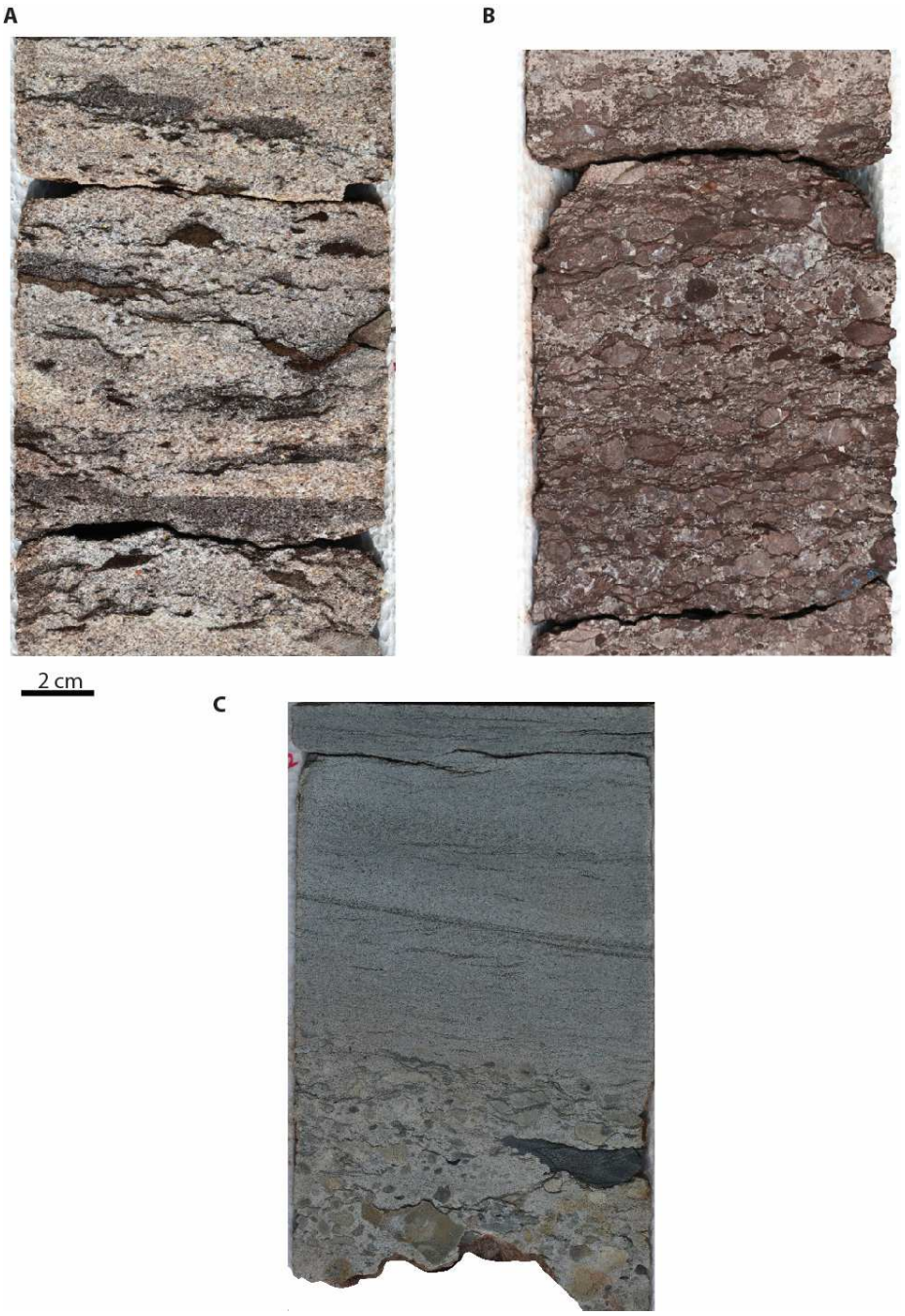

Figure 10. Photographs of slabbed core from the conglomerate facies. A) Conglomeratic sandstone; platy shale intraclasts in sandstone matrix, Well D-9-7 #2, 9,624.5 ft. B) Clast-supported conglomerate containing clay-coated caliche clasts, Well D-9-9 #2, 9,419 ft. C) Argillaceous and dolomitic mudstone clasts at the base of a siltstone layer, Well D-9-9 #2, 9,422 ft.

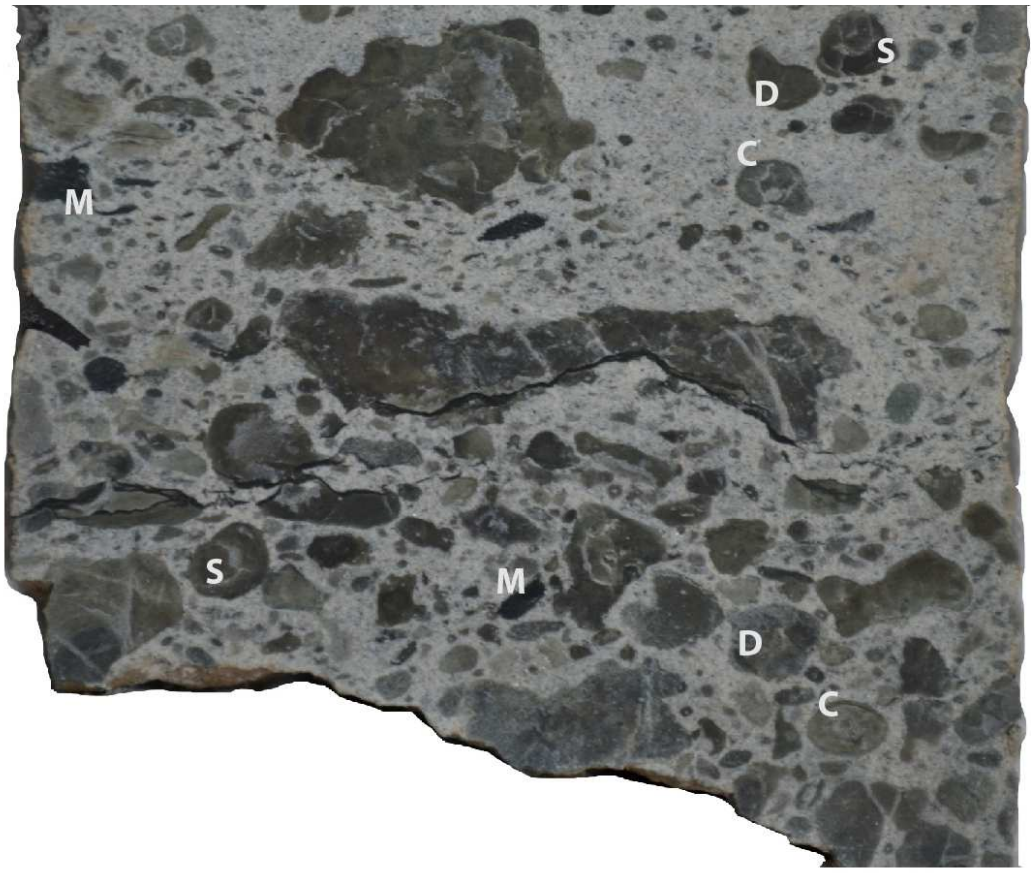

Figure 11. Conglomerate containing dolomitic and argillaceous mudstone clasts.

Figure 12. Photograph of slabbed core showing sharp basal contact and a sharp to gradational upper contact of conglomeratic beds.

Interpretation

The size, shape, and composition of the clasts in the conglomerate facies suggests that they were derived by reworking of nearby sediment. The sharp bases of the conglomerate layers provide evidence of erosion (Figure 12). The position at the base of the sandstone units suggests deposition by currents in channels. Platy mudstone clasts were most likely derived by simple erosion of the mudstone units that underlie the conglomerate and sandstone layers. Cant and Walker (1976) observed mudstone intraclasts in the Devonan Battery Point Sandstone and suggested that these intraclast lag was deposited as a result of channel development that began by scouring. Scouring may be related to strong separation eddies in the lee of advancing dunes or to local vortices developed around obstructions (Miall, 1977).

Clay coatings on the lithoclasts (Figures 10 and 11) may have multiple origins. Some may be relict clay coatings that formed as argillans in ancient soil profiles (Retallack, 2001; Pittman et al., 1992), whereas others may have formed by rolling and armoring in mud. Mud-armored clasts form where pebbles roll down muddy slopes or are rolled through mud by currents, such as river currents (Hall et al., 1984).

Imbricated platy clasts and clast clusters are commonly found in this facies (Figures 10C, 11, and 12A). A similar orientation of pebble sized clasts was observed by Bridge and Lunt (2005) in the Sagavanirktok River on the North Slope of Alaska. Miall (1977) also found clasts within the pebble range (2-64 mm) to be commonly imbricated. Cross stratification also was observed in the conglomeratic sandstone and conglomerate (Figures 10 A and C).

Cross-bedding in the conglomerate and conglomeratic sandstone indicates formation of dunes by turbulent flow and accumulation of clasts near the toes of the structures. Although localized mudstone cobble clasts were observed (Figure 12B), its rare occurrence suggests a possible infrequent occurrence of a flooding stage.

Sandstone Facies

Characteristics

The sandstone facies constitutes all sandstone units in the Paluxy Formation thicker than 4 ft and includes the reservoir sandstone units that have been used and are prospective for CO_2 injection. The sandstone is very fine- to coarse-grained and contains a variety of sedimentary and biogenic structures (Figure 9). The Paluxy sandstone bodies typically fine upward and have gradational to sharp bases (Figure 9). Sedimentary structures include cross-beds, horizontal laminae, and climbing ripples, while biogenic structures are primarily burrows and plant debris. Paluxy sandstone ranges in color from gray to very dusky red. The sandstone typically exhibits deep color, although pale pink to gray colors are common in the coarser-grained units near the base of the sandstone bodies.

Thickness of sandstone beds ranges from about 4 to more than 40 ft. Cross-bedding includes planar and tangential forms (Figures 13B and C), and bedsets are typically 0.5 to 2 ft thick and form cosets locally approaching 10 ft in thickness.

Horizontal laminae also are common in this facies (Figure 13A). Convolute bedding is present locally (Figure 13D). Some of the cross-beds have mica-draped foresets (Figure 13B). Micaceous partings are common, as are local layers of mudstone chips (≤ 1 ft). These chips are preserved as isolated clasts or in solitary laminae (Figure 9). Current ripple cross-laminae are common in very fine- to medium-grained sandstone, and rippled intervals are typically thinner than 2 ft.

Ripple forms are varied and include trough-shaped laminasets characteristic of lunate, linguoid, and cuspate ripples and planar laminasets indicative of straight- to sinuous-crested ripples (Figures 14A and B). Climbing ripples with uniform orientation were observed in some intervals (Figures 14A and B).

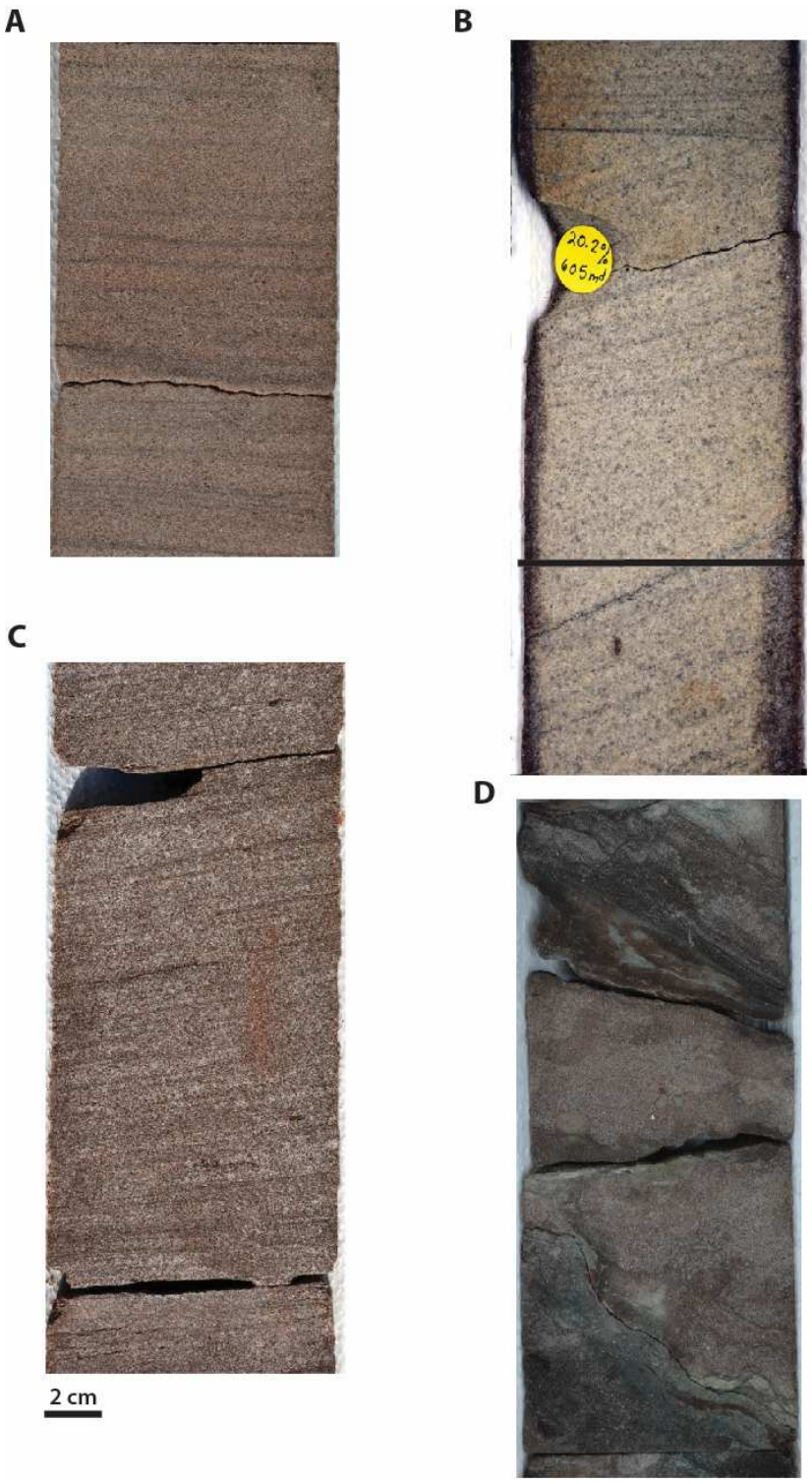

Figure 13. Photographs of slabbed core from the sandstone facies. A) Horizontally laminated sandstone containing faint micaceous laminae, Well D-9-7, 9,614 ft. B) Planar cross-beddded sandstone, Well D-9-8 #2, 9,449 ft. C) Tangential cross-bedded sandstone, Well D-9-7 #2, 9,582 ft. D) Fine grained sandstone with convoluted beds, D-9-8 #2, 9,436 ft.

Burrows as large as 0.5 inch in diameter are abundant in the upper parts of the sandstone bodies. Intense burrowing typically gives the sandstone a mottled texture in which it is difficult to identify the types of ichnofossils that are present (Figure 15B). Where internal structure can be distinguished, the burrows are meniscate. A few ichnofossils are identifiable, such as a vertical branching burrow is about 0.5 ft long (Figure 15A).

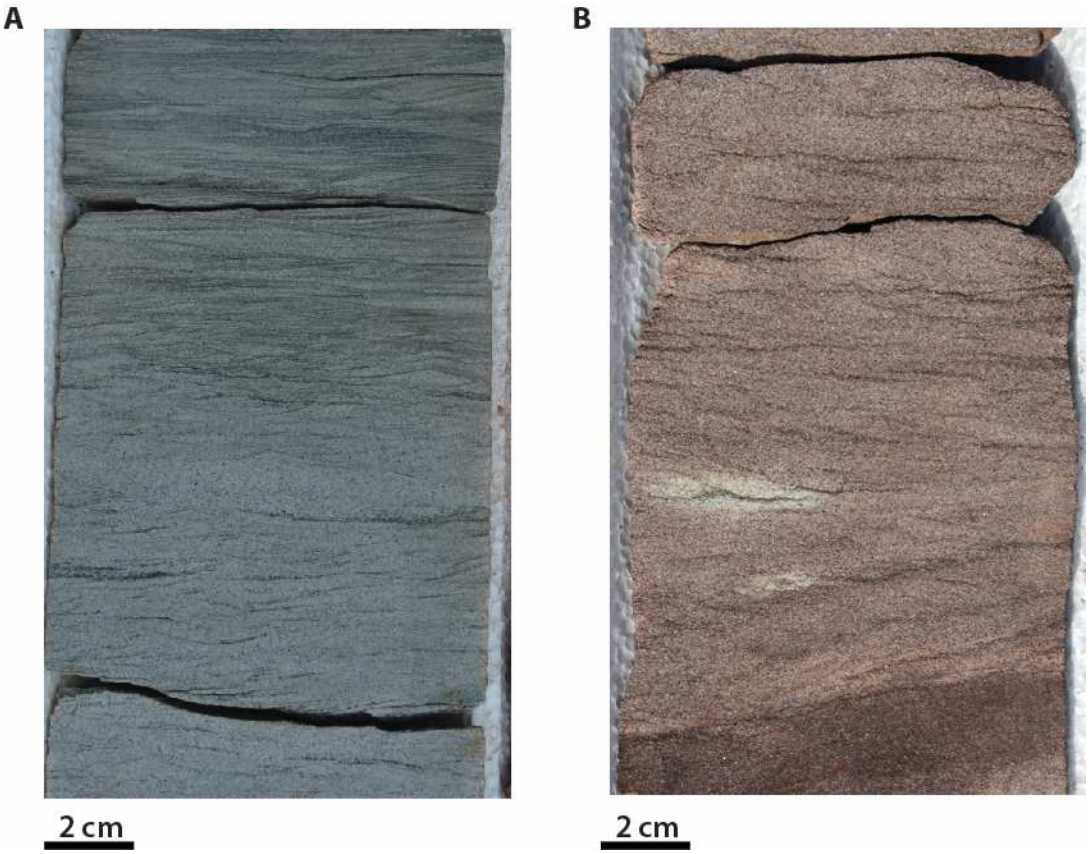

Figure 14. Photographs of slabbed core from the sandstone facies. A) Vey fine-grained sandstone with ripple foresets draped with mica and organic matter, Well D-9-9 #2, 9,422 ft. B) Fine-grained sandstone with climbing ripples, Well D-9-7 #2, 9,568 ft.

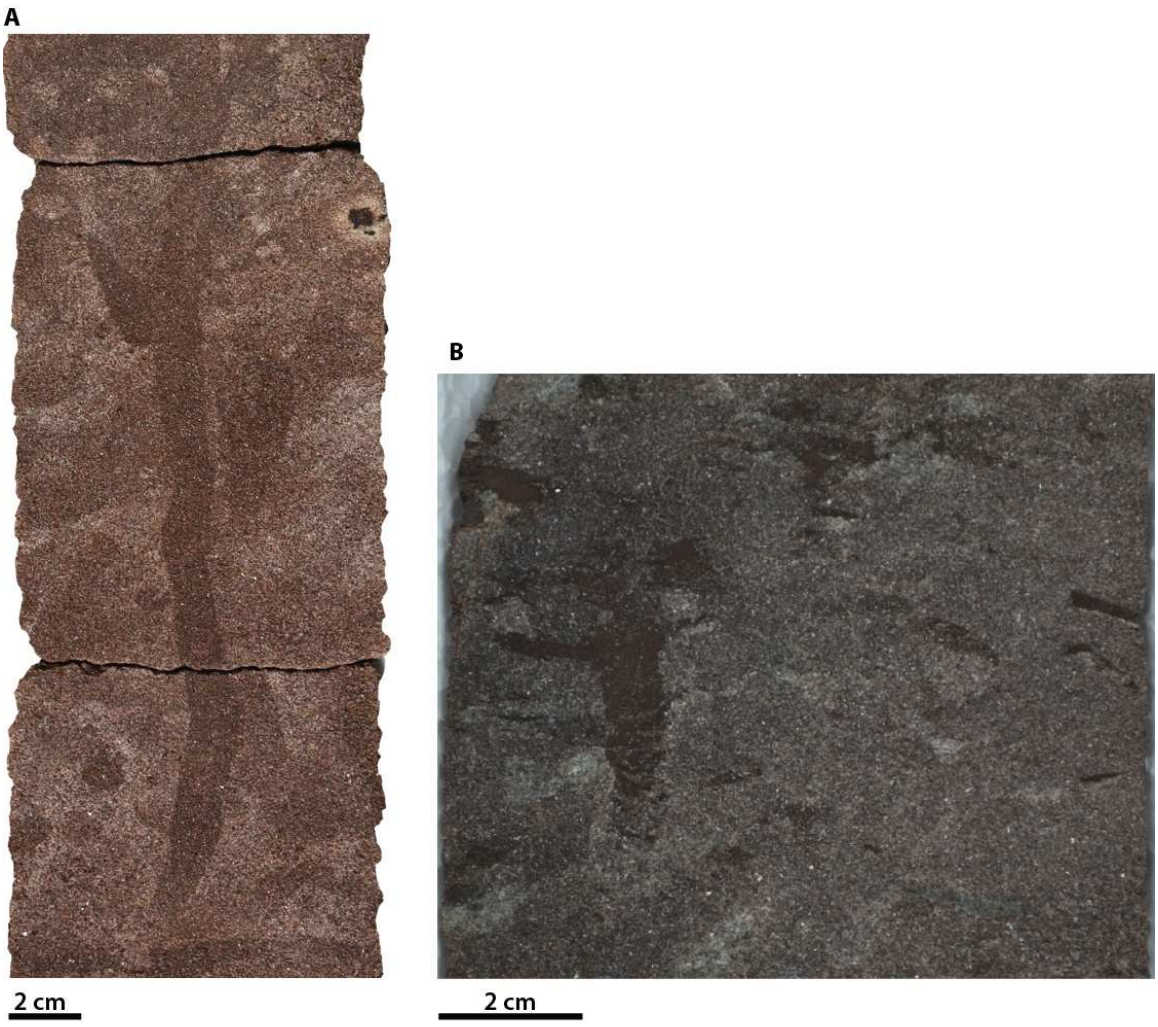

Figure 15. Photographs of slabbed core showing bioturbation in the sandstone facies. A) Sandstone containing meniscate burrows, including a long, branching vertical burrow, *Naktodemasis bownni*, Well D-9-7 #2, 9,570 ft. B) Sandstone mottled with abundant adhesive meniscate burrows, Well D-9-8 #2, 10,437 ft.

Interpretation

The sandstone facies has many characteristics of sandy, bedload-dominated fluvial deposits. The overall vertical transition from coarse- to fine-grained sandstone with cross-beds to fine- to very fine-grained sandstone with horizontal laminae and ripple cross strata suggests waning flow. Grain size indicates that the vast majority of the sandstone was deposited as bedload. Miall (1977) interpreted similar deposits as dunes and linguoid bars that formed by turbulence in upper flow regime conditions. Cant and Walker (1976, 1978) identified similar deposits in transverse and linguoid bars of the South Saskatchewan River, which is a modern sandy braided stream, and interpreted cross-bedded units in the ancient Battery Point Sandstone as transverse bars that were deposited in channels.

Horizontal laminae were deposited by laminar flow under upper plane bed conditions. Similar facies were described by Miall (1977) as laminar sandflat deposits. Ripple cross-laminated sandstone (Figure 14) was deposited by suspension settling under turbulent flow. Miall (1977) interpreted ripple cross-laminated sand with a variety of asymmetric ripple types as having been deposited under lower flow regime conditions on bar tops in straight to sinuous channel reaches. It is difficult to evaluate the consistency of cross-bed orientation because of core breakage, but consistent ripple orientation within core slabs suggests that unidirectional flows predominated, corroborating a dominant fluvial origin.

Trace fossils in the sandstone (Figure 15) are typical of continental depositional settings. Meniscate burrows like those in the Paluxy are commonly the product of insects, and other animal activity in abandoned stream beds and alluvial plains (Hasiotis, 2002).

Smith et al. (2008) called similar burrows *Naktodemasis bownni*. This recently named ichnotaxon represents burrows composed of nested ellipsoidal packets backfilled with thin, tightly spaced, menisci subparallel to the bounding packet (Smith et al., 2008; Figure 15).

Following the widely used classification of Miall (1978), the predominance of sand-size particles and intraclastic conglomerate indicates that the Paluxy deposits are of South Saskatchewan type. Therefore cross-bedded, sandstone (Figures 13 B, C and D) probably accumulated mainly in transverse and lateral bar complexes within active channels, whereas the deeply burrowed and reddened sandstone (Figure 9) in the upper parts of the sandstone units represent longitudinal bars. This upper interval represents stranded channel and bar deposits that were exposed subaerially or sat in the vadose zone for extended periods of time, thereby facilitating oxidation of sediment and colonization by burrowers, such as insects.

Mudstone Facies

Characteristics

The mudstone facies constitutes all thick-bedded mudstone in the Paluxy Formation. The facies also includes sandstone beds thinner than 4 ft, as well as some conglomeratic layers with mud matrix. The signature rock type of the mudstone facies is reddish, non-fissile mudstone. Variegated mudstone is common, and rock colors include a range of reddish and gray hues. There are distinct layers of siltstone and sandstone in the mudstone facies (Figures 9 and 17B). These layers are pale red to very dusky red in

color and contain meniscate burrows, as well as some rhizoliths (i.e., root tubules). These intervals also contain abundant ripples and dewatering structures (Figure 17B)

A lot of the mudstone has a blocky appearance (Figure 16A) and contains slickensides with variable orientation (Figure 16B). This type of mudstone is quite friable, breaking readily into blocky fragments smaller than two inches. Caliche nodules are abundant in the mudstone facies. They are commonly cracked, filled with calcite, and weather to pale colors (Figures 16C and D).

Most of the mudstone has a mottled texture, which is in part the product of intense burrowing (Figure 17A). Biogenic structures are dominated by meniscate burrows resembling those in the sandstone facies. Conglomeratic layers are preserved locally in the mudstone and include dolomitic and argillaceous mudstone clasts (Figure 17C). Conglomeratic layers in the mudstone facies have a mudstone matrix, while those from the conglomerate facies have a sandstone matrix.

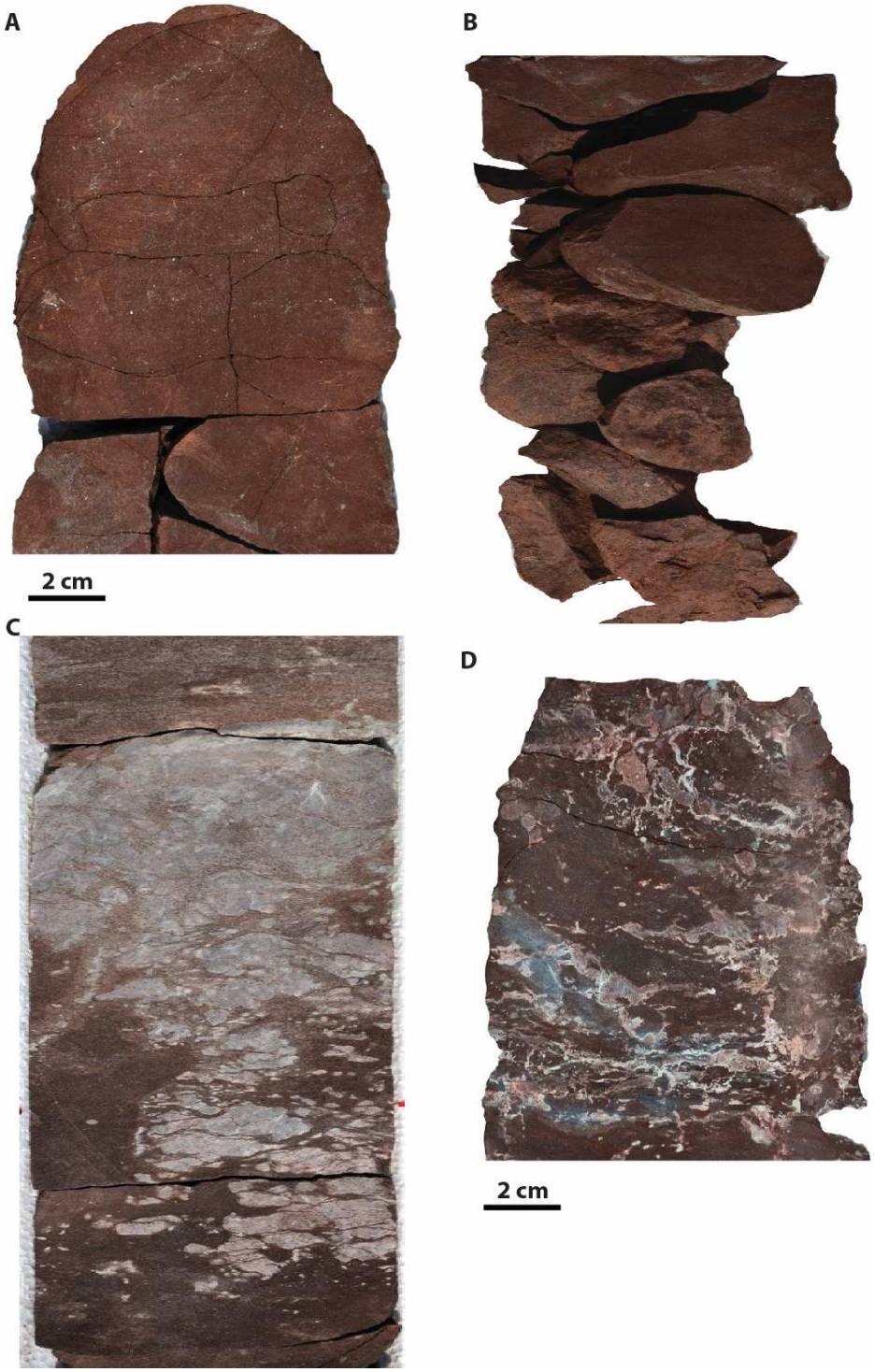

Figure 16. Photographs of slabbed core from the mudstone facies. A) Mudstone with blocky structure defined by vertical and horizontal cracks, Well D-9-7 #2, 9,634 ft. B) Mudstone containing pedogenic slickensides and blocky peds, Well D-9-7 #2, 9,635 ft. C) Mottled mudstone containing abundant calcareous nodules interpreted as caliche glaebules, Well D-9-7 #2, 9,590.5 ft. D) Mudstone containing calcite-filled cracks and small caliche nodules, Well D-9-9 #2, 9,424.5 ft.

Interpretation

The mudstone units are interpreted as paleosols. This facies is mainly a product of intense oxidation and pedogenesis. Intensely oxidized and desiccated soil profiles with abundant pedogenic slickensides are characteristic of vertic soil profiles, or vertisols (Figures 16 and 17; Mack et al, 1993, Retallack 2001). They occur in regions with subhumid to semiarid climate and a pronounced dry season. These mudstone units are characterized by thick, slickensided mudstone containing blocky peds, often with internal deformation of soil horizons (Figure 16A and B; Mack, et al., 1993, Retallack, 2001). The shape and size of the desiccated and slickensided bodies in the mudstone facies indicate that the upper parts of the soil profiles were dominated by blocky peds (Figures 16A and B).

The calcareous nodules are interpreted as caliche nodules representing precipitation of carbonate minerals that were leached from the upper part of the soil profile (Figures 16C and D). Nodules in soil profiles are termed glaebules by soil scientists. The abundance of cracks and septaria in the nodules indicate desiccation and hence alternating episodes of wetting and drying.

Clay coatings on some of the nodules suggest illuviation of clay from higher in the soil profiles and accumulation around nodules as argillans, or argillaceous cutans (soil science terms for argillaceous clay coats on soil particles). The abundance of pedogenic slickensides (Figure 16B) suggests desiccation, swelling, and compaction also occurred in the soil profile.

Figure 17. Photographs of slabbed core from the mudstone facies. A) Mudstone with intense burrow mottling and caliche nodules, Well D-9-9 #2, 9,440 ft. B Siltstone layer with dewatering structure, Well D-9-9 #2, 9,437 ft. C. Conglomeratic layer within mudstone facies composed of dolomitic and argillaceous mudstone clasts, Well D-9-9 #2, 9,445 ft.

The slickensides are interpreted as stress cutans, which are coatings of aligned clay that form where drying and wetting shrink and swell soil, causing slippage among soil particles (Retallack 2001). The presence of meniscate burrow networks like *Naktodemasis bowni* suggests periods of subaerial exposure associated with soil formation and modification under fairly to well-drained soil conditions (Smith et al., 2008).

Siltstone and sandstone layers in the thick mudstone section in core D-9-9 #2 are interpreted as the product of interchannel sheet flood events (Figure 17B). Conglomeratic layers in the mudstone facies (Figure 17C) contain argillaceous and dolomitic mudstone clasts similar to those in the conglomerate facies. The abundance of similar clasts in the conglomerate facies suggests that majority of the clasts were derived locally from the vertic soil.

Interfluvial paleosols tend to directly overlie the longitudinal bar deposits of the sandstone facies, suggesting that pedogenesis had a strong influence on the reddening of the bar deposits. Presence of abundant meniscate burrows in form of *Naktodemasis bowni* is exclusively found in paleosols. They are most likely constructed by burrowing insects, such as beetles and cicada nymphs (Smith et al., 2008). Overall observation suggests soil formation was a major process during Paluxy sedimentation.

Stratigraphic Architecture

Two stratigraphic cross sections of the Paluxy Formation and adjacent strata were constructed traversing Citronelle Field, with one cross section trending northwest-southeast along the eastern flank of the dome (Plate 1). The second cross section trends west-east across the dome (Plate 2). The cross sections are intended to show the lateral continuity and internal heterogeneity of the Paluxy sandstone bodies across the field. These cross sections were constructed using the top of the Ferry Lake Anhydrite as a datum, which is the only stratigraphic marker that can be correlated regionally with confidence near the level of the Paluxy Formation.

The Ferry Lake Anhydrite is about 50 ft thick in the stratigraphic cross sections and is overlain by the interbedded mudstone, limestone, and shale of the Mooringsport Formation. This interval has an average thickness of 240 ft. The Paluxy Formation is more than 1,150 ft thick. It can be informally divided into the basal, middle, and upper Paluxy.

The basal Paluxy sharply overlies the Mooringsport Formation. It has an average thickness of about 50 ft and extends across the entire field. The SP curve predominantly has a blocky log signature. The first sandstone body of the basal Paluxy can be interpreted as the first sequence boundary or erosional surface seen in the Paluxy Formation.

The middle Paluxy is very mud-rich with multiple isolated channel fills and discontinuous sandstone bodies. Thickness of sandstone bodies ranges from about 10 ft to 50 ft. The SP curves have variable log signatures ranging from blocky form to Christmas tree-type signatures. The blocky signatures reflect little variation in grain size and

porosity, while the Christmas tree-type signature reflects fining upward signature and vertically decreasing porosity. These variations result in significant interwell heterogenieity across the field. There is one sandstone body that is laterally continuous across the field in both cross sections. This can be interpreted as a sequence boundary that caps a variegated mudstone, which marks the boundary between the top of the middle Paluxy and the base of the upper Paluxy Formation. This sandstone unit is at a depth interval of about 9,778 ft in the NW-SE cross section and about 9800 ft in the W-E cross section.

The upper Paluxy is sand-dominated and the sandstone bodies are somewhat widespread across the field. Overall sandstone thickness is greatest in this interval. Sandstone bodies are more laterally extensive than the middle Paluxy sandstone units. The SP curves also have variable log signatures ranging from blocky form to Christmas tree-type signatures. This further demonstrates the considerable variability in sandstone geometry and continuity for each well across the field.

The sand-rich upper Paluxy may probably be a product of lateral migration of braided rivers associated with aggradation of closely stacked or sheet-like sandstone bodies that are interbedded with variegated mudstone (Boggs, 2012). Another possible cause for aggradation of these sandstone bodies is that the channel deposits vertically accreted during waning flood stages; braided rivers tend to aggrade vertically by deposition of sediment in one part of the valley with diversion of flow to other parts of the system (Cant, 1982).

The top of the cross sections is the basal shale of the Washita-Fredericksburg Interval, which serves as the confining unit. The basal shale of the Washita-

Fredericksburg interval has an average thickness of 150 ft. The western part of the field has a thinner succession of the basal shale of the Washita-Fredericksburg seal with several sandstone bodies. Plates 1 and 2 show that the Washita-Fredericksburg seal is laterally extensive but in complex facies relationship with reservoir quality sandstone units. This also implies that the Washita-Fredericksburg seal is time-transgressive.

Isopach maps of three major sand layers in the Paluxy Formation are shown in Figures 18 to 20. These maps were constructed to delineate thickness and extent of individual sandstone bodies across the Southeast unit of the field. Figures 18 and 19 are isopach maps that show a thick central core (up to 70 ft) thinning at the periphery. This peripheral thinning of the sand layers is indicative of channel sand deposits. Figure 20 is an example of a channel deposit. These isopach maps corroborates with stratigraphic analysis done on the cross sections that it would be very difficult to generate field-wide maps of individual sandstone because of considerable variability in sandstone geometry, orientation, and continuity.

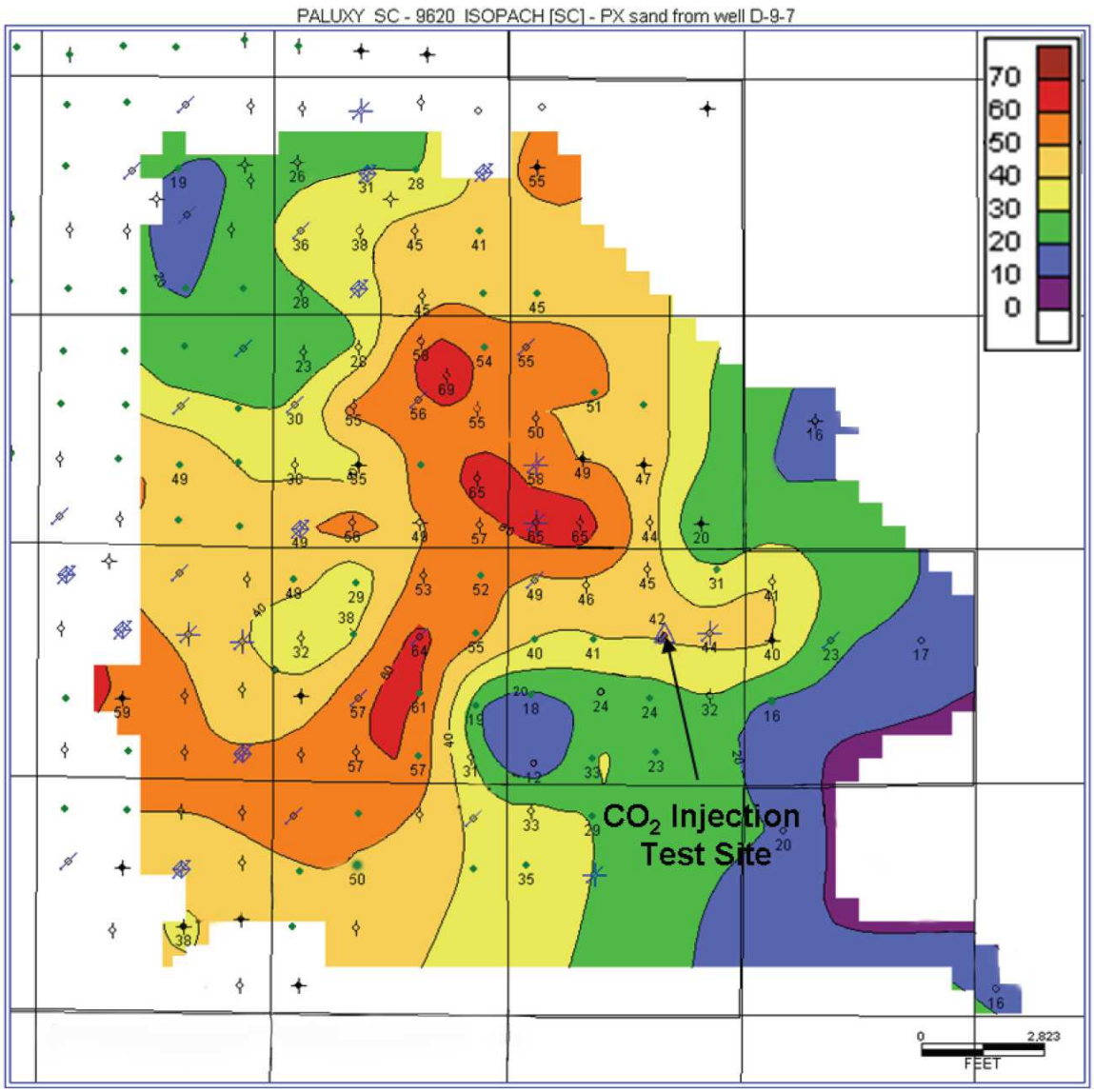

Figure 18. Isopach map of Well D-9-7 sand layer '9620' (modified from Petrusak et al., 2010).

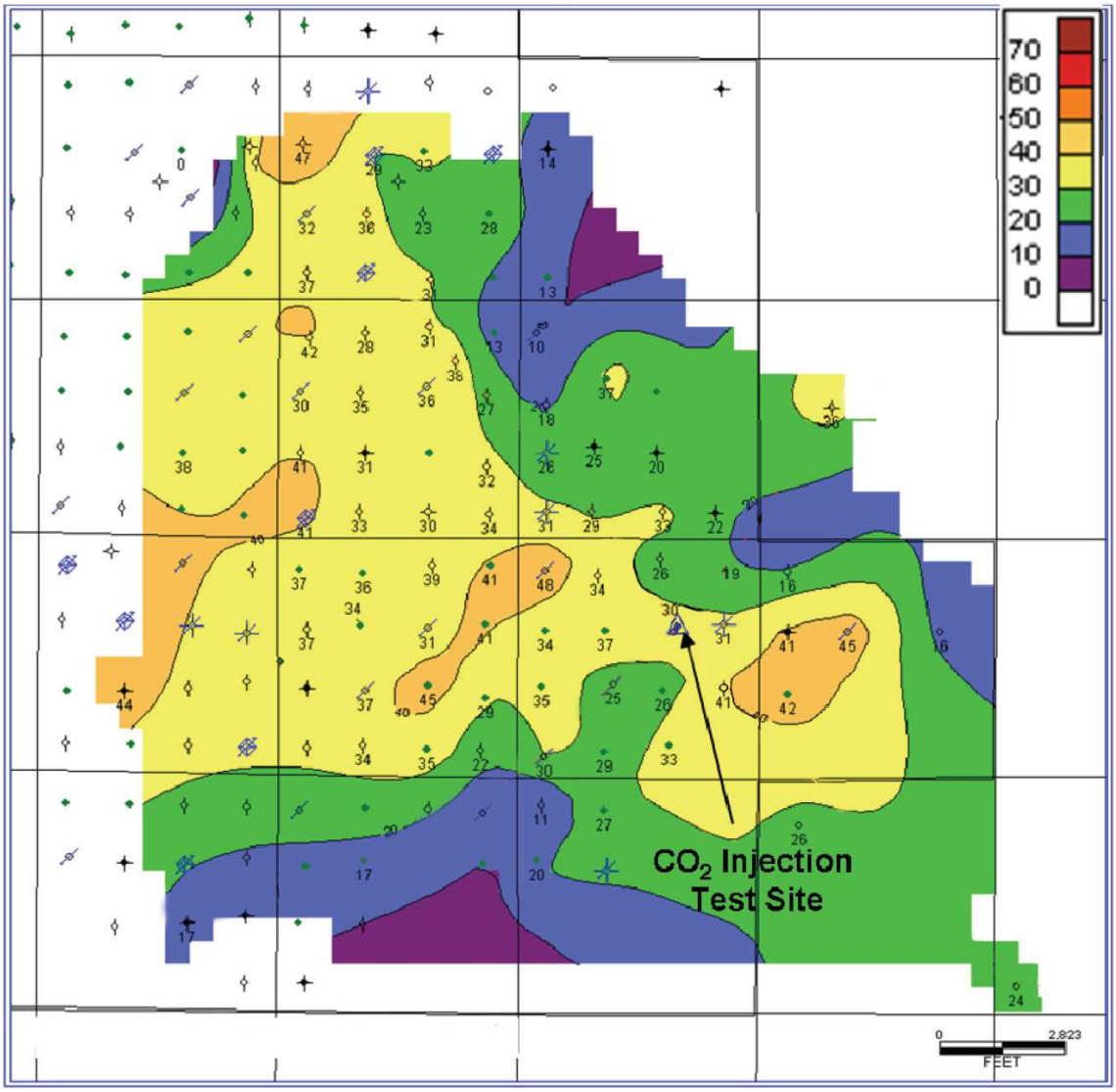

Figure 19. Isopach map of Well D-9-7 sand layer '9800' (modified from Petrusak et al., 2010).

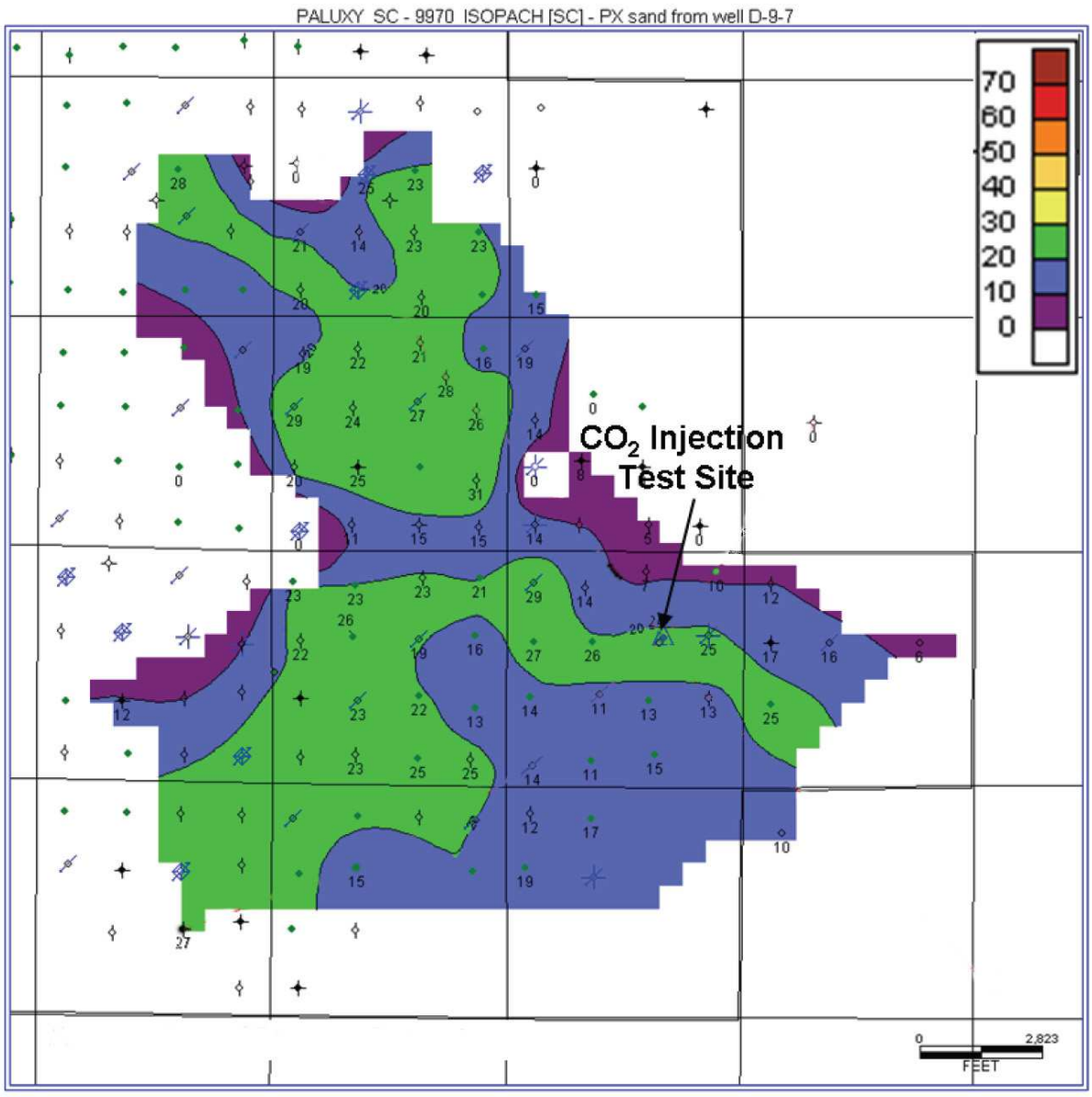

Figure 20. Isopach map of Well D-9-7 sand layer '9970' (modified from Petrusak et al., 2010).

Analogs

The proximal part of the Ganges River provides a nice visual analog, especially in depicting the reddening of the longitudinal bar as a result of intense oxidation (Figure 21). It is a great river of the plains of northern India. Current climatic conditions in the Ganges are not identical to the Paluxy Formation, because the Paluxy Formation was deposited in a semiarid to subhumid environment, while the Ganges has more vegetation and humidity. The Ganges River is also a gravelly braided system, whereas the Paluxy was deposited in sandy braided river. Nevertheless, a lot of comparisons can be made between both systems based on observations from Figure 21.

In Figure 21, the braided channel complex and longitudinal bars of the Ganges River are interpreted to be analogous to the conglomerate and sandstone facies. Higher energy deposits such as the braided channel and longitudinal bars deposits, are analogous to deposits of the braided fluvial environment of the Ganges River. The interfluves are interpreted to be analogous to the mudstone facies or vertisols. During flood events as a result of monsoons, the channel cannot contain the higher volume of water and the floodplains become inundated with sediment-laden water streams (Allison, 1998; Goodbred et al., 2003). These flood events are analogous to the sheet flood deposits facies observed during core analysis.

The Platte River system of Nebraska is a sandy braided system carrying similar bedload to that of the Paluxy Formation. They form linguoid bars or dunes that dominate during high flow occurring in both staggered and nested arrays, as well as solitary bedforms. This geometry and stacking pattern is observed in Plates 1 and 2. During intermediate and low flow, braiding is initiated and erosional process occur modifying

linguoid bars. Flood plain materials show rippled sand, and laminated and massive sand, silt, and mud that exhibit root and burrow modification. These were deposited during suspension and bed contact transport from waning flood currents. Similar processes like that of the Paluxy Formation contribute to the preservation of sandstone bodies such as channel aggradation and braid channel avulsion. There is no evidence for much vegetation in the Paluxy Formation in comparison to the Platte River, where vegetation stabilizes the bars by inhibiting erosion of bank material (Blodgett and Stanley, 1980).

The most suitable analog for the Paluxy Formation is the South Saskatchewan River of Canada. The vertical profile is very identical showing individual fining upward sequences like those observed in the Paluxy Formation. This vertical profile was adopted by Miall (1978) as the South Saskatchewan Type of braided river deposits. Cant and Walker (1978) recognized 4 major types of geomorphological elements;

1. Channels.
2. Cross-channel bars analogous to the planar cross beds found in the Paluxy core forming linguoid and transverse bars.
3. Sand flats analogous to the deeply weathered and oxidized longitudinal bar deposits of the Paluxy Formation.
4. Vegetated islands and Floodplains; similar to the vertisol and sheet flood deposits of the mudstone facies of the Paluxy Formation.

Despite these similarities, the South Saskatchewan deposits show no evidence of intense oxidation, intense burrowing, limited vegetation, semi-arid to sub-humid conditions found in the braidplain settings of the Paluxy Formation. The South Saskatchewan braidplain is less than a mile wide (Figure 22) compared to the width of

Figure 21. Modern Day analog; Google satellite image of the Ganges River, India.

the Paluxy braidplains, which is about 500 miles wide.

Another modern day analog is the Cooper's Creek, Lake Eyre Basin, central Australia. It is a multi-channel fluvial system in the Lake Eyre Basin of arid Central Australia. The dominant channel patterns are relict braids and active anastomosing channels. Braided channels are abundant but relict and have been superimposed on the braided system. The mud has been extensively burrowed by plant roots and cattle and repetitive shrinking and swelling has led to the formation of dessication cracks in the soil profiles. Calcrete is present which is analogous to the caliche profiles found in the Paluxy mudstone facies.

Differences between both systems include the maximum width of the braidplains (~10 miles) and the braidplains are mud-dominated (Figure 23; Rust, 1981). Arid to semi-arid climate has led to formation of horizons of gypsum and other evaporate salts. The superimposition of anastomosing channels has been attributed to the change in climatic conditions from a pluvial period (5000 years ago) to present arid climates (Rust, 1981).

Modern day vertisols are found in the Houston Black series, central Texas. Climatic conditions are humid-subtropical characterized by hot summers. These vertisols have calcareous, dark-colored, clayey soils with high shrink-swell potential. When dry conditions prevail, they commonly crack.

Despite the similarities with mudstone facies/vertisols of the Paluxy Formation, these modern vertisols are smectitic, suggesting low thermal maturity compared to kaolinitic and illitic clays found in the Paluxy Formation (Driese et al., 2000). Humid

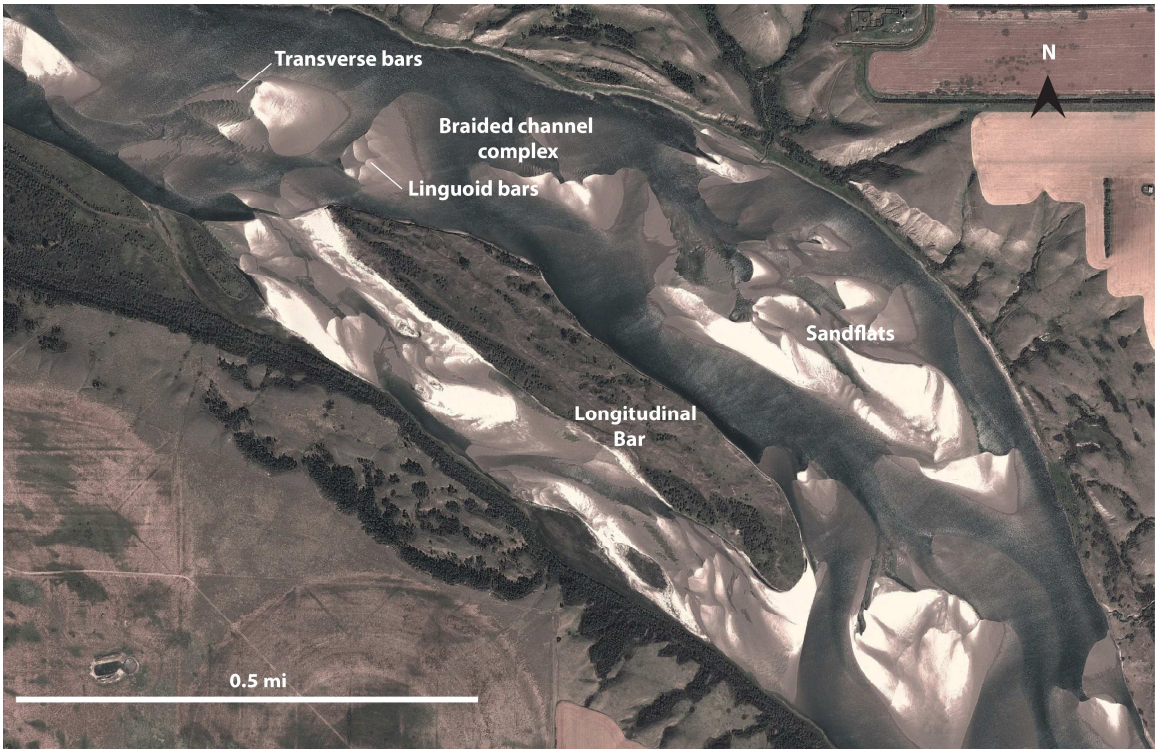

Figure 22. Modern Day analog; Google satellite image of the South Saskatchewan River, Canada.

conditions in these modern soil profiles are different from the semi-arid/sub-humid climatic conditions that existed during the deposition of the Paluxy Formation.

Despite the fact, that there are no analogs in the literature that perfectly suit the Paluxy Formation, several key elements from the discussed analogs help shed insight on the major depositional processes that may have occurred in the Paluxy Formation.

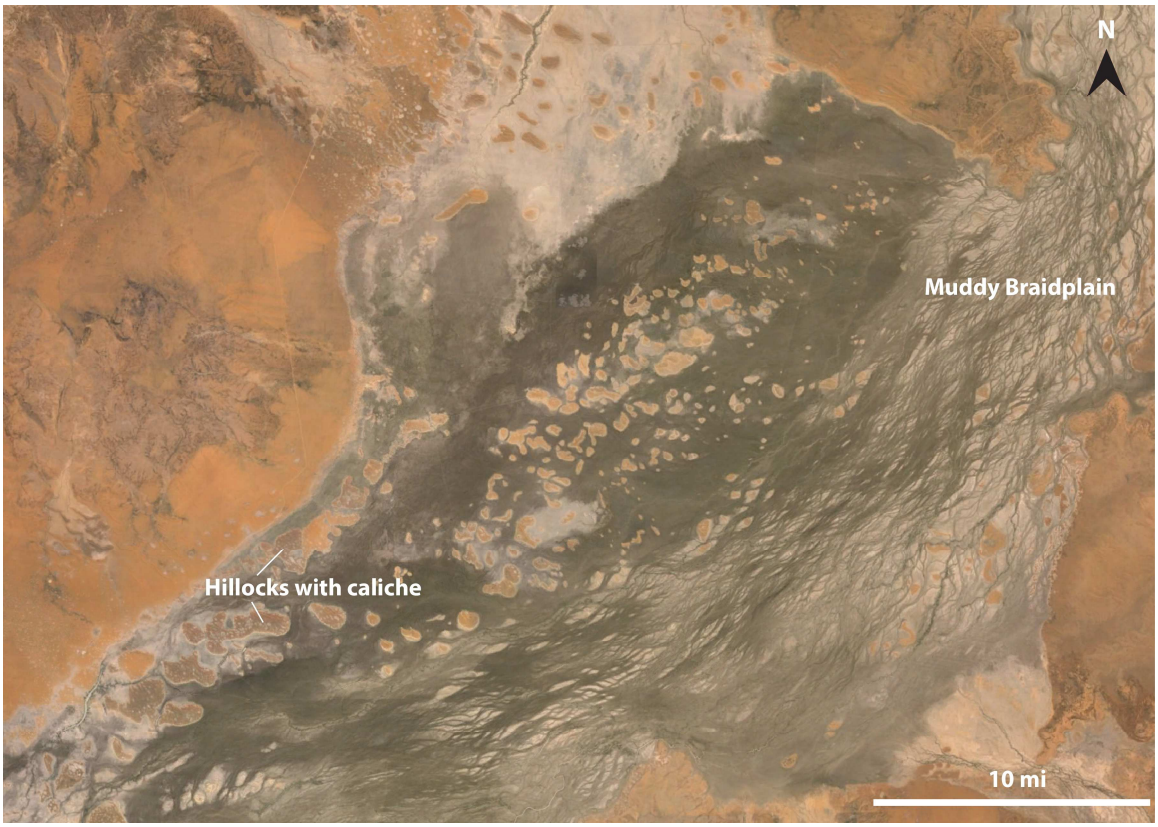

Figure 23. Modern Day analog; Google satellite image of the Cooper's Creek, Lake Eyre Basin, central Australia.

CHAPTER V

PETROLOGY

Framework Sandstone Composition

The three main classes of framework grains in Paluxy sandstone are quartz, feldspar, and lithic fragments, and the sandstone plots mainly as subarkose in the ternary diagram of Folk (1980) (Figure 24). This diagram shows that a few outlier samples plot as quartzarenite or arkose. Monocrystalline quartz is the dominant framework grain; rare polycrystalline quartz grains were also observed (Figures 25A and B). Quartz content ranges from 67% to 96%. Quartz grains are typically sub-angular to sub-rounded (Figures 25A and B). Sphericity ranges from slightly elongated to spherical. Grain size ranges from very fine sand (0.105 mm) to coarse sand (0.598 mm). Sorting ranges from moderately sorted to well sorted.

Feldspar is the second most abundant type of framework grain. Feldspar is present as two forms; plagioclase and potassium feldspar (Figures 26A and B). Point count results indicate that feldspar content ranges from 4 to 25%. Potassium feldspar is hard to distinguish from plagioclase feldspar except when it shows albite twinning or the tartan twinning that is characteristic of microcline. Thin sections stained with sodium cobalt nitrite help distinguish potassium feldspar (Bailey et al., 1960) (Figure 26B).

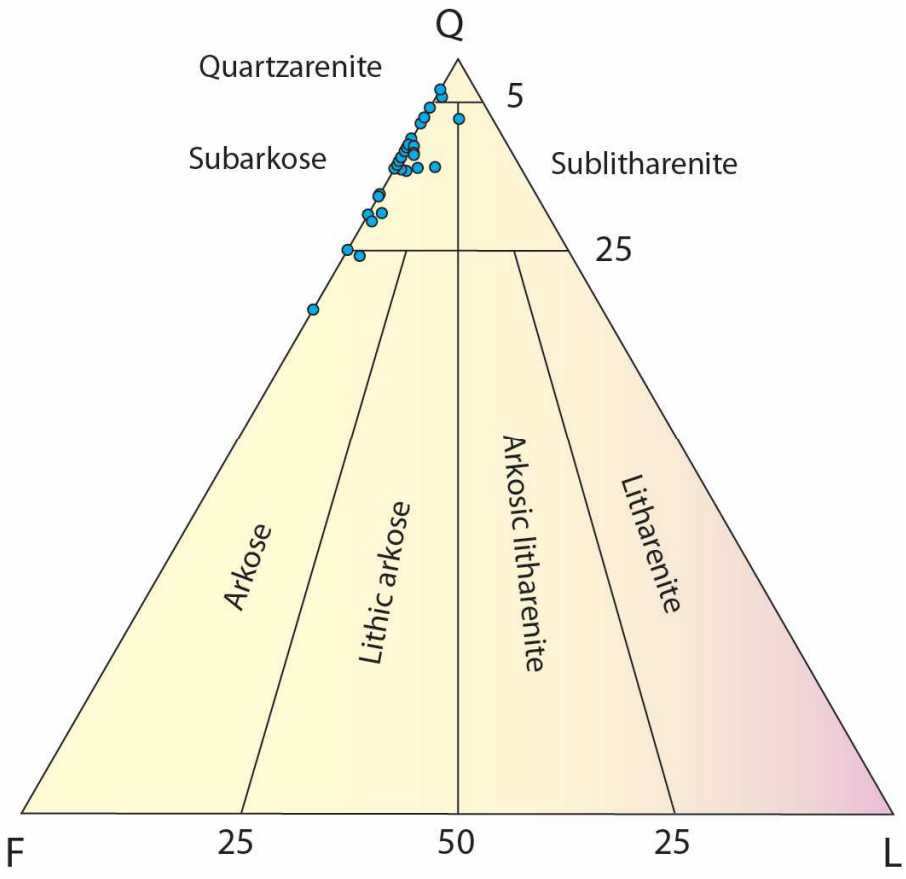

Figure 24. QFL ternary diagram showing classification of sandstone in the Paluxy Formation (modified from Folk, 1980).

Some plagioclase may be distinguished from orthoclase by albite twinning (Figure 26A), but untwined feldspar could not be identified definitively without cobalt nitrite stain. Microcline is a form of orthoclase that was identified readily based on its distinctive tartan or cross hatch twinning (Figure 27A). Feldspar grains are commonly altered or partially dissolved along the twinning planes and grain edges (Figures 26 and 27), which made it easy to distinguish feldspar and quartz grains. These partially dissolved or vacuolized grains are in places replaced by ferroan calcite cement, and vacuolized grains are a significant source of porosity (Figure 27B). Indeed, many grain-size pores may occur where feldspar has been dissolved.

Lithic fragments in Paluxy sandstone are primarily argillaceous rock fragments, no igneous or metamorphic rock fragments were observed. Argillaceous rock fragments are a common constituent, with an average composition of less than 1% of the framework. Most of the lithic fragments are opaque under plane polarized light and exhibit a brownish color under cross polarized light (Figure 28).

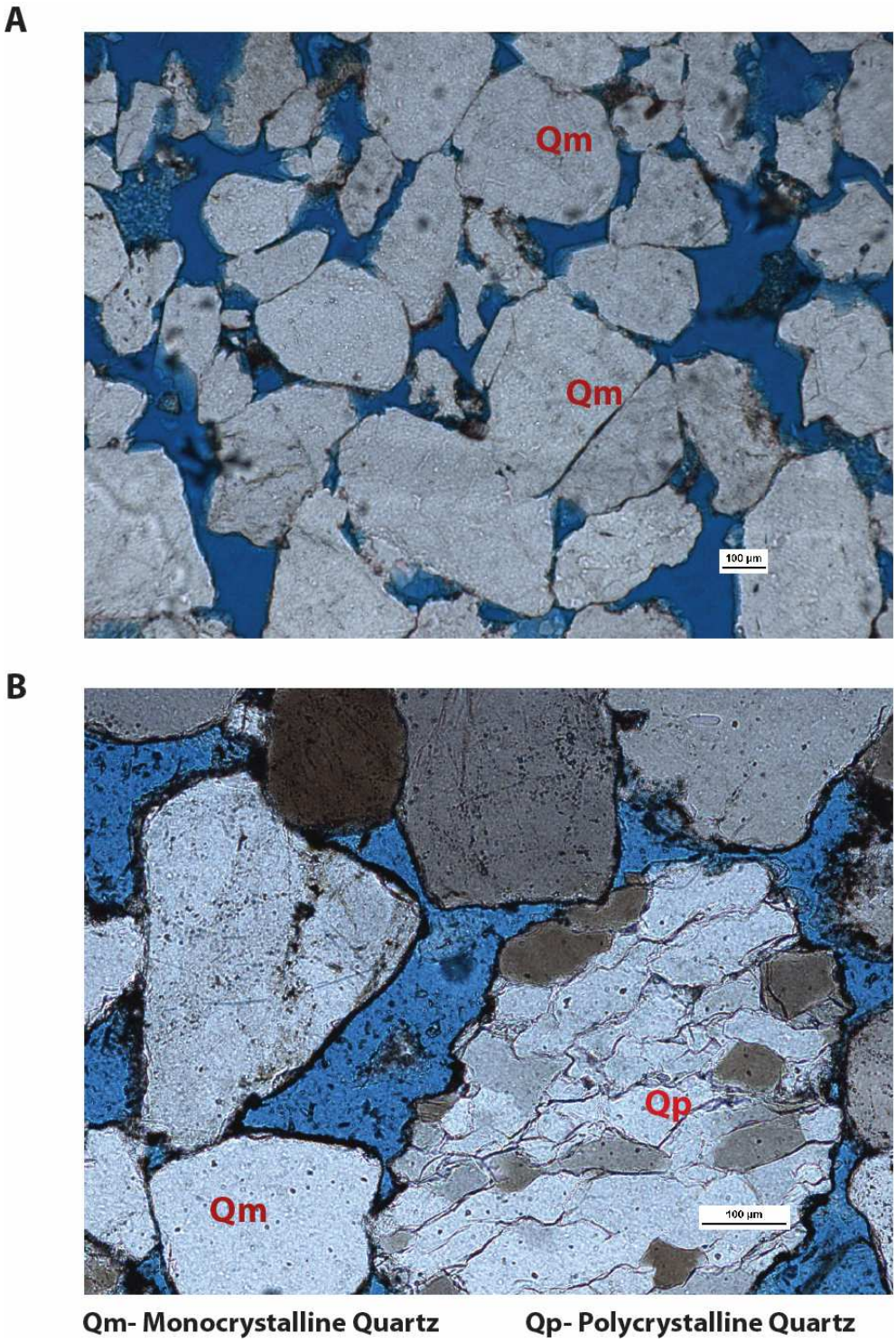

Figure 25. Thin section photomicrographs of Paluxy sandstone showing monocrystalline and polycrystalline quartz. A) Monocrystalline quartz (Qm) in plane polarized light, Well D-9-7 #2, 9,604.35 ft. B) Large polycrystalline quartz (Qp) grain in cross polarized light, Well D-9-7 #2, 9,600 ft. Note dark clay coatings on sand grains.

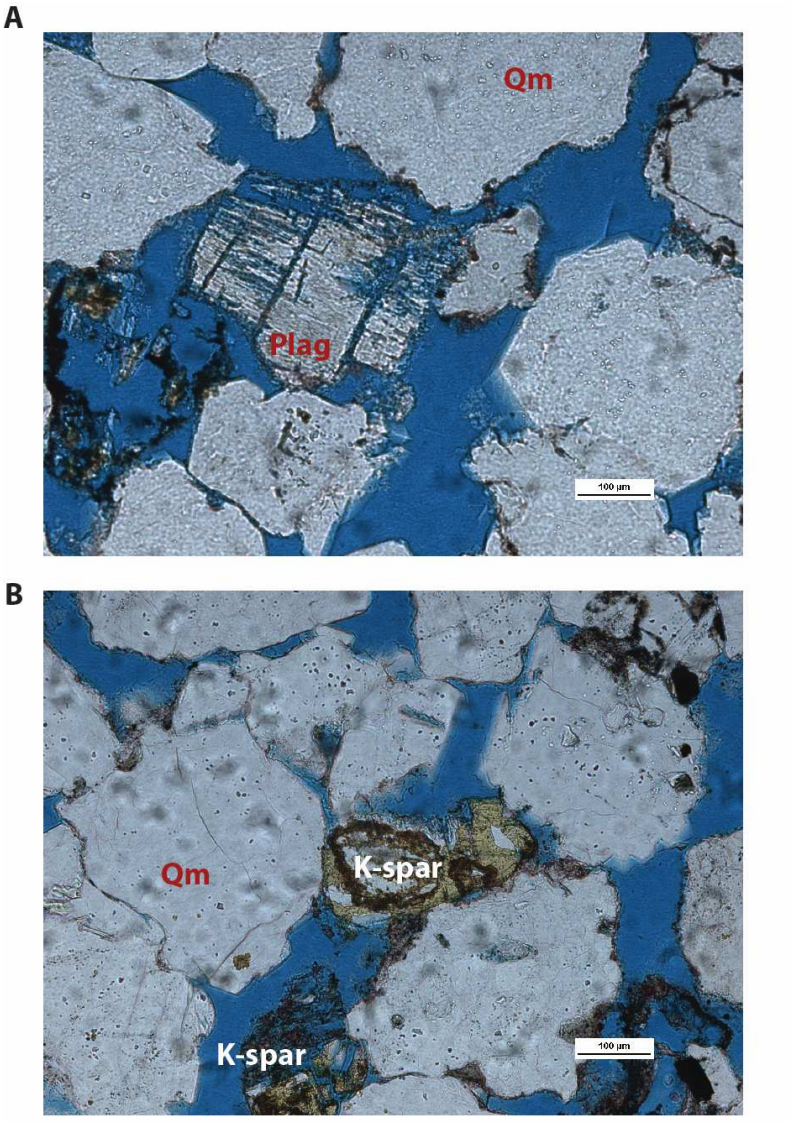

Figure 26. Thin section photomicrographs of Paluxy Formation showing feldspar in well D-9-7 #2, 9626.30 ft. A) Vacuolized plagioclase feldspar grain showing albite twinning. B) Partial dissolved potassium feldspar grains stained yellow with cobalt nitrite showing intragranular porosity.

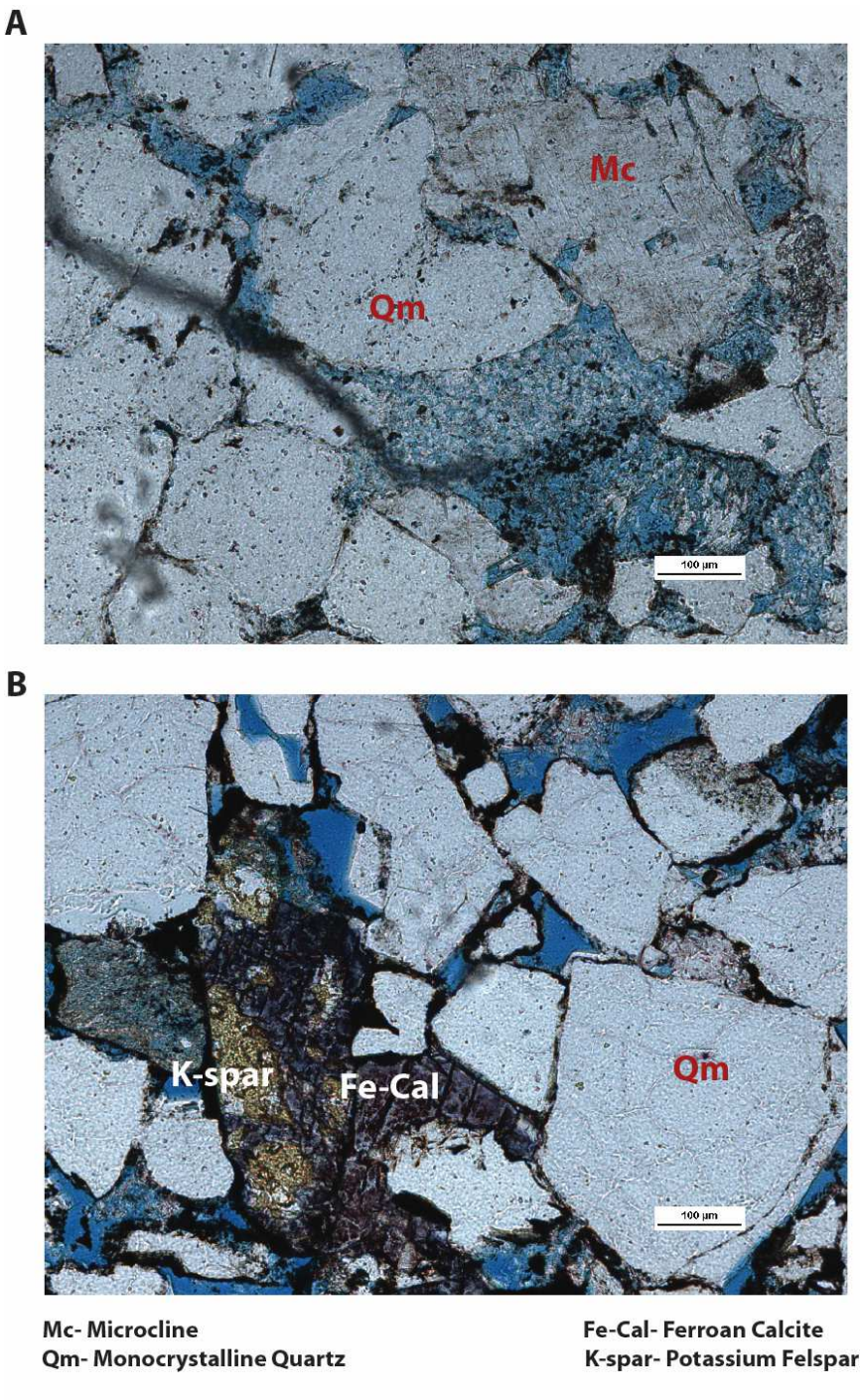

Figure 27. Thin section photomicrographs of Paluxy Formation. A) Microcline (Mc) showing the distinctive tartan/cross-hatched twinning, Well D-9-8 #2, 10,454.5 ft. B) Ferroan calcite cement replacing vacuolized potassium feldspar grain, Well D-9-7 #2, 9,575.5 ft.

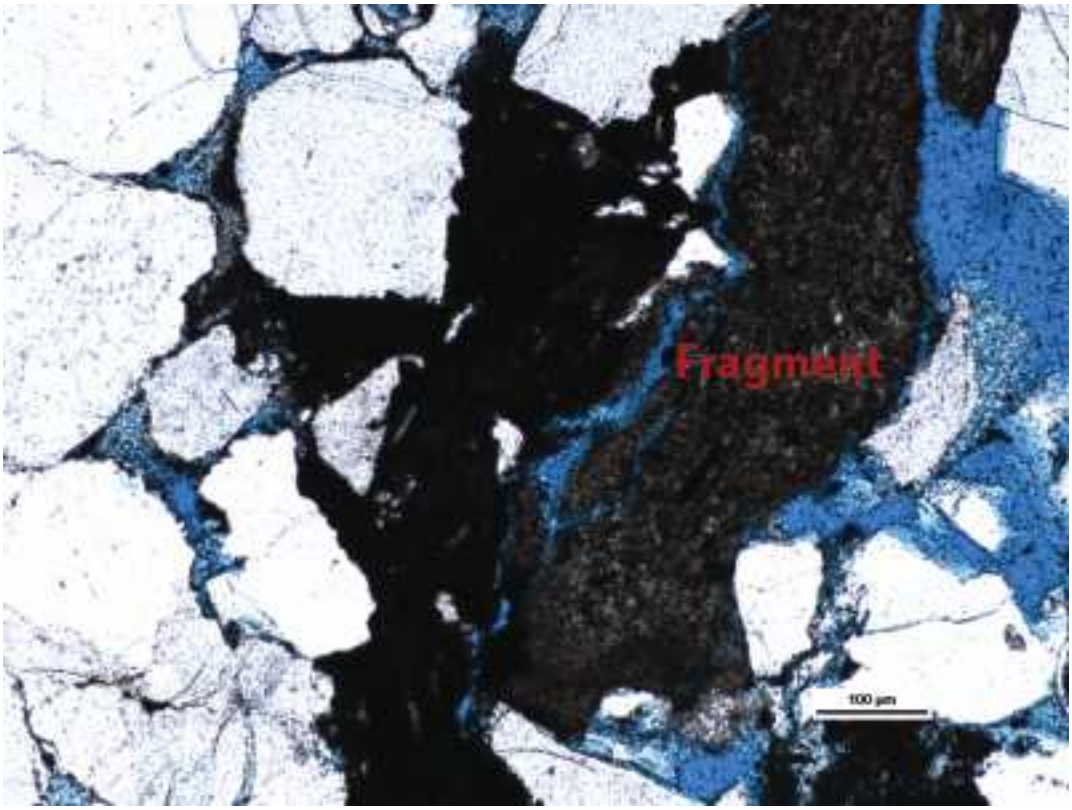

Figure 28. Thin section photomicrograph of an argillaceous lithic fragment containing silt sized quartz grains, Well D-9-7 #2, 9,625 ft.

Accessory Grains

Accessory constituents include trace quantities of detrital mica (Figure 29), amphibole, and polycrystalline quartz (Figure 25 B). Mica grains are large (0.3 mm), platy flakes of muscovite, and biotite (Figure 29). These micas have varied, but somewhat distinctive birefringence compared to surrounding grains under cross polarized light (Figure 29 B). Another way of identification was the perfect cleavage of the flakes.

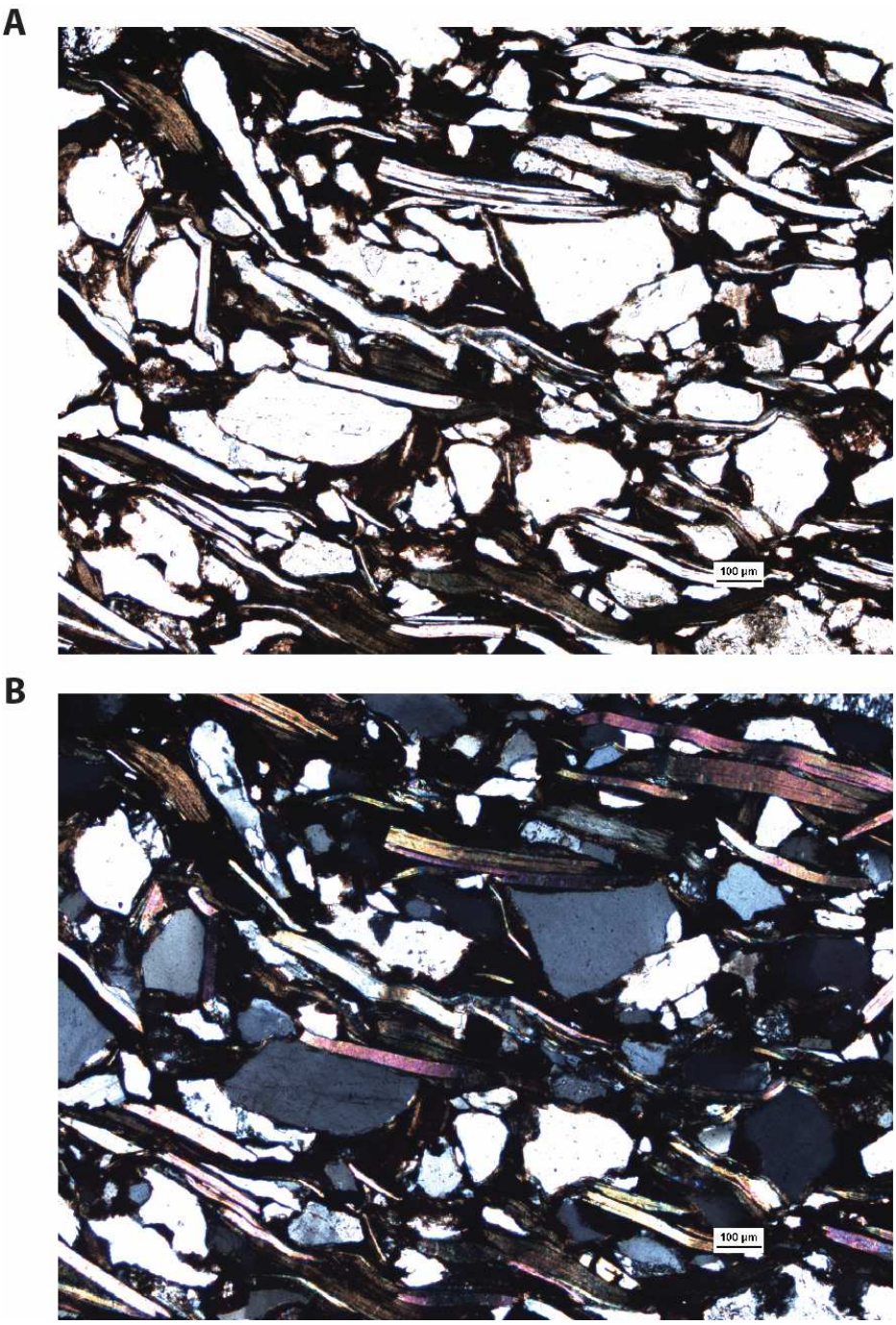

Figure 29. Thin section photomicrographs of Paluxy Formation, Well D-9-8 #2, 10,445 ft. A) Micaceous sandstone showing major concentration of platy muscovite, biotite, argillaceous rock fragments, and quartz under plane polarized light. B) Platy mica grains with distinctive birefringence under cross polarized light, most equant grains with low birefringence are quartz and feldspar. Opaque bodies are argillaceous grains.

Authigenic Minerals

X-ray diffraction (XRD) analysis identified two major clay minerals; kaolinite and illite (Figure 30). Mixed-layer montmorillonite-chlorite was found in some samples. Scanning electron microscopy (SEM) analysis also helped image the morphology of the two major clay minerals (Figure 31).

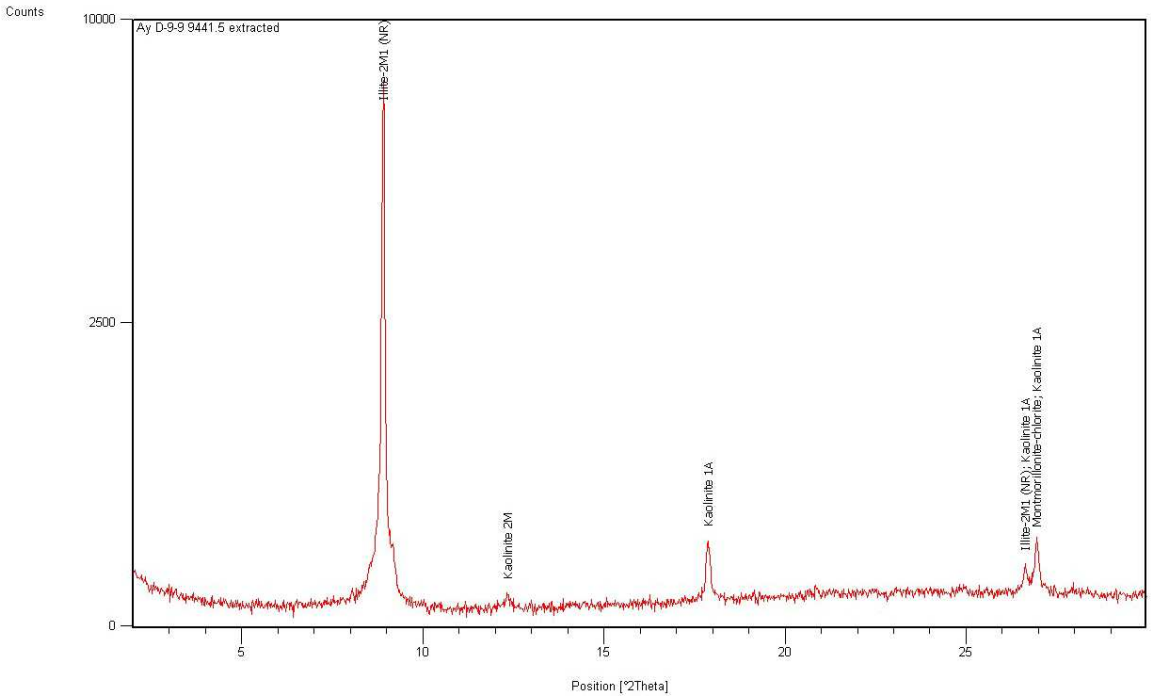

Figure 30. XRD result showing clay minerals, kaolinite, illite, and montmorillonite-chlorite. Well D-9-9 #2, 9,441.5 ft.

Quartz overgrowth is the most common type of authigenic cement in all samples observed under the microscope. Overgrowths partially fill intergranular space and do not occlude much porosity (Figure 32). Overgrowths are sometimes difficult to detect as they grow in optical continuity with the host grains. Sometimes, however, dust rims demarcate the boundary between host grain and overgrowth.

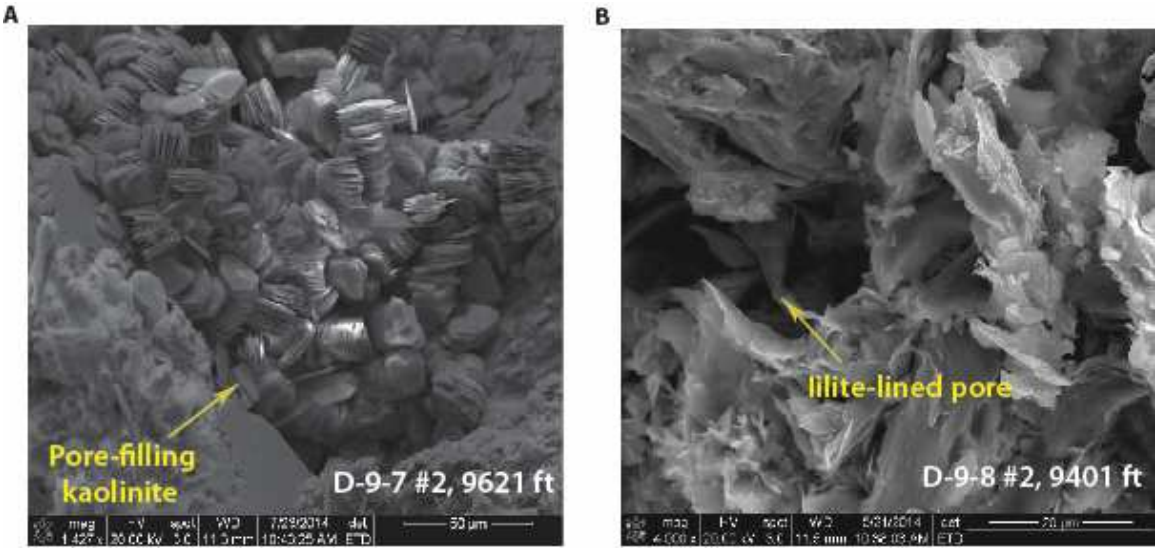

Figure 31. Photomicrograph of major clay minerals in the Paluxy Formation. A) Pore filling kaolinite with its pseudo-hexagonal booklet structure. B) Pore-lining illite with wispy platelike structure.

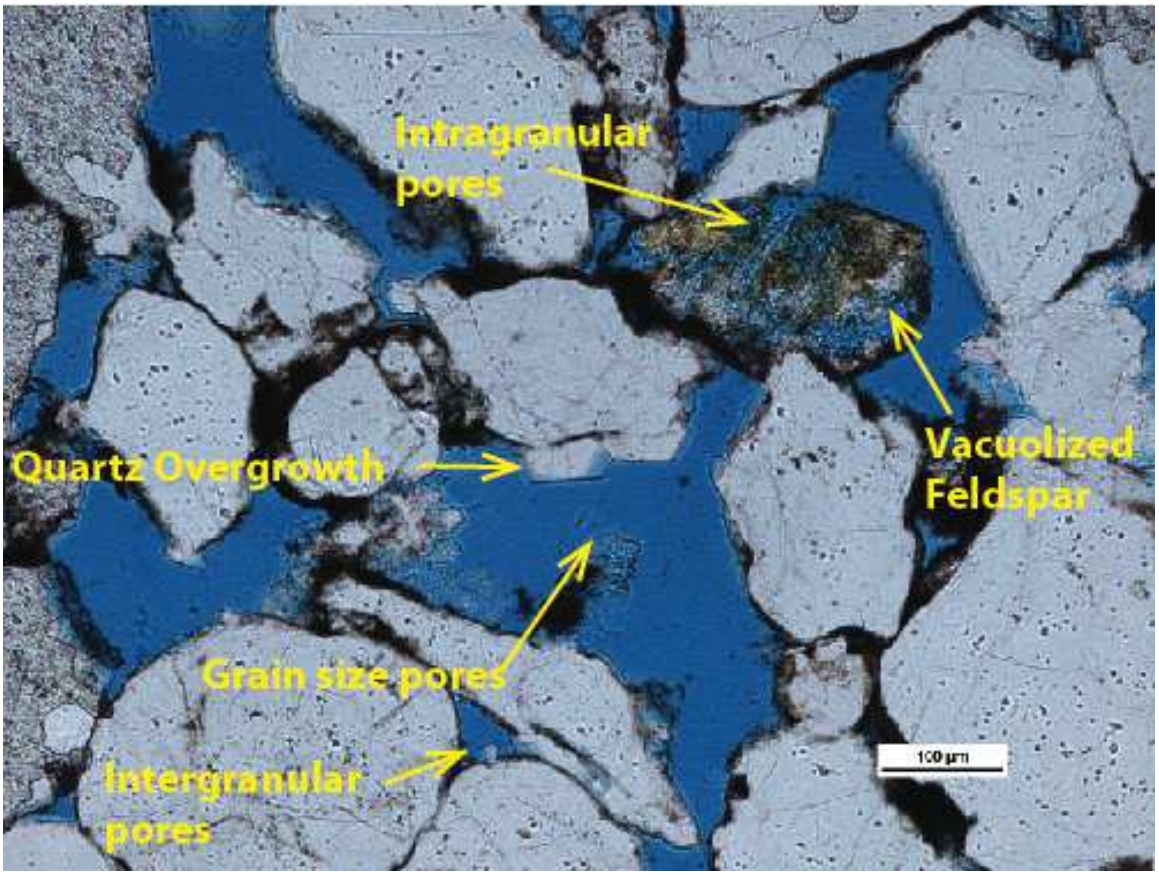

Figure 32. Thin section photomicrograph showing quartz overgrowth, primary and secondary porosity, and vacuolized feldspar. Well D-9-7 #2, 9595.60 ft.

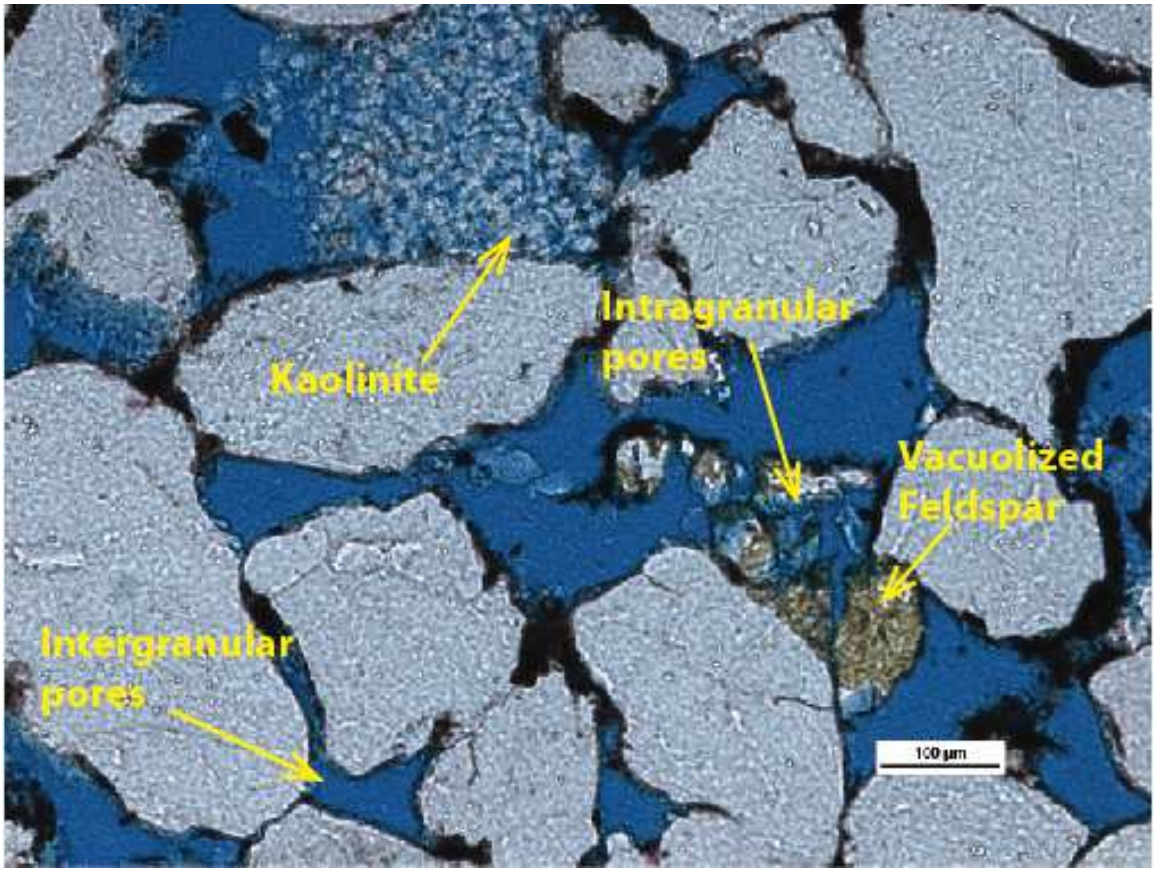

Figure 33. Thin section photomicrograph showing pore-filling kaolinite, primary and secondary porosity, and vacuolized feldspar. Well D-9-7 #2, 9595.60 ft.

Euhedral to subhedral calcite and ferroan calcite occur in trace quantities (0% to 2%) in most samples. In argillaceous sandstone, however, carbonate can form up to 18% of some samples (Figure 27B). Carbonate cements locally occlude intergranular porosity in patches ranging from 0.4 to 0.9 mm wide. In some cases, ferroan calcite fills space left by dissolution of feldspars (Figure 27B). Authigenic kaolinite was identified in all samples and occurs as clusters of small booklets. Typically, kaolinite partially fills secondary intergranular pores that resulted from dissolution of feldspar (Figure 33).

Porosity

Petrographic analysis shows that porosity is well-developed in the sandstone, where average porosity values are 20 percent (Figures 32 and 33). Two main pore types are common. Primary intergranular and secondary intragranular pores predominate (Figures 32 and 33). These pores tend to be large (i.e., sand size) and interconnected, which enhances permeability (Figure 32). Secondary porosity is in the form of intragranular pores and is the result of partial dissolution of feldspar. This is a fairly widespread phenomenon in sandstones (Figures 32 and 33; Heald and Larese, 1973). In places, dissolution of the unstable grains is so complete that secondary grain size pores are formed (Figures 32 and 33). Micropores also occur in the intercrystal areas between platelets of authigenic kaolinite (Figure 33).

Diagenesis

A number of diagenetic features were observed in the Paluxy Formation that provide crucial insight into the geochemical processes that were active during burial. Key processes that have affected the petrographic fabric and reservoir quality of the formation include mineral dissolution, fluid transport, and mineral precipitation. The effects of dissolution are obvious. This is evidenced by the significant number of feldspar grains that have been vacuolized, leaving remnants of mineral inclusions and grain-size pores where the feldspar has been dissolved (Figures 32 and 33). Turner (1980) also provided evidence of extensive in-situ dissolution of feldspar minerals in continental red beds. This has led to secondary intergranular and intragranular porosity and has almost certainly enhanced the permeability of the reservoir.

Weathering and dissolution of feldspar yields clay, which has clearly been flushed from some pores while accumulating in others (Figures 32 and 33). Some of the products of feldspar dissolution include pore-filling kaolinite (Figure 32), which probably formed parautochthonously. Heald and Larese (1973) also found feldspar to be unstable, altering into kaolinite or a replacement mineral in the Berea and Mt. Simon sandstone formations of West Virginia and Ohio. Carbonic acid formed from meteoric CO_2 tends to play a major role in leaching of grains (Schmidt and McDonald, 1979)

The paleosols of the mudstone facies and longitudinal bar deposits of the sandstone facies provide evidence for deep weathering and oxidation in the Paluxy Formation, and many thin sections reveal infiltration of clay into weathered sandstone (Figures 32 and 33). Schmidt and McDonald (1979) observed under the microscope, a characteristic property of secondary porosity in the form of oversized vug-size pores cutting across other grain boundaries. Another observation from petrologic analysis shows weathering and meteoric flushing of clay increased the porosity and permeability of some sandstone intervals.

Carbonate minerals are present in minor quantities as burial cement in the Paluxy Formation. Ferroan calcite is the most common carbonate cement and is present as large, poikilotopic bodies that occlude porosity (Figure 30B). Quartz overgrowths are the most commonly observed in thin sections, although faceted and interlocking grain boundaries of quartz grains (Figure 32), including stylolites, indicate that pressure solution and quartz overgrowth were significant processes during burial.

A chronologic paragenetic sequence based on cement-stratigraphic relationships from early to late burial of the Paluxy Formation is as follows;

1. Clay (illite) coating by rolling and saltation of sand.

2. Pedogenesis, calcite precipitation, stress cutan (slickenside) formation.

3. Illuvial illite coating.

4. Feldspar dissolution.

5. Pore-filling kaolinite, ferroan calcite, and ferroan dolomite precipitation.

Many paleosols are known for being red in color (Retallack, 1991). This is as a result of the nature and grain of iron-bearing minerals in the parent material of soils (Torrent and Schwertmann, 1987). Turner (1980) suggested several processes that might have contributed to the reddening of the sedimentary strata. Pigmentary oxides may form by intrastratal solution of detrital iron silicates, dehydration of goethite, the release of oxides during clay mineral transformations, and the oxidation of finely disseminated pyrite. Pedogenic processes play an important role in the post-depositional reddening of sedimentary strata.

Provenance

Plotting sandstone composition on the ternary provenance diagram of Dickinson and Suczek (1979) and Dickinson et al. (1983) reveals that the provenance indicators in the Paluxy Formation are dominated by monocrystalline quartz and feldspar; lithic rock fragments form only a minor component of the sandstone (Figure 34). Petrologic analysis indicates that most of the detritus represents stable minerals that originated in transitional continental to craton interior settings (Figure 34). The Paluxy Formation plots mainly in the transitional continental setting (Figure 34), suggesting an origin from denudation of

feldspar-rich basement provinces. This indicates that the sediment is far-traveled, since these types of sediment sources form only a minor fraction of the nearby Appalachian highlands, which plunge underneath the Gulf of Mexico coastal plain in eastern and central Alabama (Pashin et al., 2014). The presence of trace amounts of mica in the sandstone units (Figure 29) might suggest a possible input from metamorphic rocks, such as schist, which is abundant and widespread in the Appalachian Piedmont Province (Pashin et al., 2014).

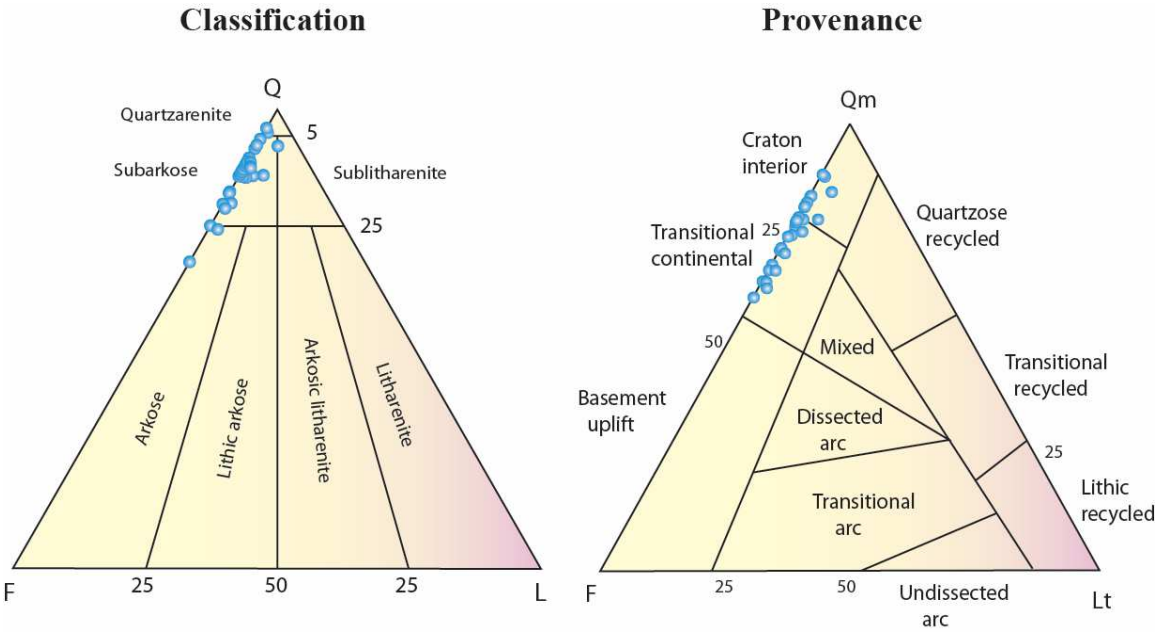

Figure 34. Ternary diagrams showing classification and provenance of the Paluxy Formation (modified from Folk, 1980; Dickinson et al., 1973, 1983).

CHAPTER VI

SUBSURFACE ANALYSIS

Log Characteristics

A robust geophysical log suite was acquired from well D-9-8 #2 (Figure 35). The entire Paluxy Formation is shown in this well log suite, as well as about 60 ft of the Washita-Fredericksburg interval. The gamma ray, shallow resistivity, deep resistivity, neutron porosity, density porosity, and fluid analysis curves were highlighted by assigning them to their respective tracks and having the headers magnified for better observation and placed on the right side of the well log.

The Paluxy Formation section can be subdivided into sandstone and mudstone based on the log curves. Sandstone has a low gamma ray value of less than 30 API units in track 1, indicative of a sandstone unit. Track 4 shows the shallow resistivity averaging 3 ohm-meters, while the deep resistivity ranges from 0.4 to 1.0 ohm-meter. There is a significant separation in the resistivity curves in track 4, suggesting deep fluid invasion and well developed porosity and permeability. Density porosity ranges from 15 to 30%, while neutron porosity ranges from 18 to 24% in track 5. Fluid analysis shows that this unit contains a lot of pore water and little to no bound water. Overall this unit depicts a permeable saline sandstone unit.

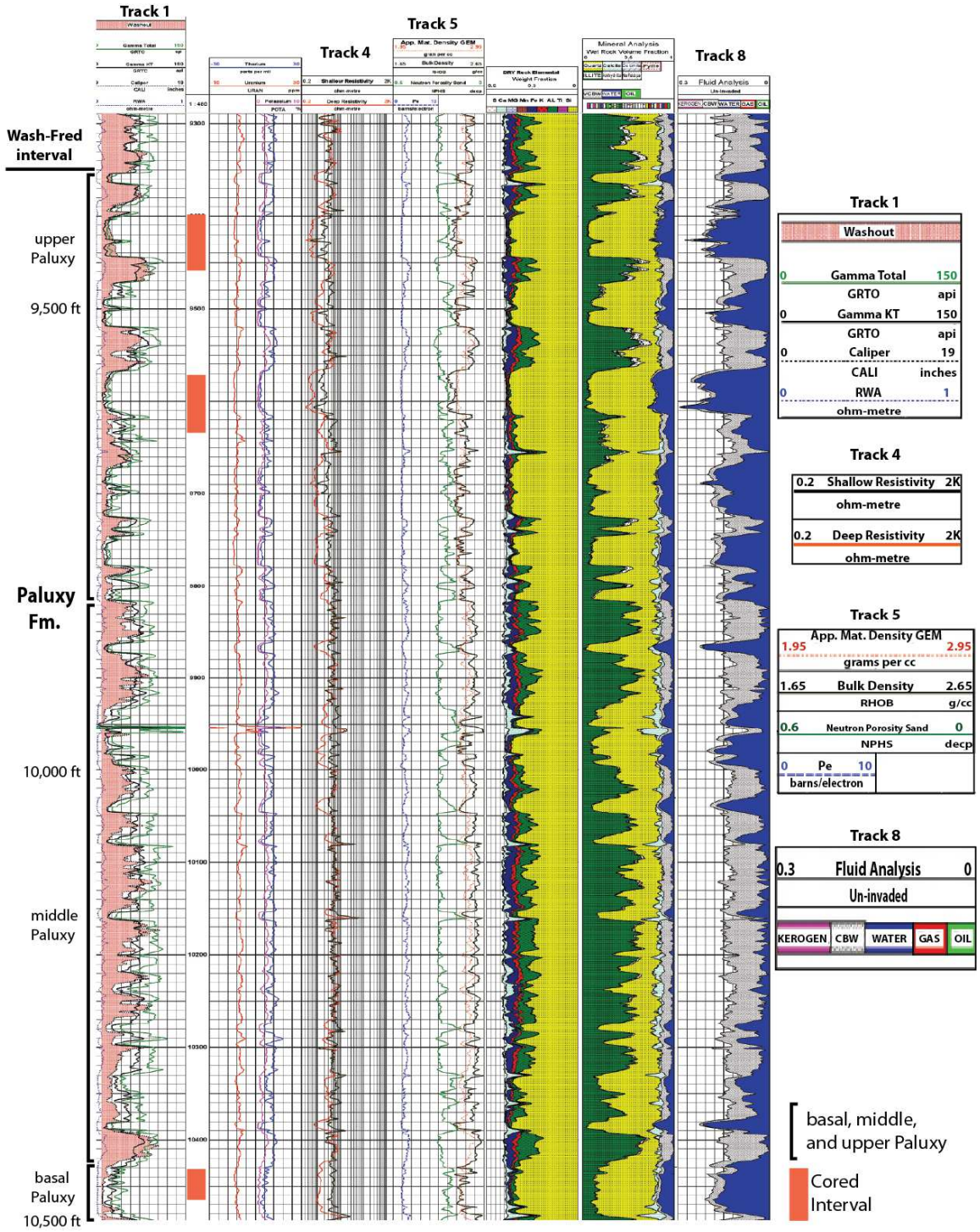

Figure 35. Well log from Well D-9-8 #2 showing the Paluxy Formation and parts of the overlying Washita-Fredericksburg interval. Adjacent key shows select track headers and cored intervals.

Paluxy mudstone units have high gamma count averaging 105 API units in track 1 suggesting a mudstone interval. Track 4 shows there is little separation between the shallow and deep resistivity curves, suggesting no invasion of fluids resulting in low permeability. Track 5 shows the neutron porosity is averaging 30% and density porosity ranges between 6 to 9%. Fluid analysis shows there is significant connate bound water in comparison to water. This unit represents an impermeable mudstone unit.

The sandstone units tend to be more abundant in the upper part of the formation, which in turn means the upper part is more sand-rich than the lower part of the Paluxy Formation. Unit 2 is a mudstone unit that is interbedded with the sandstone unit (unit 1) forming a multi-storey configuration of about thirty (30) stacked sandstone layers separated by mudstone units.

The basal section of the Washita Fredericksburg shows that the gamma ray values in track 1 average 105 API units, which is indicative of mudstone. The resistivity curves are closely spaced in track 4, which means there is no fluid invasion of the formation, and hence low permeability. Neutron porosity averages 30%, and bulk density values range from 6 to 9% in track 5. Fluid analysis shows a lot of connate bound water in track 8. The log characteristics ultimately show that this interval is an impermeable mudstone unit that has a lot of bound connate water.

Core Analysis

Figures 36 to 38 shows the relationship of porosity, permeability, and SP signature to facies. In Figure 36, conglomerate facies has porosity ranging from 5 to 12% and permeability ranges from 0.03 to 2,900 mD respectively. Conglomerate facies do not have any distinctive SP signature. Sandstone facies has porosity and permeability ranging from 10 to 26% and 4 to about 4,000 mD respectively. Sandstone facies have a large negative SP deflection from the shale baseline. Mudstone facies have porosity and permeability values ranging from 5 to 12% and 0.009 to 14 mD respectively. Mudstone facies have small negative SP deflection from the shale baseline.

In Figure 37, sandstone facies has porosity ranging from 10 to 23%, while permeability ranges from 2 to about 4,000 mD. Sandstone facies also have a large negative SP deflection from the shale baseline. Mudstone facies has porosity and permeability range from 6 to 8% and 0.012 to 0.06 mD respectively. Mudstone facies have a small negative SP deflection from the shale baseline.

Figure 38 shows conglomerate facies has porosity ranging from 5 to 6% and permeability ranges from 0.009 to 0.02 mD. Conglomerate facies do not have any unique SP signature. Sandstone facies has porosity ranging from 7 to 23% and permeability ranges from 2 to 416 mD. Sandstone facies have a large negative SP deflection from the shale baseline. Mudstone facies porosity ranges from 7 to 10% and permeability ranges from 0.002 to 0.2 mD. Mudstone facies also have a small negative SP deflection from the shale baseline.

The overall trend for all the facies shows porosity in mudstone facies ranging from 5 to 12% and permeability ranging from 0.003 to 14 mD. The mudstone facies have a small negative SP deflection from the shale baseline. This suggests poorly developed porosity and permeability in the mudstone facies. Sandstone facies ranges from 10 to 26% and permeability ranges from 2 to about 4,000 mD. The sandstone facies have a large negative SP deflection from the shale baseline. The sandstone facies have well developed porosity and permeability.

Conglomerate facies has porosity ranging from 7 to 21% and permeability values ranging from 0.009 to about 3,000 mD. Porosity and permeability range is very wide showing no distinct trend implying that the conglomerate facies can either have a poorly developed or well developed porosity and permeability. The conglomeratic facies do not show any unique petrophysical characteristics, which means that the conglomeratic facies cannot be picked on a field scale level without employing other unique tools or datasets like more core data.

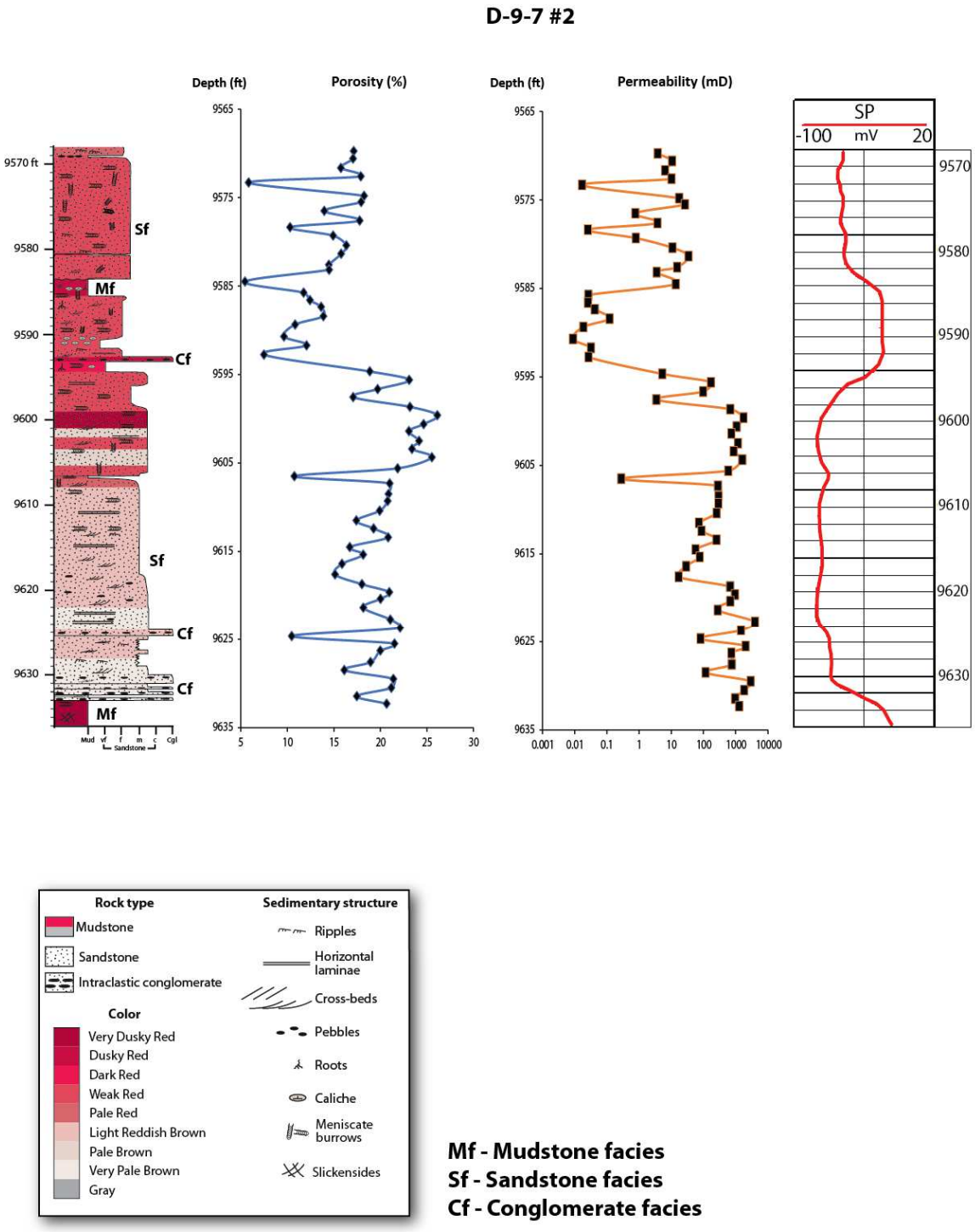

Figure 36. Relationship of porosity, permeability, and SP signature to facies, Well D-9-7 #2, 9568-9636 ft.

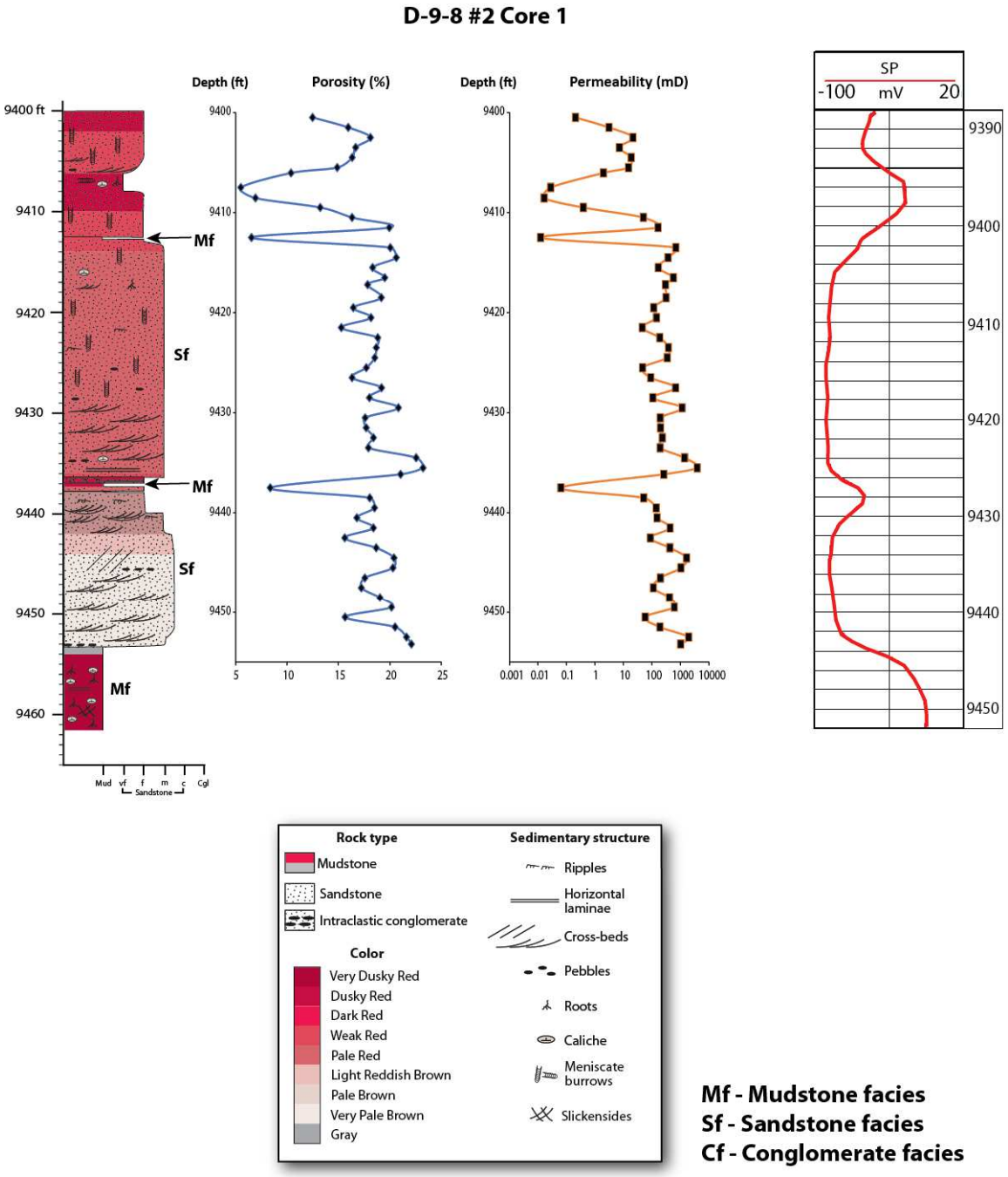

Figure 37. Relationship of porosity, permeability, and SP signature to facies, Well D-9-8 #2, 9400-9461.45 ft.

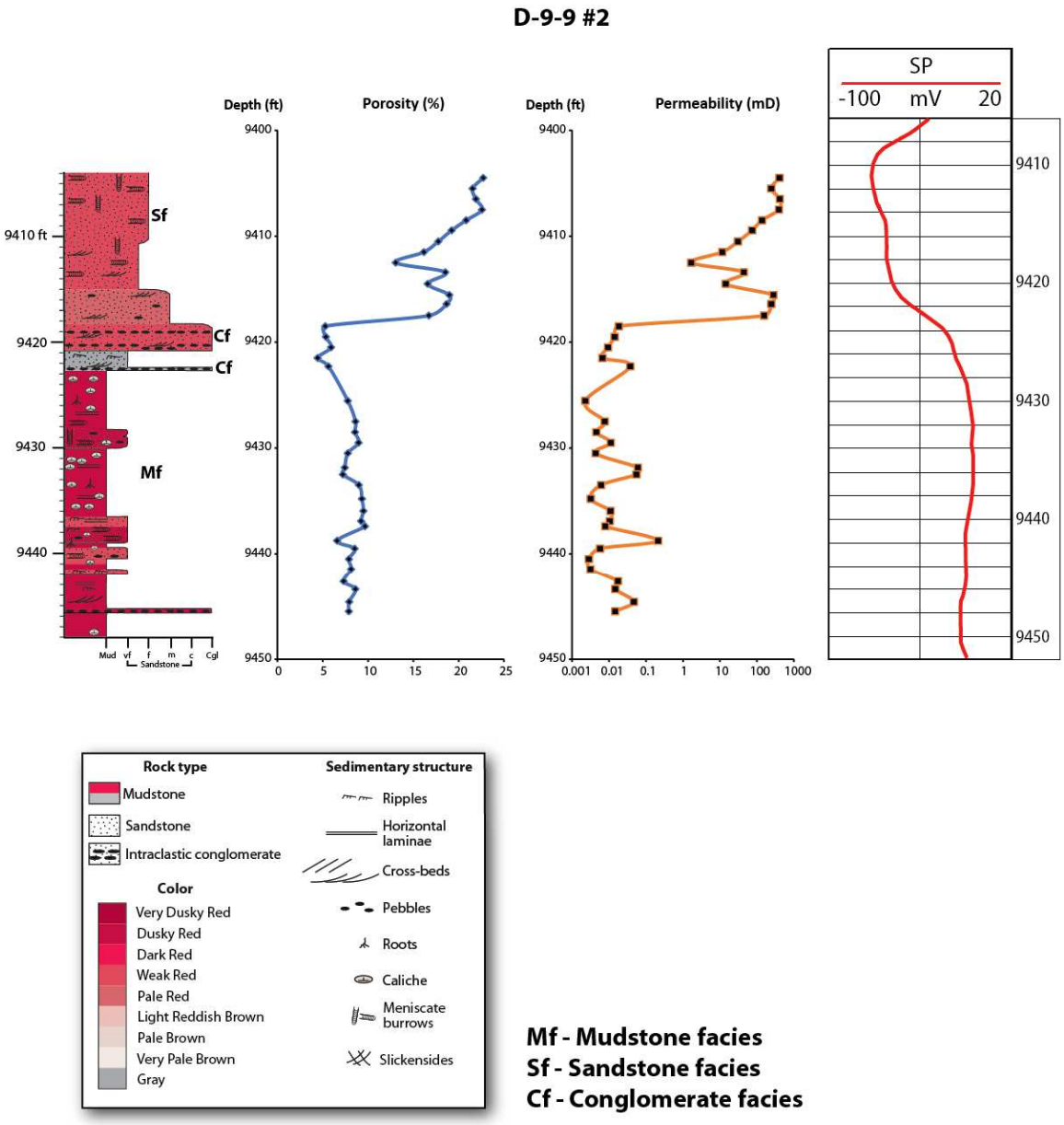

Figure 38. Relationship of porosity, permeability, and SP signature to facies, Well D-9-9 #2, 9404-9448 ft.

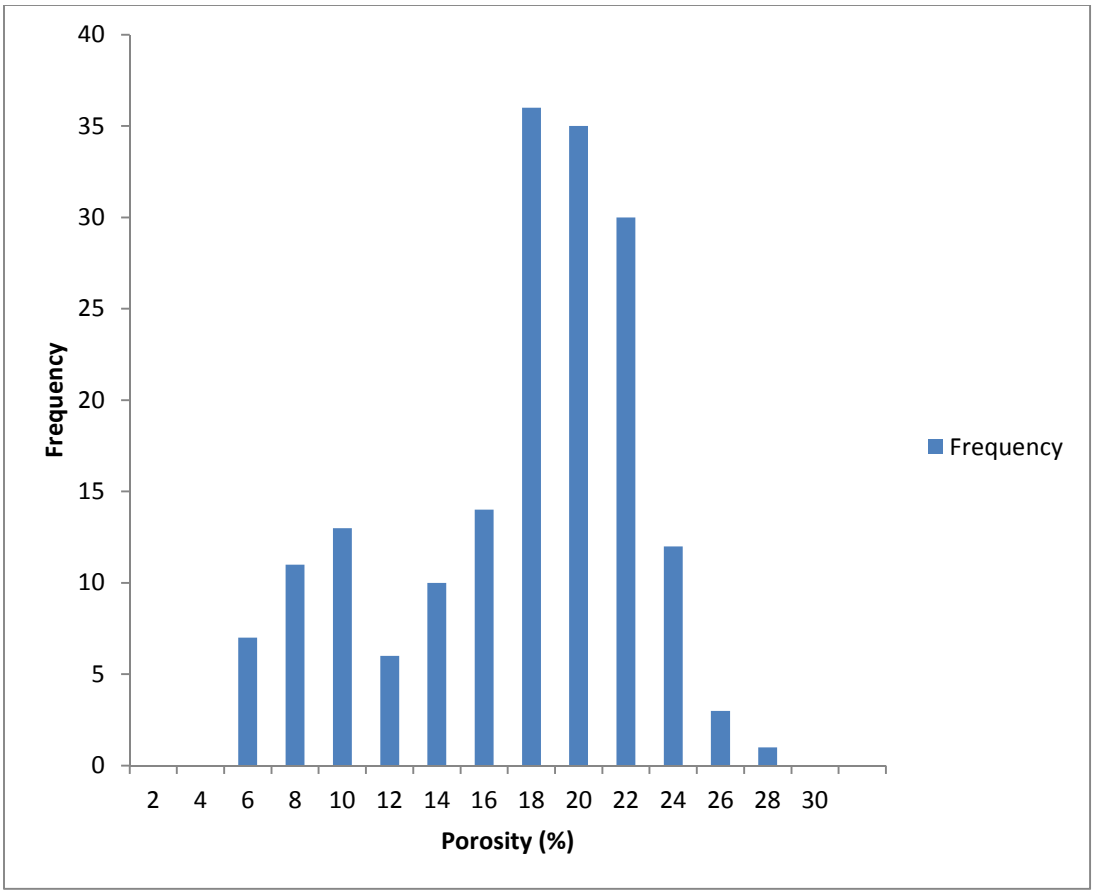

Figure 39. Histogram showing distribution of porosity determined by conventional core analysis.

The negatively skewed distribution of the histogram means that the bulk of the distribution of porosity values is towards the left of the highest values (Figure 39). Mudstone facies has porosity ranging from 5 to 12%. The sandstone facies has porosity values between 10 to 26%. Porosity values from the conglomerate facies range from 7 to 21%. The highest peak or mode is 18%. The average porosity value is 16.4%.

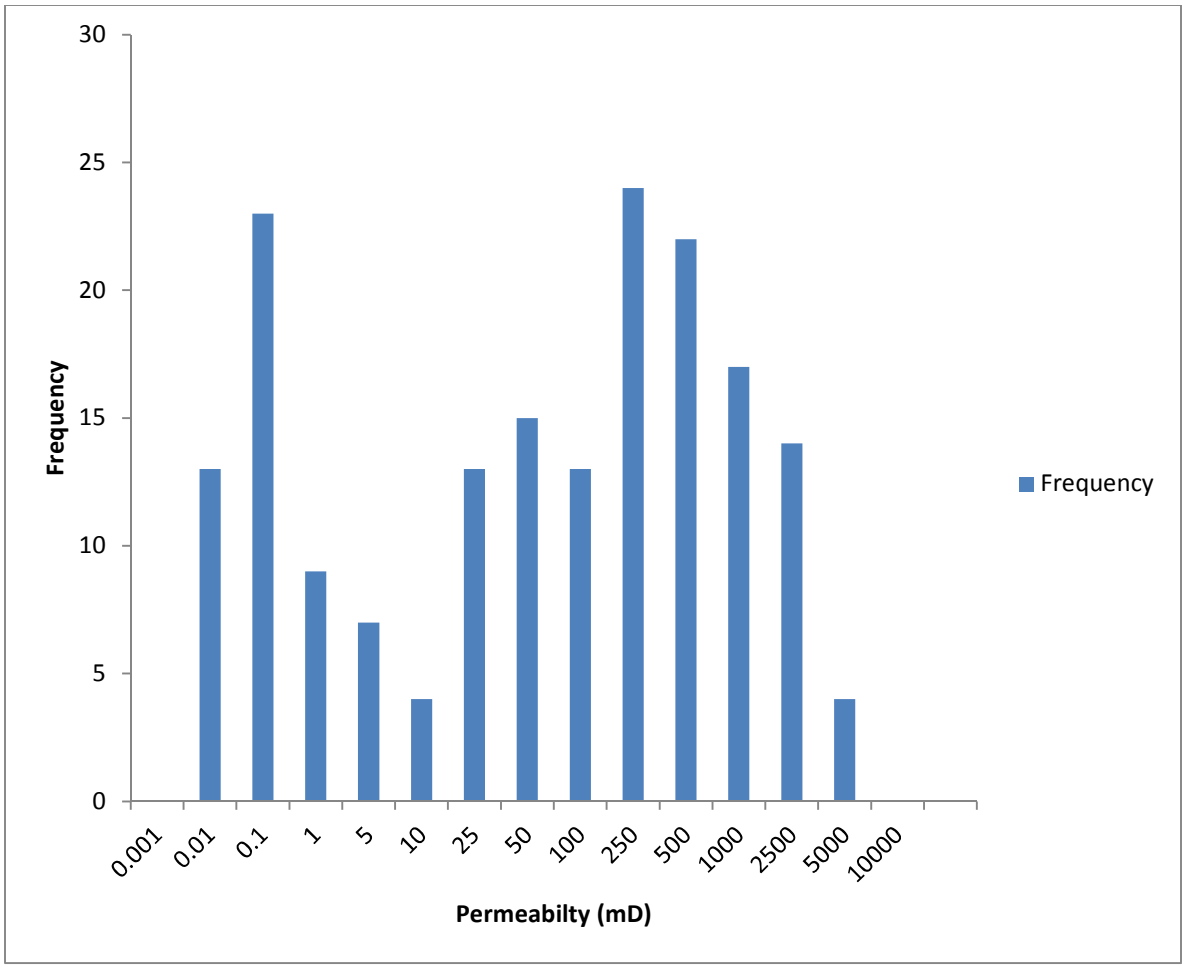

Figure 40. Histogram showing distribution of permeability determined from conventional core analysis.

Figure 40 shows a bimodal distribution of permeability. Mudstone facies has permeability ranging from 0.002 to 14 mD and the geometric mean is 0.02 mD. The sandstone facies has permeability values between 2 to about 4,000 mD and the geometric mean is 79 mD. Permeability values from the conglomerate facies range from 0.009 to 3,000 mD and the geometric mean is 6.8 mD.

CHAPTER VII

DISCUSSION

Depositional Model

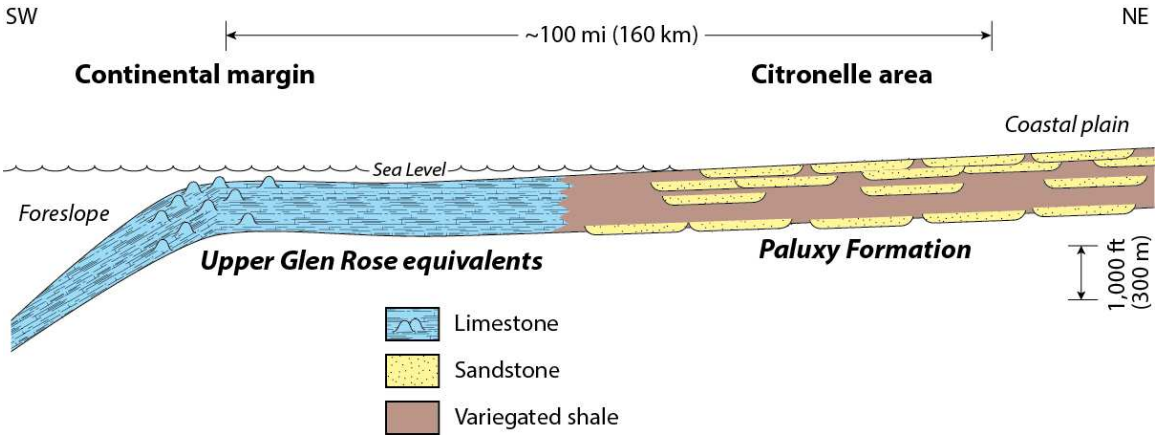

Figure 41. Generalized facies diagram showing relationship of the Paluxy Formation to equivalent carbonate deposits of the Gulf of Mexico Region (modified from Pashin et al., 2014).

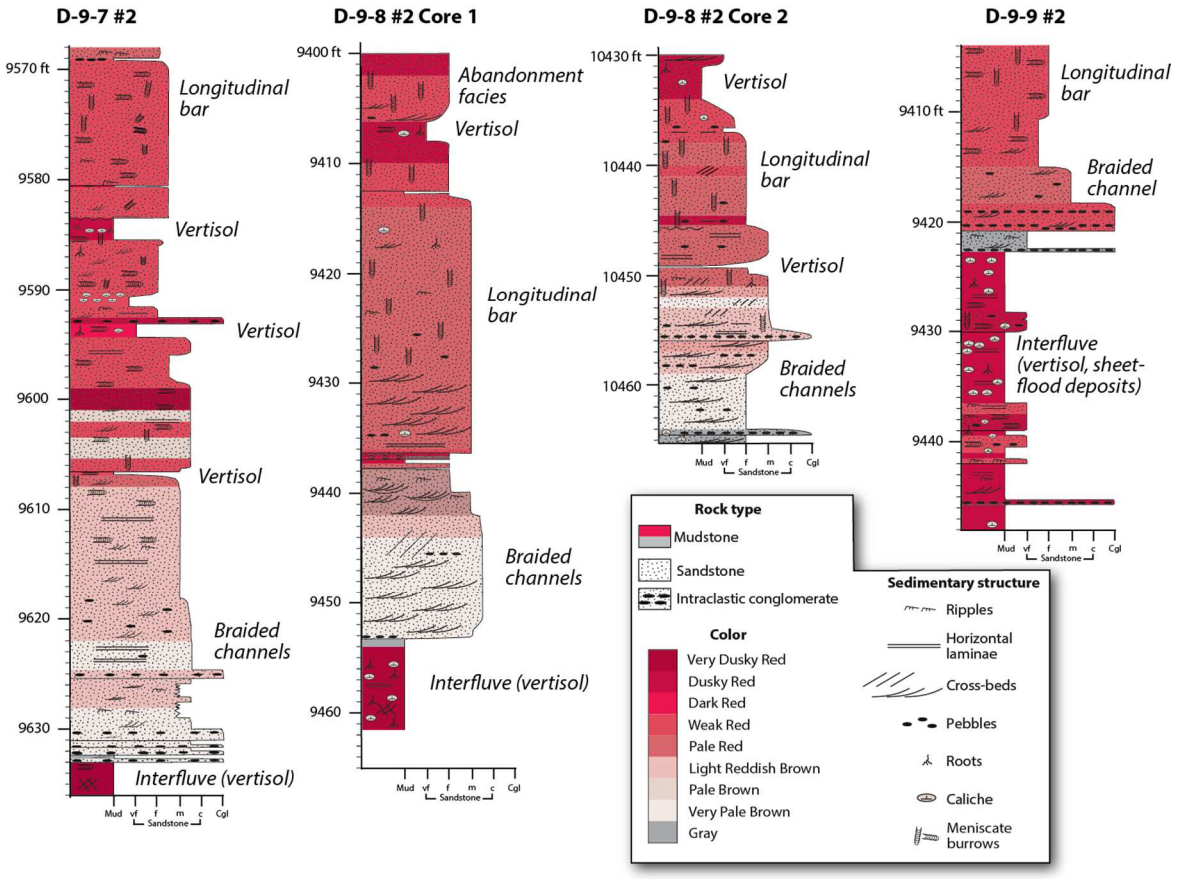

Figure 42. Graphic core logs showing schematic diagram of the depositional environment of the Paluxy Formation based on core analysis.

The Paluxy Formation is a net coarsening-upward succession composed of numerous stacked, aggradational sandstone-mudstone packages. Individual sandstone bodies have sharp bases, typically fine upward, and range in thickness from less than 10 ft to over 40 ft. Sedimentological analysis demonstrates that the Paluxy Formation was deposited in a continental environment that included bedload-dominated fluvial systems and interfluvial paleosols (Figure 41). In bedload-dominated or braided fluvial systems, multiple channels with low sinuosity carry coarse-grained sediment (Miall, 1977). The braided channel complex and longitudinal bars of the Paluxy Formation are represented

by the conglomerate facies and the sandstone facies. Cross-bedded sandstone represents braided channel complexes, while the deeply reddened and bioturbated sandstone bodies represent longitudinal bars.

The mudstone units separating the reservoir sandstone bodies are interpreted as interfluvial paleosols (Figure 42). These mudstone units are characterized by thick, very clayey, slickensided mudstone, often with internal deformation of horizons, caliche glaebules, and caliche crack fills. Soil horizons with these characteristics are classified as vertisols.They occur in regions with sub-humid to semiarid climates with a pronounced dry season (Retallack, 2001).

During flood events, the channel becomes inundated and sheet flood deposits accumulated as a result of these periodic events. These are in the form of thin layers of fine-grained sandstone and conglomerate in the mudstone units. (Figure 42).

A generalized repetitive sequence is argillaceous and dolomitic intraclasts, overlain by cross-bedded strata. The sequence ends with rippled sandstone, capped by bioturbated sandstone and mudstone. Similar sequences are observed in the modern South Saskatchewan and Devonian Battery Point Formation (Cant and Walker, 1976 and 1978; Miall, 1977; Rust, 1977).

The Paluxy Formation caps a major transgressive-regressive cycle during the Lower Cretaceous. It is the most areally extensive of three major progradational siliciclastic units in the Mississippi Interior Salt Basin (Mancini et al., 2002). Plates 1 and 2 show that the Paluxy Formation can be interpreted as a third order stratigraphic succession that has 2 major internal sequence boundaries.

The Paluxy was deposited over a period of 3 million years (Mancini et al., 2002)

during the Albian age. There are about 30 sandstone units in a typical vertical section of the Paluxy (Plates 1 and 2), which suggests that individual sandstone units have an average frequency of 100,000 years, which is equivalent to the Milankovitch short eccentricity cycle. This cyclic sedimentation is interpreted to have been driven by changes in climate with regards to the ellipticity of the earth's orbit around the sun. These climatic changes will affect rainfall occurrence during each cycle, eustatic sea level, base level, and sediment flux on the alluvial plain. These are the primary factors that would have controlled frequency of pedogenesis and bedload-dominated fluvial deposits sedimentation. Similar cyclicity was observed by Pashin (2014) in the Donovan sandstone of the Citronelle Field.

Implications for Commercialization of CO_2 Storage Technology

Although Citronelle Field is structurally simple (Figure 5), analysis of reservoir architecture (Plates 1 and 2) reveals extreme facies heterogeneity in the Paluxy Formation. There is abundant storage capacity and high injectivity due to high porosity and permeability in the reservoir. With so many porous and permeable sandstone units to consider in Citronelle Field, perhaps the greatest challenge for CO_2 storage programs is managing facies heterogeneity.

Stratigraphic cross sections (Plates 1 and 2) indicate that reservoir sandstone bodies tend to occur in clusters thus initial planning should perhaps focus on assessment of these clusters in specific focus areas. Another factor for consideration when designing injection programs is stratigraphic isolation and hydraulic confinement of the target

sandstone bodies. Although there are intra-formational barriers, baffles and seals that limit the vertical migration of CO_2 plume, keeping injectate in zone may be a significant problem where successive sandstone bodies are amalgamated into multi-storey successions, and this may limit the predictability of CO_2 flow.

Interwell heterogeneity is another key consideration in Citronelle Field. Although some sandstone units have great lateral continuity, each well may have a substantially different geophysical log signature, reflecting major variation of reservoir properties among wells (Plates 1 and 2).

The basal shale of the Washita-Fredericksburg, which serves as the primary seal tends to get thinner towards the western part of the field, with clusters of sandstone bodies overlying the seal. Care must be exercised when injecting in these areas, but the presence of numerous additional seals nullify the threat of surface leakage of CO_2.

Primary facies heterogeneity and diagenetic processes associated with pedogenesis are the major causes of reservoir heterogeneity. Primary facies heterogeneity is expressed in the form of isolated channel fills in discontinuous sandstone units and nesting of multiple channels within widespread sandstone bodies. Pedogenesis enhances porosity through the dissolution of feldspar and the dissolution products are flushed out of the sandstone. These flushed products accumulate as clay and can plug the sandstone altering the petrophysical properties of the reservoir. It is therefore important to consider diagenetic and depositional processes, when selecting and mapping out ideal sandstone bodies with geophysical logs.

Citronelle Field is ultimately a suitable host for CO_2 sequestration and the criteria for selecting ideal sandstone bodies to inject CO_2 should not only include reservoir

quality, but reservoir heterogeneity has to be considered and well understood when planning injection programs.

CHAPTER VIII

CONCLUSIONS

Citronelle Field is the product of a complex geologic history that is associated with the evolution of the Mississippi Interior Salt Basin. The field is in a structurally simple domal structure that formed above a broad salt pillow; Louann Salt. The dome forms an elliptical, four way closure that lacks faults. It contains multiple reservoir sandstone units and a range of mudstone, evaporate, and carbonate seals. The primary confining unit above the Paluxy Formation is the basal shale of the Washita-Fredericksburg interval, and secondary seals higher in the section provide additional storage security and include the marine shale of the Tuscaloosa Group and the chalk of the Selma Group.

The Paluxy Formation is an Early Cretaceous (Albian age) redbed succession that includes a heterogeneous assemblage of sandstone reservoirs in which conglomerate and mudstone units form baffles and barriers to flow. The conglomerate facies are characterized by variegated, predominantly pebble-sized clasts of mudstone and carbonate origin embedded in a sandstone matrix. The sandstone facies is variegated, fine to coarse grained with several sedimentary and biogenic structures. Mudstone facies

constitute all the mudstone and thin-bedded sandstone units, with the signature rock type being the reddish non-fissile mudstone.

Facies analysis of the Paluxy Formation indicates that reservoir facies were deposited primarily in a bedload-dominated fluvial systems. The cross bedded conglomerate and sandstone facies probably accumulated as dunes within active channels, while deeply burrowed and weathered sandstone facies formed longitudinal bars. The mudstone facies are interfluvial paleosols that formed as a result of weathering and soil formation. The siltstone and sandstone layers found within the mudstone facies are interpreted as the product of inter-channel sheet flood events. Overall observation suggests pedogenesis was a major contributor during the deposition of the Paluxy Formation.

Petrologic analysis shows that the Paluxy sandstone is mainly subarkosic.with trace amounts of argillaceous lithic fragments and detrital mica. Major authigenic clay minerals are in the form of Kaolinite and Illite, while quartz overgrowth is the most common authigenic cement. Euhedral to subhedaral calcite and ferroan calcite are found in trace quantities. Porosity is well-developed in the sandstone with an average porosity values of 20 percent. Two main pore types are common; primary intergranular and secondary intragranular pores. These pores tend to be quite large (i.e., sand size) and interconnected, which enhances permeability. Provenance analysis indicates that most of the detritus originated in transitional continental to craton interior settings.

Integration of core facies, porosity and permeability values from core plug analysis, and geophysical well analysis can help in delineating attractive reservoir targets. Results showed a trend of small negative SP deflection from the shale baseline, low

porosity, and low permeability values in the mudstone units; while the sandstone facies depicted large negative SP deflection from the shale baseline, high porosity and high permeability values. Reservoir porosity commonly exceeds 20 percent and permeability values can range up to 4,000 mD.

Despite several similarities in the certain elements of other braided systems, there are no modern analogs that encompass the extensive width of the Paluxy braidplain setting (~500 miles). The South Saskatchewan River has a humid, vegetated, and narrow braidplain setting. The Cooper Creek is muddy, narrow, too arid, and has been superimposed by anastomosing channels. The Platte River vegetative stability leads to enhanced sinuosity of the river system. The Ganges River is gravelly, narrow, vegetated, and humid. Modern day vertisols of the Houston Black series, central Texas are smectitic and too humid

The Paluxy braidplains can be interpreted as regionally extensive sand-dominated braidplains that were deposited in semi-arid to sub-humid climatic conditions. Deposition occurred in a braided dryland river system that relied on a probable 100,000 year cycle flooding events. Tooth (2000) review of the process, form and change in dryland rivers corroborated this observation, by noting the impact of large floods to dryland river form and change.

Diagenesis was driven in large part by pedogenic processes. Feldspar dissolution during pedogenesis was a fundamental control on reservoir quality in the Paluxy Formation and effectively differentiates CO_2 injection zones from baffle and barrier layers. The Washita-Fredericksburg seal is laterally extensive but is in a complex facies relationship with reservoir quality sandstone.

The interplay of depositional and diagenetic processes resulted in the deposition and quality of reservoir sandstone bodies in which reservoir heterogeneity occurs at a multitude of scales. Reservoir heterogeneity is therefore a key factor in identifying and prioritizing CO_2 injection zones and understanding reservoir confinement and subsurface flow pathways. This will ultimately give a predictive framework for the management of commercial-scale CO_2 injection in the Paluxy Formation.

REFERENCES

Allison, M.A., 1998, Geologic framework and environmental status of the Ganges-Brahmaputra Delta: Journal of Coastal Research, v. 14, no. 3, p. 826-836.

Bailey, E.H., and Stevens, R.E., 1960, Selective staining of K-feldspar and plagioclase on rock slabs and thin section: American Mineralogist, 45, 9-10, p. 1020-1025.

Blodgett, R.H., and Stanley, K.O., 1980, Stratification, bedforms, and discharge relations of the Platte braided river system, Nebraska, Journal of Sedimentary Petrology, v. 50, no. 1, p. 139-148.

Boggs, S., Jr., 2012, Principles of sedimentology and stratigraphy, 5th ed., Prentice Hall.

Bridge, J.S., and Lunt, I.A., 2006, Depositional models of braided rivers: Braided Rivers, Processes, Deposits, Ecology and Management, International Association of Sedimentologists. Special Publication 36, p. 11-50.

Cant, D.J., and Walker, R.G., 1976, Development of a braided-fluvial facies model for the Devonian Battery Point Sandstone, Quebec: Can. J. Earth Sci., v. 23, p. 102-119.

Cant, D.J., and Walker, R.G., 1978, Fluvial processes and facies sequence in the sandy braided South Saskatchewan River, Canada, Sedimentology, v. 25, no. 5, p. 625-648.

Cant, D.J., 1982, Fluvial facies models and their application, In: Sandstone Depositional Environments, (eds. P.A. Scholle and D. Spearing), AAPG Memoir, 31, p.115-137.

CH2M Hill, 1986, A class one injection well durvey, Phase I Report: Survey of delected ditesz; unpublished report to the Underground Injection Practices Council, unpaginated.

Cottingham, J. P., 1988, A kinematic model for interpreting the structural evolution of the Citronelle dome, Mobile County, Alabama: Tuscaloosa, Alabama, University of Alabama, unpublished Master's thesis, 94 p.

Dickinson, W. R., and Suczek, C. A., 1979, Plate tectonics and sandstone compositions: AAPG Bulletin, v. 63, p. 2164-2182.

Dickinson, W. R., Beard, S. L., Brakenridge, G. R., Erjavec, J. L., Ferguson, R. C., Inman, K. F., Knepp, R. A., Lindberg, F. A., and Ryberg, P. T., 1983, Provenance of North American Phanerozoic sandstones in relation to tectonic setting: GSA Bulletin, v. 94, p. 222-235.

Driese, S.G., Mora, C.I., Stiles, C.A., Joeckel, R.M., and Nordt, L.C., 2000, Mass-balance reconstruction of a modern Vertisol: implications for interpreting the geochemistry and burial alteration of paleo-Vertisols, Geoderma 95, p. 179-204.

Eaves, E., 1976, Citronelle Oil Field, Mobile County, Alabama: AAPG Memoir 24, p. 259-275.

Esposito, R. A., Pashin, J. C., Hills, D. J., and Walsh, P. M., 2008, Citronelle Dome: a giant opportunity for multi-zone carbon storage and enhanced oil recovery in the Mississippi Interior Salt Basin of Alabama: Gulf Coast Association of Geological Societies Transactions, v. 57,p.213-224.

Esposito, R. A., Pashin, J. C., Hills, D. J., and Walsh, P. M., 2010, Geologic assessment and injection design for a pilot CO_2-enhanced oil recovery and sequestration

demonstration in a heterogeneous oil reservoir: Citronelle Field, Alabama: Environmental Earth Sciences, v. 60, p. 431-444.

Esposito, R., Rhudy, R., Trautz, R., Koperna, G., and Hill, G., 2011, Integrating carbon capture with transportation and storage: Energy Procedia, v. 4, p. 5512-5519.

Folk, R.L., 1980, Petrology of sedimentary rocks, Hemphill Publishing Company, 182 p.

Gilchrist, R. E., 1981, Miscibility Study (Repeat 50% P.V. Slug) in Cores, Citronelle Unit, Mobile County, Alabama: unpublished report prepared for Unit Manager of Citronelle Field.

Gilchrist, R. E., 1982, Evaluation of Produced Fluids from the Carbon Dioxide Pilot Area in the Citronelle Unit, Mobile County, Alabama: unpublished report prepared for Unit Manager of Citronelle Field.

Goodbred, S.L. Jr., Kuehl, S.A., Steckler, M.S., and Sarker, M.H., 2003, Controls on facies distribution and stratigraphic preservation in the Ganges-Brahmaputra delta sequence: Sedimentary Geology, v. 155, p. 301-316.

Hall, A. M., and Fritz, W. J., 1984, Armored mud balls from Cabretta and Sapelo barrier islands, Georgia: Journal of Sedimentary Research, v. 54, p. 831-835.

Hasiotis, S. T., 2002, Continental trace fossils: SEPM Short Course Notes 51, 132 p.

Hayward, O. T. & Brown, L. F., 1967, Comanchean (Cretaceous) rocks of central Texas. In Comanchean (Lower Cretaceous) stratigraphy and paleontology of Texas (ed. Hendricks, L.), Permian Basin Section, Society of Economic Paleontologists and Mineralogists, p. 31–48.

Heald, M.T., and Larese, R.E., 1973, The significance of the solution of feldspar in porosity development, Journal of Sedimentary Petrology, v. 43, no. 2, p. 458-460.

Koperna, G., Riestenberg, D., Kuuskraa, V., Rhudy, R., Trautz, R., Hill, G. R., and Esposito, R., 2012, The SECARB Anthropogenic Test: A US Integrated CO_2 Capture, Transportation and Storage Test: International Journal of Clean Coal and Energy, v. 1, 13 p.

Kuuskraa, V. A., Lynch, R., and Fokin, M., 2004, Site selection and process identification for CO_2 capture and storage test centers: Arlington, Virginia, Advanced Resources International, Electric Power Research Institute Report, Agreement E2-P79/C5887, 184 p.

Mack, G.H., James, W.C., and Monger, H.C., 1993, Classification of paleosols, Geological Society of America Bulletin, v. 105, p. 129-136.

Mancini, E. A., and Puckett, T. M., 2002, Transgressive-regressive cycles in Lower Cretaceous strata, Mississippi Interior Salt Basin area of the northeastern Gulf of Mexico, USA, Cretaceous Research, v. 23, p. 409-438.

Mancini, E. A., and Puckett, T. M., 2005, Jurassic and Cretaceous transgressive-regressive (T-R) cycles, Northern Gulf of Mexico, USA: Stratigraphy, v. 2, no. 1, p. 31-48.

Martin, C.A., and Brian, R.T., 1998, Origins of massive-type sandstones in braided river systems, Earth Science Reviews, 44, no.1, p. 15-38.

Miall, A. D., 1977, A review of the braided-river depositional environment, Earth-Science Reviews 13, 62 p.

Miall, A.D., 1977, Lithofacies types and vertical profile models in braided river deposits: a summary; in A.D. Miall, ed., Fluvial sedimentology, Canadian Society of Petroleum Geologists, Memoir 5, p. 597-604

NETL, 2012, The United States 2012 Carbon Utilization and Storage Atlas, 4th Edition, 130 p.

http://www.netl.doe.gov

Nunnally, J. D. and Fowler, H. F., 1954, Lower Cretaceous stratigraphy of Mississippi. Mississippi State Geological Survey, Bulletin 79, 54 p.

Pashin, J. C., Kopaska-Merkel, D. C., and Hills, D. J., 2014, Reservoir geology of the Donovan sandstone in Citronelle Field, in Walsh, P. M., ed., Carbon dioxide-enhanced oil production from the Citronelle oil field in the Rodessa Formation, South Alabama: Final Scientific/Technical Report, U.S. Department of Energy Award DE-FC26-06-NT43029, p. 13-65.

Pashin, J. C., and Guohai Jin, 2004, Geometry and evolution of Mesozoic-Cenozoic salt structures in the DeSoto Canyon and eastern Mississippi interior salt basins: Final Report, U.S. Minerals Management Service, Order 0101PO18256, 191 p.

Pashin, J. C., McIntyre, M. R., Grace, R. L. B., and Hills, D. J, 2008, Southeastern Regional Carbon Sequestration Partnership (SECARB) Phase III: Final Report prepared for Advanced Resources International, 57 p.

Pashin, J. C., Raymond, D. E., Alabi, G. G., Groshong, R. H., Jr., and Guohai Jin, 2000, Revitalizing Gilbertown oil field: Characterization of fractured chalk and glauconitic sandstone reservoirs in an extensional fault system: Alabama Geological Survey Bulletin 168, 81 p.

Petrusak, R., Cyphers, S., Baumgardner, S., Hills, D., Pashin, J., C., and Esposito, R. A., 2010, Saline reservoir storage in an active oil field: extracting maximum value form existing data for initial site characterization; Southeast Regional Carbon

Sequestration Partnership (SECARB) Phase III Anthropogenic CO_2 Test at Citronelle Field: New Orleans, SPE International Conference on CO_2 Capture, Storage and Utilization, paper SPE 139700, 25 p.

Pittman, E. D., Larese, R. E., and Heald M. T., 1992, Clay coats: occurrence and relevance to preservation of porosity in sandstones: SEPM Special Publication 47, p. 241-255.

Raymond, D.E., Osborne, W.E., Copeland, C.W., and Neathery, T.L., 1988, Alabama stratigraphy, Geological Survey of Alabama, Stratigraphy and Paleontology Division, v. 140, 97 p.

Retallack, G. J., 1991, Untangling the effects of burial alteration and ancient soil formation, Annual Review of Earth and Planetary Sciences, 19, p. 183-206.

Retallack, G. J., 2001, Soils of the past: an introduction to paleopedology, 2nd edition, Blackwell Science Ltd, 404 p.

Rust, B.R., 1977, Depositional models for braided alluvium, in A.D. Miall, ed., Fluvial sedimentology, Canadian Society of Petroleum Geologists, Memoir 5, p. 605-625.

Rust, B.R., 1981, Sedimentation in an arid-zone anastomosing fluvial system: Cooper's Creek, central Australia, Journal of Sedimentary Petrology, v. 51, no. 3, p. 745-755.

Schmidt, V., and McDonald, D.A., 1979, The role of secondary porosity in the course of sandstone diagenesis, The Society of Economic Paleontologists and Mineralogists, Special Publication, no. 26, p. 175-207.

Shanley, K.W., and McCabe, P.J., 1994, Perspectives on the sequence stratigraphy of continental strata, AAPG Bulletin, v. 78, no.4, p. 544-568.

Smith, J. J., Hasiotis, S. T., Kraus, M. J., & Woody, D. T., 2008, Naktodemasis bowni: new ichnogenus and ichnospecies for adhesive meniscate burrows (AMB), and paleoenvironmental implications, Paleogene Willwood Formation, Bighorn Basin, Wyoming: Journal of Paleontology, v. 82, no. 2, p. 267-278.

Tooth, S., 2000, Process, form and change in dryland rivers: a review of recent research: Earth Science Reviews, v. 51, p. 37-107.

Torrent, J., and Schwertmann, U., 1987, Influence of hematite on the color of red beds, Journal of Sedimentary Petrology, 57, p. 682-686.

Turner, P., 1980, Continental red beds, Amsterdam, Elsevier, 562 p.

Withjack, M.O., Schlische, R.W., and Olsen, P.E., 1998, Diachronous rifting, drifting, and inversion on the passive margin of central eastern North America: an analog for other passive margin: AAPG Bulletin, v. 82, p. 817-835

Young, K., 1967, Ammonite zonations, Texas Comanchean (Lower Cretaceous). In Comanchean (Lower Cretaceous) stratigraphy and paleontology of Texas (ed. Hendricks, L.), Permian Basin Section, Society of Economic Paleontologists and Mineralogists, p. 65–70.

Yurewicz, D. A., Marler, T. B., Meyerholtz, K. A. & Siroky, F. X., 1993, Early Cretaceous carbonate platform, north rim of the Gulf of Mexico, Mississippi and Louisiana. In Cretaceous carbonate platforms (eds Simo, J. A. T., Scott, R. W. & Masse, J. P.), American Association of Petroleum Geologists, Memoir 56, p. 81–96.

VITA

Ayobami Timothy Folaranmi

Candidate for the Degree of

Master of Science

Thesis: GEOLOGIC CHARACTERIZATION OF A SALINE RESERVOIR FOR CARBON SEQUESTRATION: THE PALUXY FORMATION, CITRONELLE DOME, GULF OF MEXICO BASIN, ALABAMA.

Major Field: Geology.

Biographical:

Education:

Completed the requirements for the Master of Science in Geology at Oklahoma State University, Stillwater, Oklahoma in May, 2015.

Completed the requirements for the Bachelor of Science in Geosciences at Midwestern State University, Wichita Falls, Texas in 2012.

Experience:

Graduate Research Assistant, Oklahoma State University, Stillwater (August 2013-May 2015).
Geological Technician, Gunn Oil Company, Wichita Falls, Texas (May 2011-June 2013).

Professional Memberships:

Member of American Association of Petroleum Geologists.
Member of Geological Society of America.